The National Academies of SCIENCES ENGINEERING MEDICINE
THE NATIONAL ACADEMIES PRESS

This PDF is available at http://nap.edu/24612

SHARE

Exhaust Emissions from In-Use General Aviation Aircraft (2016)

DETAILS

122 pages | 8.5 x 11 | PAPERBACK
ISBN 978-0-309-45233-5 | DOI 10.17226/24612

GET THIS BOOK

FIND RELATED TITLES

CONTRIBUTORS

Tara I. Yacovitch, Zhenhong Yu, Scott C. Herndon, Rick Miake-Lye, David Liscinsky, W. Berk Knighton, Mike Kenney, Cristina Schoonard, and Paola Pringle; Airport Cooperative Research Program; Transportation Research Board; National Academies of Sciences, Engineering, and Medicine

SUGGESTED CITATION

National Academies of Sciences, Engineering, and Medicine 2016. *Exhaust Emissions from In-Use General Aviation Aircraft*. Washington, DC: The National Academies Press. https://doi.org/10.17226/24612.

Visit the National Academies Press at NAP.edu and login or register to get:

- Access to free PDF downloads of thousands of scientific reports
- 10% off the price of print titles
- Email or social media notifications of new titles related to your interests
- Special offers and discounts

Distribution, posting, or copying of this PDF is strictly prohibited without written permission of the National Academies Press. (Request Permission) Unless otherwise indicated, all materials in this PDF are copyrighted by the National Academy of Sciences.

Copyright © National Academy of Sciences. All rights reserved.

AIRPORT COOPERATIVE RESEARCH PROGRAM

ACRP RESEARCH REPORT 164

Exhaust Emissions from In-Use General Aviation Aircraft

Tara I. Yacovitch
Zhenhong Yu
Scott C. Herndon
Rick Miake-Lye
AERODYNE RESEARCH, INC.
Billerica, MA

IN ASSOCIATION WITH

David Liscinsky
UNITED TECHNOLOGIES RESEARCH CENTER
East Hartford, CT

W. Berk Knighton
DEPARTMENT OF CHEMISTRY & BIOCHEMISTRY,
MONTANA STATE UNIVERSITY
Bozeman, MT

Mike Kenney
Cristina Schoonard
Paola Pringle
KB ENVIRONMENTAL
St. Petersburg, FL

Subscriber Categories
Aviation • Environment

Research sponsored by the Federal Aviation Administration

TRB TRANSPORTATION RESEARCH BOARD
The National Academies of
SCIENCES • ENGINEERING • MEDICINE

2016

Copyright National Academy of Sciences. All rights reserved.

AIRPORT COOPERATIVE RESEARCH PROGRAM

Airports are vital national resources. They serve a key role in transportation of people and goods and in regional, national, and international commerce. They are where the nation's aviation system connects with other modes of transportation and where federal responsibility for managing and regulating air traffic operations intersects with the role of state and local governments that own and operate most airports. Research is necessary to solve common operating problems, to adapt appropriate new technologies from other industries, and to introduce innovations into the airport industry. The Airport Cooperative Research Program (ACRP) serves as one of the principal means by which the airport industry can develop innovative near-term solutions to meet demands placed on it.

The need for ACRP was identified in *TRB Special Report 272: Airport Research Needs: Cooperative Solutions* in 2003, based on a study sponsored by the Federal Aviation Administration (FAA). ACRP carries out applied research on problems that are shared by airport operating agencies and not being adequately addressed by existing federal research programs. ACRP is modeled after the successful National Cooperative Highway Research Program (NCHRP) and Transit Cooperative Research Program (TCRP). ACRP undertakes research and other technical activities in various airport subject areas, including design, construction, legal, maintenance, operations, safety, policy, planning, human resources, and administration. ACRP provides a forum where airport operators can cooperatively address common operational problems.

ACRP was authorized in December 2003 as part of the Vision 100—Century of Aviation Reauthorization Act. The primary participants in the ACRP are (1) an independent governing board, the ACRP Oversight Committee (AOC), appointed by the Secretary of the U.S. Department of Transportation with representation from airport operating agencies, other stakeholders, and relevant industry organizations such as the Airports Council International-North America (ACI-NA), the American Association of Airport Executives (AAAE), the National Association of State Aviation Officials (NASAO), Airlines for America (A4A), and the Airport Consultants Council (ACC) as vital links to the airport community; (2) TRB as program manager and secretariat for the governing board; and (3) the FAA as program sponsor. In October 2005, the FAA executed a contract with the National Academy of Sciences formally initiating the program.

ACRP benefits from the cooperation and participation of airport professionals, air carriers, shippers, state and local government officials, equipment and service suppliers, other airport users, and research organizations. Each of these participants has different interests and responsibilities, and each is an integral part of this cooperative research effort.

Research problem statements for ACRP are solicited periodically but may be submitted to TRB by anyone at any time. It is the responsibility of the AOC to formulate the research program by identifying the highest priority projects and defining funding levels and expected products.

Once selected, each ACRP project is assigned to an expert panel appointed by TRB. Panels include experienced practitioners and research specialists; heavy emphasis is placed on including airport professionals, the intended users of the research products. The panels prepare project statements (requests for proposals), select contractors, and provide technical guidance and counsel throughout the life of the project. The process for developing research problem statements and selecting research agencies has been used by TRB in managing cooperative research programs since 1962. As in other TRB activities, ACRP project panels serve voluntarily without compensation.

Primary emphasis is placed on disseminating ACRP results to the intended users of the research: airport operating agencies, service providers, and academic institutions. ACRP produces a series of research reports for use by airport operators, local agencies, the FAA, and other interested parties; industry associations may arrange for workshops, training aids, field visits, webinars, and other activities to ensure that results are implemented by airport industry practitioners.

ACRP RESEARCH REPORT 164

Project 02-54
ISSN 1935-9802
ISBN 978-0-309-44601-3
Library of Congress Control Number 2016956783

© 2016 National Academy of Sciences. All rights reserved.

COPYRIGHT INFORMATION

Authors herein are responsible for the authenticity of their materials and for obtaining written permissions from publishers or persons who own the copyright to any previously published or copyrighted material used herein.

Cooperative Research Programs (CRP) grants permission to reproduce material in this publication for classroom and not-for-profit purposes. Permission is given with the understanding that none of the material will be used to imply TRB, AASHTO, FAA, FHWA, FMCSA, FRA, FTA, Office of the Assistant Secretary for Research and Technology, PHMSA, or TDC endorsement of a particular product, method, or practice. It is expected that those reproducing the material in this document for educational and not-for-profit uses will give appropriate acknowledgment of the source of any reprinted or reproduced material. For other uses of the material, request permission from CRP.

NOTICE

The research report was reviewed by the technical panel and accepted for publication according to procedures established and overseen by the Transportation Research Board and approved by the National Academies of Sciences, Engineering, and Medicine.

The opinions and conclusions expressed or implied in this report are those of the researchers who performed the research and are not necessarily those of the Transportation Research Board; the National Academies of Sciences, Engineering, and Medicine; or the program sponsors.

The Transportation Research Board; the National Academies of Sciences, Engineering, and Medicine; and the sponsors of the Airport Cooperative Research Program do not endorse products or manufacturers. Trade or manufacturers' names appear herein solely because they are considered essential to the object of the report.

Published research reports of the

AIRPORT COOPERATIVE RESEARCH PROGRAM

are available from

Transportation Research Board
Business Office
500 Fifth Street, NW
Washington, DC 20001

and can be ordered through the Internet by going to

http://www.national-academies.org

and then searching for TRB

Printed in the United States of America

Copyright National Academy of Sciences. All rights reserved.

The National Academies of
SCIENCES • ENGINEERING • MEDICINE

The **National Academy of Sciences** was established in 1863 by an Act of Congress, signed by President Lincoln, as a private, non-governmental institution to advise the nation on issues related to science and technology. Members are elected by their peers for outstanding contributions to research. Dr. Marcia McNutt is president.

The **National Academy of Engineering** was established in 1964 under the charter of the National Academy of Sciences to bring the practices of engineering to advising the nation. Members are elected by their peers for extraordinary contributions to engineering. Dr. C. D. Mote, Jr., is president.

The **National Academy of Medicine** (formerly the Institute of Medicine) was established in 1970 under the charter of the National Academy of Sciences to advise the nation on medical and health issues. Members are elected by their peers for distinguished contributions to medicine and health. Dr. Victor J. Dzau is president.

The three Academies work together as the **National Academies of Sciences, Engineering, and Medicine** to provide independent, objective analysis and advice to the nation and conduct other activities to solve complex problems and inform public policy decisions. The Academies also encourage education and research, recognize outstanding contributions to knowledge, and increase public understanding in matters of science, engineering, and medicine.

Learn more about the National Academies of Sciences, Engineering, and Medicine at **www.national-academies.org**.

The **Transportation Research Board** is one of seven major programs of the National Academies of Sciences, Engineering, and Medicine. The mission of the Transportation Research Board is to increase the benefits that transportation contributes to society by providing leadership in transportation innovation and progress through research and information exchange, conducted within a setting that is objective, interdisciplinary, and multimodal. The Board's varied committees, task forces, and panels annually engage about 7,000 engineers, scientists, and other transportation researchers and practitioners from the public and private sectors and academia, all of whom contribute their expertise in the public interest. The program is supported by state transportation departments, federal agencies including the component administrations of the U.S. Department of Transportation, and other organizations and individuals interested in the development of transportation.

Learn more about the Transportation Research Board at **www.TRB.org**.

Copyright National Academy of Sciences. All rights reserved.

COOPERATIVE RESEARCH PROGRAMS

CRP STAFF FOR ACRP RESEARCH REPORT 164

Christopher J. Hedges, *Interim Director, Cooperative Research Programs*
Michael R. Salamone, *ACRP Manager*
Marci A. Greenberger, *Senior Program Officer*
Jeffrey Oser, *Program Coordinator*
Eileen P. Delaney, *Director of Publications*
Hilary Freer, *Senior Editor*

ACRP PROJECT 02-54 PANEL
Field of Environment

Karen A. Scott, *Tetra Tech, Louisville, KY* (Chair)
Patti Clark, *Embry-Riddle Aeronautical University—Worldwide, Daytona Beach, FL*
Robert D. Freeman, *Los Angeles World Airports, Los Angeles, CA*
Samuel J. Hartsfield, *Portland, OR*
Corbett Smith, *Mead & Hunt, Santa Rosa, CA*
Phillip Soucacos, *Booz Allen Hamilton, Washington, DC*
Carl Ma, *FAA Liaison*
Christine Gerencher, *TRB Liaison*

AUTHOR ACKNOWLEDGMENTS

The measurements presented within could not have been done without the cooperation of GA airports. The authors gratefully acknowledge Stephen Bourque and the users at Boire Field, and Robert Mezzetti, A.A.E., and the Beverly Regional Airport for their support of this project and logistical assistance during engine testing.

We thank Joe Sarcione for operating aircraft during early-stage engine tests and whose knowledge of engine operation helped us design a streamlined engine test matrix. We also thank the individual pilots, flight schools, fixed-base operators, charter services, and companies who provided the aircraft and experienced pilots for ground testing, including Mark Scott at Falcon Air, Arne Nordeide at Beverly Flight Center, Paul Beaulieu at Perception Prime Flight Instruction, and Ron Emond at Air Direct Airways, as well as Drew Gillett, Sheera Kaizerman, Brian Stoughton, and Aeroptic, LLC.

Copyright National Academy of Sciences. All rights reserved.

FOREWORD

By Marci A. Greenberger
Staff Officer
Transportation Research Board

Aircraft emissions data for smaller aircraft such as piston and small turbine-powered aircraft either do not exist or have not been independently verified. The emissions data obtained as part of this project is available on the TRB website and can be added to the FAA's AEDT database of aircraft engines so as to better understand and estimate general aviation (GA) aircraft emissions. This report provides the findings from the emissions testing and the data. A PowerPoint presentation provides an overview of the findings and is available on the TRB website.

The FAA's Emission and Dispersion Modeling System (EDMS) used to perform air quality analysis is going to be replaced with the Aviation Environmental Design Tool (AEDT). Both modeling systems use emissions data for various aircraft engines, but there is greater confidence in the data for larger commercial aircraft engines. For smaller aircraft, such as piston and small turbine-powered aircraft, emission factor data, which is either non-existent or has not been independently verified, can result in under- or overestimating aircraft emissions and can make it difficult for airports with significant general aviation (GA) operations to characterize their emissions inventories.

Aerodyne, as part of ACRP Project 02-54, was selected to validate existing data for GA aircraft engines, supplement the existing data, and recommend substitutions for when aircraft engine data does not exist. Their research consisted of measuring emissions from 47 engines while those engines were in use. The resulting data is available in a spreadsheet on the TRB website. Piston engine emissions were found to be extremely variable due to the flexible way in which they are operated. The effect on airports of these new emissions factors and their variability is quantified and discussed.

This report, with the PowerPoint presentation, provides the information in different formats so as to be accessible to both those with a deep understanding of air quality modeling and those needing to understand the effect at their airport. The layperson can read the italicized sections without having to read the technical mechanics, allowing any reader to better understand emissions overall.

Copyright National Academy of Sciences. All rights reserved.

CONTENTS

1 Summary

4 **Chapter 1** Background

6 **Chapter 2** Research Approach
6 Pollutants in Exhaust
6 From Exhaust Pipe to Airport Emission
8 Test Procedures

11 **Chapter 3** Trends in Emission Indices
11 Gas Turbine Engines
14 Piston Engines
18 GA Emission Indices Show a Great Deal of Variability
18 Quantitative Validation of Existing Data

21 **Chapter 4** Sensitivity Analysis on Airport Emissions
21 Sensitivity Analysis Using EDMS/AEDT Tools
21 Introduction and Purpose
21 Assessment
21 Step 1—Identifying a Hypothetical National GA Airport Fleet
22 Step 2—Engine Matching and Substitutions
25 Step 3—Sensitivity Analysis
27 Baseline Scenario
28 Updated Scenarios
28 Results of the Sensitivity Analysis
30 Using Monte Carlo Methods to Improve Airport Emissions Estimates

36 **Chapter 5** Other Parameters Affecting Emissions
36 Pilot Mindset on Fuel Mixture
37 CO_2 Carbon Fraction as an Indicator of Combustion
39 Thermal NO_x and Rich vs. Lean Combustion
40 Transient Emissions Are Negligible
43 Ambient Conditions
44 Fuel Additives
45 Hydrocarbon Emissions from GA Are Primarily Unburned Fuel
46 New Measures of PM to Replace "Smoke Number"
47 PM Volatility Is High for Piston Engines
48 PM Size Is Small, < 20nm, for Piston Engines
50 GA Turbofan Engines

53 **Chapter 6** Conclusions
54 Future Research
55 Policy Implications of This Research

Copyright National Academy of Sciences. All rights reserved.

56 **Appendix A** Engine Prioritization List
57 **Appendix B** Test Matrix
60 **Appendix C** ICAO vs. FOCA Databases
61 **Appendix D** Method for Calculating Emission Ratios
64 **Appendix E** Method for Calculating Emission Indices
65 **Appendix F** Variability in Emissions Results from Variability in the Engine
68 **Appendix G** Gas-Phase Measurement Instruments
70 **Appendix H** PM Measurement Instruments
73 **Appendix I** PM Line Losses
76 **Appendix J** Estimating Fuel Flows for Piston Engines
79 **Appendix K** Carbon Content of AVGAS 100 LL
81 **Appendix L** Hypothetical Airport Engine Mapping
85 **Appendix M** Terminology and Abbreviations
87 **Appendix N** References
89 **Appendix O** List of Data Products
90 **Appendix P** Emission Index Data Tables

Copyright National Academy of Sciences. All rights reserved.

SUMMARY

Exhaust Emissions from In-Use General Aviation Aircraft

Available data on exhaust emissions of general aviation (GA) aircraft is limited, particularly for piston engines. For this research, the research team measured emissions and computed emission indices for dozens of real in-use aircraft. **Forty-seven complete engine tests are reported**, including **10 engines from a list of the top 20 national piston engines**.

The major findings described in this report are as follows:

- **Gas turbine engines and piston engines have very different emissions**, both in terms of magnitude and in trends with power. These differences can be understood based on the much higher combustion efficiencies in modern gas turbine engines versus piston engines. Piston engines emit more carbon monoxide and hydrocarbons (unburned or partially burned fuel) and less nitrogen oxides than gas turbine engines.
- **Emission trends from piston engines agree with basic principles of combustion**. Emission indices exhibit a large dependence on the fuel/air mixture (see Figure S-1).
- **Emissions from piston engines show a great deal of variability** that is directly related to the nature of piston engines and the flexible way in which they are operated.
- **Skewed distributions of emission indices are observed for piston engine emissions** of hydrocarbons, oxides of nitrogen, and particulate matter (PM) (see Figure S-1). This means that the most common emission index is not equal to the average emission index. For carbon monoxide, piston engine emissions, distributions are not skewed.
- The **variability of an average emission can be measured using 95% confidence intervals**. A confidence interval consists of an upper limit and a lower limit such that one is 95% sure that the true average emission falls between them. Existing data is considered invalid (statistically different) if it falls outside this confidence interval. See Figure S-2 for illustration.
- Replicate measurements of several tested engines were used to perform a statistical **validation of existing data**. Several invalid data points were found. The most important of these data points is the 2.3-times underestimate of the hydrocarbon emissions data for the very common Lycoming O-320 engine by the FAA-mandated software used for calculating airport emissions (Emission and Dispersion Modeling System [EDMS]/AEDT).
- A hypothetical GA airport representative of the U.S. national fleet was constructed. The effect of changing emission indices on this hypothetical airport was investigated with a **sensitivity analysis**. The effect of emission index variability was also investigated. **The effect of updated emission factors is much smaller than the effect of emissions variability**.
- **Standard statistical methods combined with FAA-mandated methods yield undesirably large confidence intervals on an airport's emissions**. For example, the hypothetical airport has an average NO_x emission of 2.7 megagrams per year, but it could be up to 3.9 times that amount within 95% confidence.

Copyright National Academy of Sciences. All rights reserved.

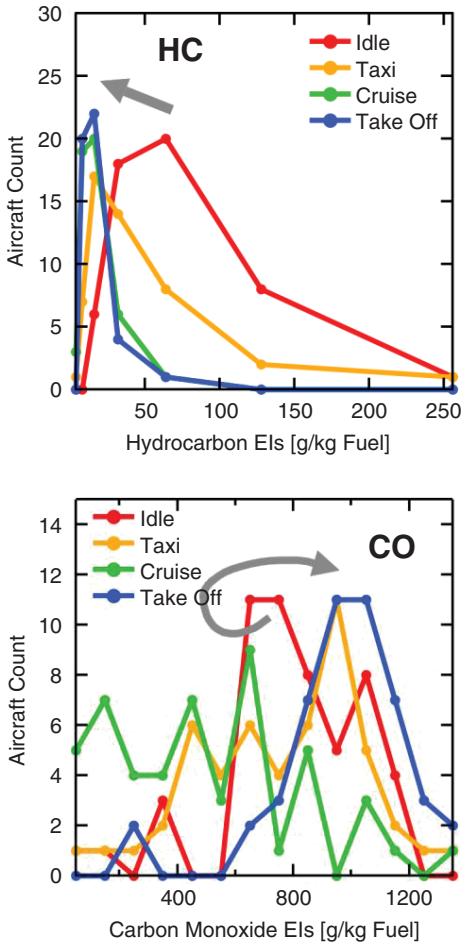

Figure S-1. Distributions of piston engine emission indices (EIs) for hydrocarbons (HC) and carbon monoxide (CO) as a function of power state (idle, taxi, cruise, take-off). The grey arrows show how the peak of the distribution moves with increasing power.

Copyright National Academy of Sciences. All rights reserved.

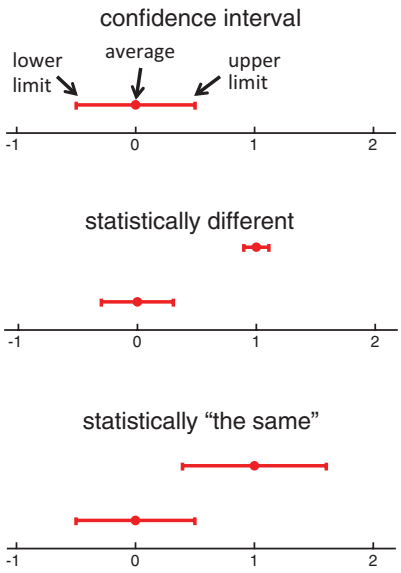

Figure S-2. Using confidence intervals to compare data points. Confidence intervals must not overlap for data to be considered statistically different.

- The research team demonstrated an **alternate statistical method (Monte Carlo simulations) that can constrain these confidence intervals**.
- **Many factors can affect emissions**. Several causes for high variability in emission indices are explored. The research team found that pilot mindset and their operation of an aircraft's mixture setting allows for a great deal of freedom in combustion parameters. The researchers also investigated several other technical details related to GA piston engine emissions, including trends in particle size and volatility, the effect of fuel additives, and thermal production of oxides of nitrogen and its relationship to lean combustion.
- A full list of measured emission indices is provided in Appendix P.

Copyright National Academy of Sciences. All rights reserved.

CHAPTER 1

Background

Much work has been done in quantifying the emissions from large commercial aircraft and their engines during operation in large airports. Regional airports serving the GA community are much smaller than a typical hub airport for commercial aircraft. However, in a local community that supports a regional airport, the airport can make a significant contribution to the community's burden of criteria pollutants like particulate matter (PM), oxides of nitrogen (NO_x), and hydrocarbon emissions. Although some studies have examined the issue of lead emissions from GA aircraft burning available aviation gasoline (AVGAS) (Heiken 2015), there has been relatively less examination of these criteria pollutants from GA aircraft.

Because small piston aircraft represent a small part of the overall airspace operations and are very small in terms of national gasoline fuel usage, the regulating authorities have largely given small aircraft little attention relative to large commercial aircraft and road traffic, respectively. Thus, much legacy technology is still in use in GA operations and has not been subject to regulatory emissions control. When aviation emissions regulations were first being imposed, it was reasonable to assume this small part of global aviation was a negligible part of the total pollution problem. Now, as large commercial engines have gotten cleaner and more efficient, it is important to assess the contribution that general aviation makes as a result of their operations in local communities.

Because general aviation uses different engine technologies than those of large commercial aircraft, one cannot simply use emissions inventories developed for large airports and scale them for use in regional airport analysis. General aviation extensively uses piston engines burning AVGAS, and these engines have different emissions characteristics from the large commercial aircraft gas turbine engines and from ground transport piston engines. Even the smaller gas turbine engines, used in smaller business jets and similar smaller jet-propelled aircraft, can have different emissions performance than the large modern turbofans used by major commercial carriers. Thus, there is a strong need to understand the emissions performance of GA engines.

The Swiss Federal Office of Civil Aviation (FOCA) made an initial study on a limited set of piston engine aircraft. *ACRP Research Report 164* extends and expands this FOCA study to examine a wider range of engines and to assess multiple examples of engines and operators to evaluate the variability in the emissions performance during actual day-to-day operation. The emissions measured in this research include PM, where multiple characteristics were quantified, NO_x, carbon monoxide (CO), and hydrocarbons. These are all considered criteria pollutants by the US EPA, and are emissions that are controlled for large aircraft through the EPA in concert with international standards established by the International Civil Aviation Organization (ICAO).

The pollutants in this research were measured in ways different from how certification is done on new engines for regulatory purposes. The research team took advantage of cooperating operators so that the engines could be measured "on-wing" using in-service engines. This offered the

Copyright National Academy of Sciences. All rights reserved.

advantage of acquiring data reflecting actual operation of in-use engines in the airframe, rather than idealized states of new engines in certification testing rigs. This distinction is especially important for piston engine aircraft, because there is large variability in how piston engines are operated and, thus, in the emissions performance for even the same engine model. Furthermore, testing of these in-use engines has further advantages over certification testing of new engines, given that the GA fleet has slow turnover, and many decades-old aircraft are still in-use.

Throughout this report, summaries in layperson's terms are italicized to guide the casual reader to the main conclusions of each section.

ACRP Research Report 164 has six chapters and numerous appendices. Chapters 1 and 2 provide background information about aircraft emissions and describe how testing and data analysis is done. In Chapter 3, the main results of the emissions measurements are described and compared to previous data. Chapter 4 shows how these emission results can be used to estimate the environmental impact of a GA airport. Chapter 5 examines the details of the emissions results with an eye to understanding the effect of everything from pilot mindset to transients. Finally, Chapter 6 summarizes the main conclusions of this research and identifies topics for future research. Appendixes A through P provide supporting detail and useful data sets.

Copyright National Academy of Sciences. All rights reserved.

CHAPTER 2

Research Approach

Pollutants in Exhaust

Four main pollutant types were measured as a part of this study: nitrogen oxides, carbon monoxide, total hydrocarbons, and PM. The sources and importance of these pollutant species are described.

In this research the focus is on the main pollutant species (see Figure 2-1).

Nitrogen oxides (NO_x) play an important role in smog formation and can be particularly important for airports situated in ozone non-attainment zones. Such zones are areas that do not meet National Ambient Air Quality Standards (NAAQS) for ozone, a pollutant in smog.

Carbon monoxide (CO) is a product of incomplete combustion. In high concentrations and in enclosed spaces, CO can be dangerous, so many households and some aircraft cockpits have CO monitors or alarms.

Hydrocarbons (HC), sometimes referred to as unburned hydrocarbons (UHC), are a third pollutant of interest. HCs come from fuel that has not been completely burned in the engine. HC includes a large range of individual chemical components, including volatile organic hydrocarbons (VOCs), unchanged components from the fuel, as well as partially broken down fuel. Depending on their exact composition, HC emissions can be of concern to both human health and local air quality.

PM emissions are a last category of engine pollutant. PM is fundamentally different from the previous pollutants because it is non-gaseous; any type of smoke is made up of PM. PM contains both volatile and non-volatile substances. The predominant component of non-volatile PM (nvPM) is soot, which is formed during the incomplete combustion process. Volatile PM is generated by the nucleation or condensation on soot from gaseous precursors such as sulfuric acid and organic compounds. The sum of volatile and non-volatile PM is called total PM (totPM). There are two general ways to quantify PM: count them to get the number (PM_n) or weigh them to get the mass (PM_m).

Although it is not a reported emission species, carbon dioxide (CO_2) is central to all emissions measurements. Carbon dioxide is the result of **complete** combustion of fuel. Combined with the products of incomplete combustion (CO and HC), CO_2 allows us to relate the emissions to the total amount of fuel burned.

From Exhaust Pipe to Airport Emission

The aircraft's operation (power states, time spent in each mode, landing and take-off cycle at the airport) can be combined with measured emission indices and fuel flows to estimate the total emissions from an airport.

Copyright National Academy of Sciences. All rights reserved.

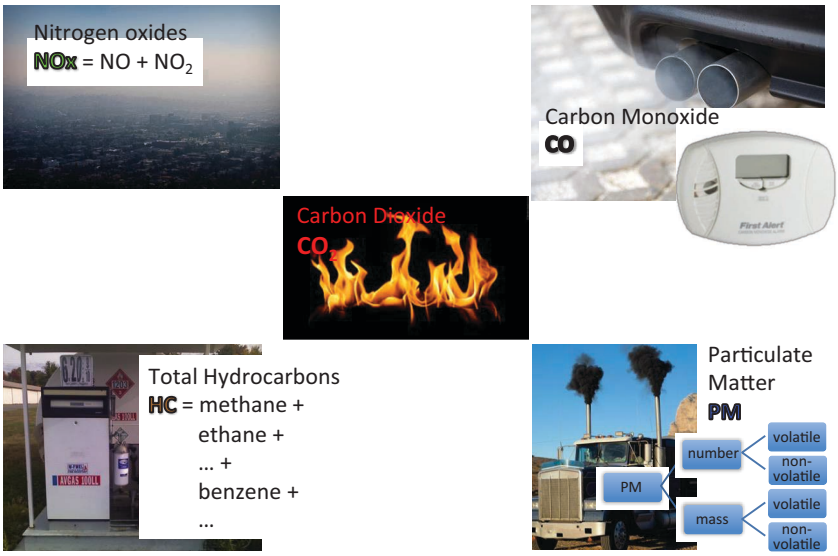

Figure 2-1. Important species in aircraft exhaust: nitrogen oxides (NO_x), carbon monoxide (CO), carbon dioxide (CO_2), total hydrocarbons (HC), and particulate matter (PM).

Suppose an airport's environmental manager wants to know how plans to construct a new runway will affect the total emissions from the airport. Emissions data tables such as those in Appendix P, when combined with some additional information about the airport, will allow the environmental manager to estimate current and future emissions. With these estimates in hand, an informed decision on the future of construction can then be made. So how do we get all the way from the exhaust pipe of an aircraft engine to the final airport emissions estimate? This section defines terms and explains the math needed.

We start at the greatest level of detail with an **emission index (EI)**. The EI is a measure of the amount of a pollutant (or "chemical species") that is emitted per amount of fuel burned for a given engine type. EIs are expressed in terms of grams of pollutant per kilogram of fuel burned (g/kg fuel). In practice, an **emission ratio (ER)**, the molar ratio of a measured species versus the sum of carbon-containing species, is determined experimentally for each chemical species of interest (see Appendix D for a discussion of ER calculation methods) and then combined with the known carbon content of the aircraft fuel to calculate the EIs. Appendix E details the mathematics of this procedure. Tables of EIs (such as those in Appendix P) list EIs for many different engines and many different pollutants at many different power states.

The **power states**, based on the operation of an aircraft, will be familiar to any pilot. The power states used in this report are idle, taxi, climb-out (C/O), cruise, approach (App), and take-off (T/O). The report defines the additional power state of final approach (Final App) with less power than approach, based on anecdotal evidence from pilots that the crosswind and upwind leg of the approach are distinct and different. The precise definitions of these power states vary depending on the emissions database in question. For example, Appendix C compares the power states defined by the ICAO, which has data for large commercial jets, to the Swiss FOCA, which has data for small piston engines. Throughout this report, power is usually plotted in terms of the percentage of the maximum fuel flow, because this is most indicative of thrust for piston engines.

Depending on the size of an airport, the time that a typical aircraft spends in each power state can vary. These characteristic times are referred to as "**times in mode**." In this report, the

Copyright National Academy of Sciences. All rights reserved.

standard times-in-mode are as defined by the ICAO for commercial airports; however, these times may not always be appropriate for typical operations at many GA airports. The development of GA-specific times in mode was beyond the scope of this research.

With the defined power states and known times in mode, it is possible to construct a **landing take-off cycle (LTO)** for an airplane; for example: idle, taxi, take-off, climb-out, approach, final approach, taxi, and idle. The cruise state is not included in the LTO framework—cruise emissions, while important for national inventories, are not relevant when considering emissions at the airport.

For a given aircraft, the emission indices can be multiplied by fuel flow and the times in mode to yield an **emission burden**. The burden represents the amount of pollutant emitted by a given engine over the course of the LTO and will be expressed in units of grams of pollutant per engine (g/engine).

Any given airport will have a certain number of operations per unit time. An operation in this sense refers to the number of LTO cycles that occur at the airport. The airport will also have a characteristic fleet, where the number and type of aircraft are known. Each aircraft will have a known airframe type (e.g., Cessna 172), engine model type (e.g., Lycoming O-320-E2G), and number of engines per aircraft (1 or 2). With this known information about the airport fleet, a burden for each aircraft can be calculated and summed to produce the final emission estimate for the whole airport. This type of estimate is often done before (a "baseline scenario") and after ("updated scenario") some proposed change.

The FAA-mandated tool used to perform these calculations is the AEDT. Prior to 2016, the Emission and Dispersion Modeling System (EDMS) was the mandated software. Both pieces of software have the same small set of built-in emission indices, which for piston engines amounts to eight different types of piston engines (see Appendix P). This limited data can now be supplemented by the new EIs measured over the course of this project.

Test Procedures

To measure a large number of different engines, engine tests were performed on the ground with real in-use aircraft. The measurement equipment sampled from a probe placed behind the aircraft (no contact). The pilot was instructed to operate the aircraft at different simulated power states (e.g., idle, take-off, and so forth) and an observer in the passenger seat noted relevant cockpit parameters.

A primary goal of ACRP Project 02-54 was to supplement the available data on GA engine emissions. To maximize the number of engines measured, measurement equipment was brought to GA airports and ground testing of the local aircraft fleet was done. Flight instructors or owner-pilots operated the aircraft in exchange for hourly fees and/or fuel vouchers. All measurements were performed using a no-contact probe set up 1 to 10 meters behind the tail of the aircraft. Figure 2-2 shows a typical sampling setup for a propeller plane.

An alternative type of engine testing involves laboratory measurements of an engine in a dynamometer setup (i.e., no aircraft, highly controlled input parameters like fuel flow and torque). While providing detailed information on engine operation, this type of test cannot compete with the low relative cost per engine sampled of real in-use testing. Furthermore, testing the engine in the airframe is more representative of true conditions at a GA airport where many different engine/airframe combinations are operated by many different pilots in different ways.

Measurement campaigns were conducted in the spring and fall to avoid large extremes in temperature. Test airports were also at similar altitudes to avoid large differences in ambient pressure. Ambient temperature and pressure are reported for each measured emission index, but no further correction has been made.

Copyright National Academy of Sciences. All rights reserved.

Figure 2-2. Preparing for a test of a Lycoming O-320 engine. The tripod to the right of the image supports two sampling lines for gas-phase and particle-phase measurements, respectively.

Two measurement platforms were used: the Aerodyne Mobile Lab (AML) supported instrumentation for gas-phase measurements; the Aerodyne trailer, towed by a pickup truck, supported instrumentation for all particulate phase measurements. A third vehicle towed a generator for power while stationary. These three vehicles are shown in Figure 2-3 (see also Figure 2-4).

The suite of instrumentation is described in more detail in Appendixes G and H. A welded steel tripod with narrow cross-section was used to support sampling lines for gas and particle-phase measurements. The measurement tripod is visible in the center of the frame of Figure 2-3, with

Figure 2-3. Measurement setup. The tow-behind trailer to the left houses the particulate matter instrument suite. The white truck in the middle is the Aerodyne Mobile Laboratory, housing the gas-phase instrumentation and data acquisition computers. The red truck to the right is towing a construction generator that powers all the instrumentation.

Copyright National Academy of Sciences. All rights reserved.

Figure 2-4. Ideal geometry for engine testing. The aircraft test is performed next to an unused taxiway. The exhaust and propeller wash are directed into an open field with no buildings or aircraft. The probe is placed just off the taxiway. The measurement equipment (the white truck) is out of the way.

sampling lines going back to the AML and trailer. The tripod is weighted with sandbags before any measurement.

A test matrix was constructed to guide the measurements. This test matrix, reproduced in Appendix B, was used by a cockpit observer to direct the engine test and note relevant cockpit parameters. A key development in this testing procedure was the addition of "return to idle" points between each high-power state. The aircraft engine can be idled for long periods on the ground, allowing the measurement team the time to gain an understanding of the "idle signature" and allowing for the cockpit observer to collect information on the aircraft and engine and describe the next test point. Idle then provided a chemical marker defining the beginning and end of the higher engine states, which can only be accessed for short periods on the ground without overheating.

Live, preliminary analysis of the emission ratios was performed by a scientist sitting in the passenger seat in the AML. This scientist could then determine whether data was of sufficient quality to proceed with the next test point. Communication with the cockpit observer was achieved through radio communication or SMS messaging. These test procedures allowed an experienced scientist team and a pilot without any previous ground-testing experience to complete a full engine test in less than 15 minutes.

Copyright National Academy of Sciences. All rights reserved.

CHAPTER 3

Trends in Emission Indices

By design, gas turbine engines installed in turboprop and turbofan (jet) aircraft operate in a prescribed manner. The combustion in these engines is well controlled by aircraft computers, and there is a strong link between the power produced by an engine and the resulting emissions.

In contrast, piston engines, which drive small propeller planes, operate in a much more flexible manner. Piston engines are rugged and imprecise and pilots can operate them in various ways with simple levers (e.g., the throttle and mixer) in the cockpit. Power and emissions are weakly linked, particularly in low-power states like idle and taxi. The nature of piston engines means that there is also a great deal of variability in their emissions, even for the same pilot operating the same airplane.

Gas Turbine Engines

Gas turbine engines operate in a very controlled manner. Engine operation is always lean (excess air) and combustion efficiency is high throughout the range of operational states. Figure 3-1 shows the expected trends in emission indices. This schematic was constructed based on trends observed during a 2006 field study of a General Electric CFM56-2-C1 jet engine (Anderson et al. 2006). HC and CO drop off precipitously above taxi, while NO_x emissions increase steadily with power.

For ACRP Project 02-54, the researchers measured gaseous and particulate emissions from four gas turbine aircraft engines:

- A TPE331-6-252B turboprop engine from Garrett AiResearch,
- A PT6A-60A turboprop engine from Pratt & Whitney,
- A FJ44-1AP turbofan engine from Williams International, and
- A CF34-3A1 turbofan engine from General Electric.

Among these measurements, the CF34-3A1 and TPE331 engine tests were performed with a cockpit observer and well-defined engine states (the other two jets were fortuitous measurements), so the trends in emissions from these two engines were investigated as a function of engine state.

Figure 3-2 shows the emission indices of gas-phase species. The CO EIs and HC EIs decrease with engine thrust for both the CF34 jet and the TPE331 turboprop, while NO_x EIs increase with engine thrust. This inverse-correlation of NO_x to CO and HC is primarily due to incomplete combustion at lower combustor temperatures, leading to the appreciable production of CO and unburned hydrocarbons. As the combustor temperature increases at high power, the CO and HC emissions are minimized and the NO_x emission index increases.

Figure 3-2 shows that both the emissions magnitude and trends for CO and NO_x EIs are similar among the very different gas turbines. However, although the trends are similar for the

Copyright National Academy of Sciences. All rights reserved.

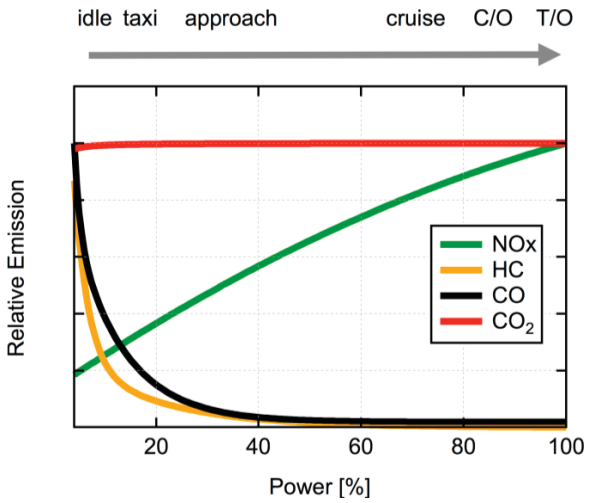

Figure 3-1. The trends in emissions for gas turbine engines.

HC emissions, the Garrett AiResearch TPE331 turboprop engine has systematically higher HC emissions than the GE CF34 jet by about 8 g/kg fuel.

Data for the General Electric CF34 jet is available in the ICAO database (ICAO 2013). Figure 3-3 shows a plot of these certified EI values for the CF34 engine along with the research team's data. Except for the approach power condition, the ACRP Project 02-54 research team's results are in relatively good agreement with the ICAO-certified CF34 EIs. For instance, at idle, EIs of CO, HC, and NO_x from the ICAO emission data bank are 42.6, 3.95, and 3.85 g/kg fuel, respectively. The research team obtained EIs of CO, HC, and NO_x of 67, 2.8, and 3.5 g/kg fuel, respectively. The ICAO values are averaged over several minutes of engine operation and use engine testing rigs (not in-use aircraft) and multiple sampling probes. All of these sampling differences may explain why the research team's instantaneous approach readings with a single sampling probe differ from ICAO's published values.

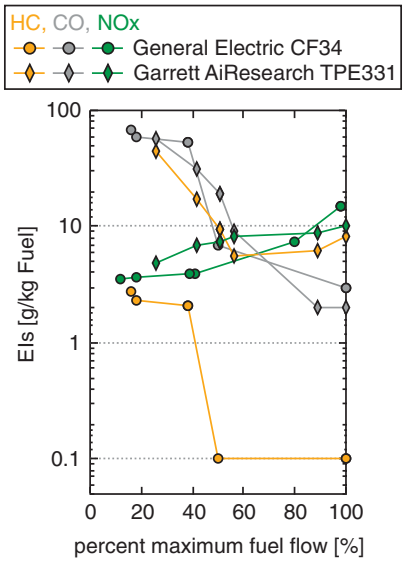

Figure 3-2. Emission indices of CO, HC, and NO_x for jet (CF34) and turboprop (TPE331) engines.

Copyright National Academy of Sciences. All rights reserved.

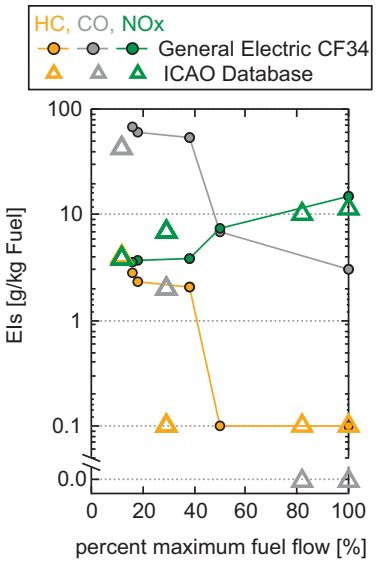

Figure 3-3. Comparison of the General Electric CF34-3A1 engine with ICAO database results.

In general, modern gas turbine aircraft engines have much higher combustion efficiencies than the conventional piston engines used in general aviation. The research team observed this phenomenon in the ACRP Project 02-54 research. For example, consider the CO emissions from the CF34 jet engine. At idle, CO constitutes about 3% of the total carbon emissions, but contributes <0.1% at T/O. HC emissions from this same engine are an order of magnitude smaller than CO emissions in these two states; this observation indicates that the CF34 engine has a combustion efficiency of 97% at idle and runs much more efficiently at the higher temperatures and pressures associated with high-power settings. On the contrary, for the measured piston engines discussed in the following sections, the averaged CO EI is 997 g/kg fuel at idle and 798 g/kg fuel at T/O and the averaged HC EI is 167 g/kg fuel at idle and 42 g/kg fuel at T/O. These results imply that, even at the highest engine power condition, the combustion efficiency of a piston engine is approximately 50%. Thus gas turbine engines are more than 10 times better at idle and more than two orders of magnitude better at high power than the conventional piston engines in terms of CO and HC emissions. ("CO_2 Carbon Fraction as an Indicator of Combustion" in Chapter 5 presents more detail.)

Both volatile and non-volatile PM are present in the exhaust of aircraft gas turbine engines. Emitted to the ambient air, the engine exhaust is diluted and cooled by the surrounding environment, so partitioning of the volatile species (e.g., volatile organic compounds and sulfuric acid) from gas phase to PM starts after the engine exit via condensation and new particle formation. This process will continue via microphysical interactions over a distance of hundreds of meters downstream. Accurate quantification for both the non-volatile PM emissions and the volatile contributions to particle mass is necessary to estimate environmental and health impacts.

The non-volatile PM number and mass emissions (nvPMn and nvPMm) as well as the total particulate matter number emissions (tPMn) are determined for the two turbine engines in question and plotted in Figure 3-4. The research team found that, in general, the total PM number EIs (tPMn, pink) are much larger than the non-volatile PM number EIs (nvPMn, red) at each engine power condition. The total particulate count contains the non-volatile count, and so this is expected. This phenomenon has been observed in plumes encountered in flight, in staged engine testing, and at airports. The difference between the two EIs is probably driven

Copyright National Academy of Sciences. All rights reserved.

14 Exhaust Emissions from In-Use General Aviation Aircraft

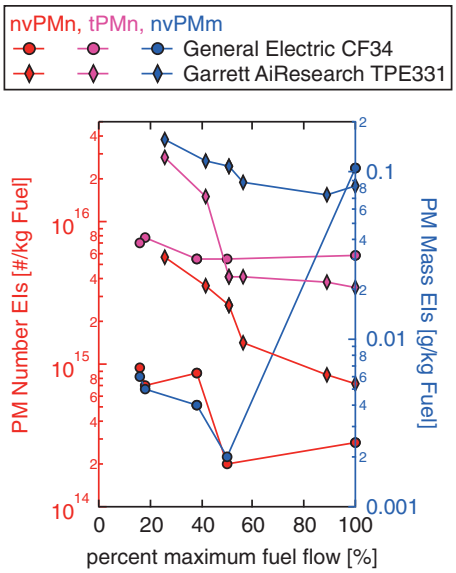

Figure 3-4. Emission indices for non-volatile particulate matter number (nvPMn), total particulate matter number (tPMn), and non-volatile particulate matter mass (nvPMm) in number and mass.

by the amount of condensable organic and sulfate species present in the engine exhausts. This is true for both the CF34 jet and the TPE331 turboprop engines.

As for nvPM, both the number and mass emissions of the CF34 engine are highly dependent on engine power condition. As shown in Figure 3-4, the lowest values of emissions in both nvPM mass and number occur near cruise power condition for the CF34 engine (40 – 50% of maximum fuel flow, 67% thrust). This character in emission with respect to engine power results in the U-shaped EI curves, which have been observed during many previous emissions measurements on modern gas turbine aircraft engines. These U-shaped curves occur because PM mass emissions are minimized at the highly efficient mid-power range typical of the cruise conditions, but increase at both take-off and idle where combustion efficiency is lower. The TPE331 turboprop engine also shows this U-shaped character in nvPMm, although the minimum is shifted toward slightly higher powers. Conversely, the TPE331 shows continuously decreasing tPMn and nvPMn with increasing power state. Data does not exist for full tests on turboprop engines, so this is the first time such a PM signature has been characterized.

For the CF34 engine, the highest EI for nvPMm is 0.106 g/kg fuel at the highest engine thrust, T/O, while the lowest nvPMm EI is 0.002 g/kg fuel at cruise (50% of maximum fuel flow, 67% thrust). This is in excellent agreement with previous measurements (Lobo et al. 2015) on a CFM56-7B24/3 engine that resulted in nvPMm EI of ~0.100 g/kg fuel at full power and ~0.001 – 0.002 g/kg fuel at cruise. Unlike PM mass, the EI in number (nvPMn) peaks at engine idle 9.3×10^{14} #/kg fuel, compared to 2.8×10^{14} #/kg fuel at full thrust.

Piston Engines

The large variability in piston engine emissions can be shown by plotting distributions of emission indices. Except for CO, the distributions are very skewed—the most common emission index is not equal to the average emission index.

Copyright National Academy of Sciences. All rights reserved.

EI distributions change with increasing power (idle > taxi > cruise > take-off) as expected. HC emissions decrease with power. CO emissions largely stay the same. NO_x emissions increase with power, peak at cruise, and then fall again. PM distributions behave differently depending on their measure (count vs. mass) and on their composition (total vs. non-volatile only).

This section explores the variability and trends in observed in carbon monoxide (CO), hydrocarbons (HC), nitrogen oxides (NO_x), and PM emissions from GA piston engines. Figure 3-5 shows the expected behavior of the gaseous exhaust species as a function of the oxygen left in the exhaust, which scales inversely with the fuel/air (F/A) ratio. At the vertical 0 line, one achieves ideal stoichiometric combustion where all fuel is combusted to CO_2, and all oxygen is consumed. Left of this line, the engine is operating with excess fuel (rich) and produces high amounts of CO and HC and low NO_x. Right of this line, the engine is operating with excess air (lean) and produces high NO_x but low CO and HC. The grey arrow in Figure 3-5 shows the expected behavior of the expected fuel/air ratio as a function of power state; for the piston engines examined here, one would not expect lean of stoichiometric behavior (hashed area). Although take-off (T/O) is the highest power state, it is not the leanest state; cruise is generally the leanest power state measured. (The reasons behind this are explored in "Pilot Mindset on Fuel Mixture" in Chapter 5.)

The emissions trends suggested by Figure 3-5 are borne out in the data from the piston engines. In Figure 3-6, aircraft count is plotted against emission index bins to yield distributions of EIs for measured piston engines. Four selected power states were chosen: idle, taxi, cruise and take-off. The approach, final approach, and climb-out states resembled the take-off state and were omitted for clarity. All EI axes were logarithmically scaled, except for CO, to highlight the orders-of-magnitude differences observed among emissions from different aircraft. Grey arrows show how the peak emissions distributions change with increasing power state.

As shown in Figure 3-6, except for CO emission index, lognormal distributions were observed for HC, NO_x, and PM emissions. Lognormal distributions are skewed distributions: the most common emission index (the mode) is smaller—sometimes much smaller—than the average emission index. These distributions demonstrate orders-of-magnitude difference in emissions among piston engines, even of the same engine model. Given that a lognormal distribution often results from a statistical multiplicative product of several independent variables, the research

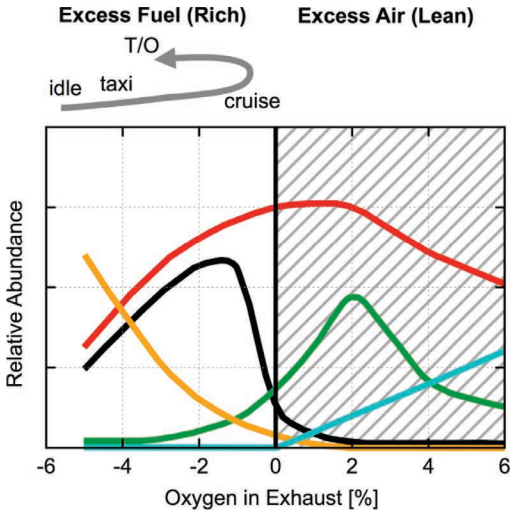

Figure 3-5. Expected exhaust gas composition as a function of the richness of combustion.

Copyright National Academy of Sciences. All rights reserved.

16 Exhaust Emissions from In-Use General Aviation Aircraft

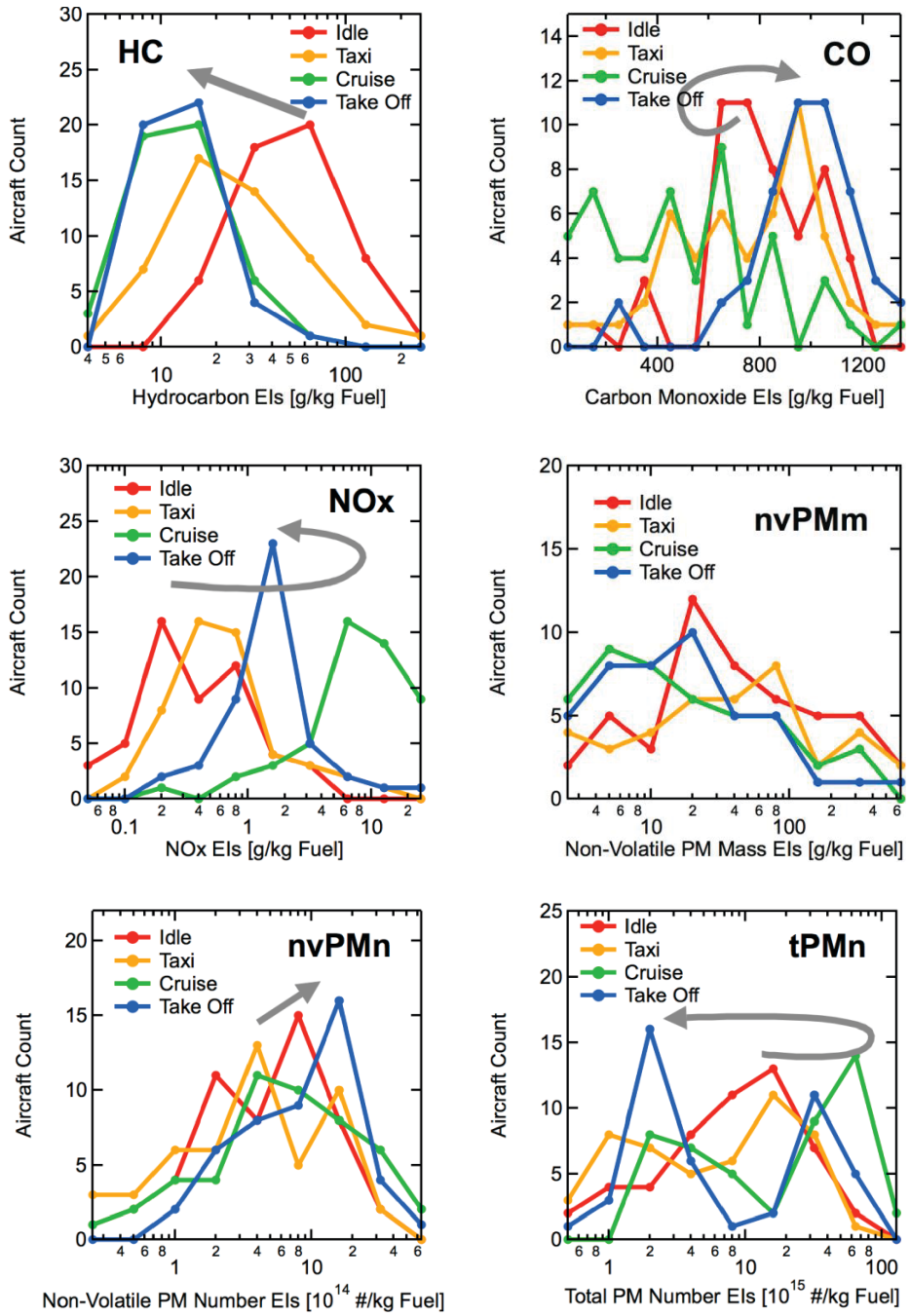

Figure 3-6. Distributions of emission indices as a function of power state (idle, taxi, cruise, take-off). Logarithmic axis for all EIs except carbon monoxide. The grey arrows show how the peak of the distribution moves with increasing power.

team's observation of lognormal distributions indicates that many random variables (e.g., fuel-to-air ratio (F/A), ambient temperature, and pilot preference of aircraft operation) are involved in determining the HC, NO_x, and PM emissions from piston aircraft engines.

In contrast to other species, CO emissions follow a normal distribution. The CO emissions are relatively constant with engine power, except at cruise condition, where CO emissions flatten out with the lowest mean value. Given that CO is an indicator of incomplete combustion

Copyright National Academy of Sciences. All rights reserved.

(see "CO_2 Carbon Fraction as an Indicator of Combustion" in Chapter 5), formation of CO is sensitive to the internal combustion engine temperature and F/A ratio. At fuel-rich combustion conditions, CO concentration normally increases with F/A ratio. When the F/A ratio closes to the stoichiometric condition, CO starts to decrease dramatically. As shown in Figure 3-6, CO emission increases from idle to taxi, to take-off, and then to cruise, indicative of a decreasing F/A. The research team's CO emission results reflect that pilots prefer to operate rich in all engine states except for cruise (see "Pilot Mindset on Fuel Mixture" and "CO_2 Carbon Fraction as an Indicator of Combustion" in Chapter 5). CO emissions at this lean-cruise condition are, on average, almost half those in the T/O or C/O conditions (rich).

The lognormal distributions in Figure 3-6 indicate that HC emissions decrease with increasing engine power. HC emissions from piston engines mainly consist of unburned and slightly burned fuel (see "Hydrocarbon Emissions from GA Are Primarily Unburned Fuel" in Chapter 5). Three main processes are expected to contribute:

1. Engine misfire,
2. Wall quenching, and
3. Combustion chamber deposits.

Additionally, HC concentrations can be influenced by the temperature of the fuel-to-air (F/A) mixture as it enters the combustion chamber, so large changes in ambient temperature could have an effect. The effect of ambient temperature on piston engine measurements is explored in Chapter 5. The observed lognormal distributions for HC emissions are consistent with these multiple influential variables.

As demonstrated in Figure 3-6, NO_x emissions from piston engines are inversely correlated with F/A and lognormally distributed. In this research, NO_x emissions are highest at cruise, decreasing in the following order: cruise → take-off → taxi → idle. This order implies that F/A at cruise is the lowest and is the highest at idle—this is in agreement with the observations from CO and HC emission measurements.

Shapes of the PM emission distributions are broader and harder to define than those for HC and NO_x emissions. In addition, the skewness, or asymmetry, of the distributions also becomes much larger, especially for the nvPMm emissions. The broad distribution and large skewness imply that additional measurements and analysis are necessary to understand the source and evolution of PM emissions from piston aircraft engines.

For piston aircraft engines, measurement results indicate black carbon soot emissions (nvPMm) are larger at the low-power conditions (idle and taxi), contrary to the observation from turbofan aircraft engines. The total soot emissions at a GA airport will be dominated by a few high emitters. At take-off, for example, the largest three emitters contribute 50% to the total emissions from 44 aircraft engines.

Emissions of nvPMn, which include contributions from both black carbon soot and $PbBr_2$ particles, are much less sensitive to power condition, compared to nvPMm emissions. Figure 3-6 shows a slight increase of nvPMn emission with engine power. This observation implies that $PbBr_2$ particles are significant contributors to the nvPMn emissions, since $PbBr_2$ emission is independent of engine power. Further investigation is necessary to distinguish the contributions from $PbBr_2$ and black carbon soot.

In general, total PM number emissions (tPMn) are ten times larger than the nvPMn emissions, indicative of predominance of volatile PM over non-volatile PM. Given the high level of incomplete combustion for piston aircraft engines, this observation is understandable. However, the research team also observed bimodal lognormal distributions for the tPMn emissions at each engine condition. The difference between the two modes is more than one order of magnitude.

Copyright National Academy of Sciences. All rights reserved.

18 Exhaust Emissions from In-Use General Aviation Aircraft

The smaller of these two modes may come from nucleation mode particles generated from volatile material/unburned fuel, whereas the larger particles can come from black carbon soot. The contribution of lead particles to these modes is still under investigation.

GA Emission Indices Show a Great Deal of Variability

A major finding from this research is that emissions from GA piston engines show a great deal of inherent variability. Piston aircraft are operated somewhat by "feel." For example, in the idle state, pilots reduce the throttle (and therefore the engine RPM) until the engine starts to run too roughly. The pilot also has direct control over the fuel/air mixture, and the research team has seen evidence of fuel additives (see following sections). Thus, for piston aircraft, the parameters that define a valid idle (or any other state) span a large multidimensional parameter space, particularly when compared to a turbojet engine, where mixture is handled automatically, and the pilot can dial in a percent power for each state.

The research team's recommendation for dealing with this variability is to understand that any airport emissions inventory produced for GA will carry uncertainty bars directly related to the nature of piston engines and their operation.

Policies, such as encouraging pilots to run lean (less excess fuel), could be investigated, especially during taxi and idle where there is no safety issue with stalling the engine. This is one way of mitigating airport emissions of hydrocarbons and CO, but with a potential increase in NO_x.

Quantitative Validation of Existing Data

The inherent variability in the data means that few existing data points can be invalidated with certainty. The most important invalid data point is the hydrocarbon emission index from the Lycoming O-320 engine, which is underestimated by a factor of 2.3 versus the results from this study.

The research team investigated three sources of existing aircraft emissions data:

1. The Swiss Federal Office of Civil Aviation (FOCA 2007a), which includes
   a. Original measurements
   b. Data from FAA's Aircraft Engine Emissions Database (FAEED)
2. FAA's Emission and Dispersion Modeling System (EDMS), which will be the same data used in the new standard, the AEDT, and which includes
   a. Data from the Environmental Protection Agency's Compilation of Air Pollutant Emission Factors – Mobile Sources (AP-42) (EPA 1989)
   b. Data from jet engine manufacturers like Pratt & Whitney
3. The International Civil Aviation Organization Database (ICAO 2013), which includes data from commercial jet engines

To quantitatively validate (or invalidate) this data, the research team considered the emissions burden of a given engine type for a standard landing-take-off cycle (LTO). This burden, expressed as g/LTO, rolls up the emissions factors and the fuel flows for all engine states of interest. Calculating LTO burdens allowed the research team to turn a 28-dimensional problem (seven engine states multiplied by four emission species) into a 4-dimensional problem. Validation was done for engines that the research team measured several times. These repeat measurements allowed the research team to determine with confidence the true variability between different instances of the same engine. The research team thus reports 95% confidence intervals on the average measured emissions burden. Four emission types were compared: hydrocarbons (HC), carbon monoxide (CO), oxides of nitrogen (NO_x), and non-volatile PM mass (nvPMm)

Copyright National Academy of Sciences. All rights reserved.

Table 3-1. LTO time-in-modes used in calculating emissions burdens. Engine states considered are *take-off* (T/O), *climb-out* (C/O), *cruise*, *approach* (App), *final approach* (Final App), *taxi* and *idle*.

Condition	T/O	C/O	Cruise	App	Final App	Taxi	Idle
Secs (Tot)	42	132	0	210	30	660	900

measured via engine exhaust particle sizer (EEPS). Table 3-1 lists the LTO times used. For the existing data, which does not differentiate between idle and taxi, nor between approach and final approach, the sum of the relevant times was used. Different characterization technologies were used to compare particulate quantification. The FOCA data was collected using a combination of the scanning mobility particle sizer (SMPS) and the EEPS 3090.

Table 3-2 shows selected experimental data used in the comparisons. Color bars guide the eye to the magnitude of the emission burden. Variability confidence intervals are expressed as a percentage of the average so that they can be compared on equal footing:

$$\%CI = \frac{\sigma \circ T_{95\%}^{DF}}{avg}$$

where

%CI is the percent confidence intervals,
avg is the average of the replicate determinations of emissions burden per LTO,
σ is the standard deviation of these replicates, and
$T_{95\%}^{DF}$ is the student's T at 95% confidence for degrees of freedom (DF = count − 1).

In these results, engine subtypes are neglected because no repeat measurements of any of the particular subtypes of FOCA data were acquired, and EDMS does not differentiate among subtypes.

Table 3-2. Experimental data for use in validation. The size of the color bars is proportional to the magnitude of the emissions burden for HC (orange), CO (pink), NO_x (green) and tPMm (blue).

Engine	Full Tests	HC Avg	Variability	CO Avg	Variability	NOx Avg	Variability	tPMm Avg	Variability
		g/LTO	% at 95% Conf	g/LTO	% at 95% Conf	g/LTO	% at 95% Conf	g/LTO	% at 95% Conf
Full Engine									
General Electric CF34-3A1	1	292		7315		1278		7.04	
Engine Family	Count								
Lycoming O-320	16	258	38%	4083	47%	32	246%	0.90	120%
Lycoming IO-360	4	598	116%	4387	47%	44	434%	2.04	358%
Lycoming O-360	6	406	95%	4924	58%	16	220%	1.68	186%
Lycoming IO-520	1	968		6960		13		1.95	
TCM O-470	1	391		3441		11		1.02	
Lycoming O-540	3	747	236%	6457	108%	21	32%	3.06	444%
Lycoming IO-540	4	795	115%	8483	96%	39	212%	3.33	230%
Horse Power Family									
diverse Prop-200hp	35	346	112%	4056	51%	26	255%	1.27	169%
diverse Prop-300hp	10	753	95%	7078	79%	27	171%	2.83	188%
diverse Prop-160hp	25	275	75%	3841	52%	25	256%	1.00	123%

Copyright National Academy of Sciences. All rights reserved.

Table 3-3. Validation of existing data. The size of the color bars is proportional to the magnitude of the emissions burden for HC (orange), CO (pink), NO_x (green) and tPMm (blue).

Engine	Data Source	HC [g/LTO]	valid?	CO [g/LTO]	valid?	NOx [g/LTO]	valid?	tPMm [g/LTO]	valid?
diverse Prop-200hp	FAEED162	116	YES	5350	YES	8	YES	0.27	YES
diverse Prop-300hp	FAEED160	345	YES	5481	YES	20	YES	2.02	YES
Lycoming O-320	FOCA	69	NO	3426	YES	36	YES	0.26	YES
Lycoming O-360	FOCA	115	YES	5948	YES	17	YES	0.32	YES
Lycoming IO-360	FOCA	168	YES	6988	NO	9	YES	1.30	YES
Lycoming O-540	FOCA	215	YES	8470	YES	3	NO		
Lycoming IO-540	FOCA	244	YES	7974	YES	23	YES	1.11	YES
General Electric CF34-3A1	ICAO	313	YES 1 rep	3350	NO 1 rep	1137	YES 1 rep		
Lycoming IO-360	EDMS	104	YES	4017	YES	20	YES		
Lycoming O-320	EDMS	115	NO	5326	YES	8	YES		

In Table 3-2 confidence intervals are generally the best (smallest) for the Lycoming O-320 engine family because the 16 replicate tests contribute to good statistics of these inherently highly variable emissions burdens (4 partial tests were excluded). When we apply the EDMS protocol of grouping all engines at or below 200 horsepower (HP), somewhat poorer statistics for the HC burden emerge, despite a greater number of measurements. Table 3-2 shows that a better grouping of engines would be anything below or equal to 160 HP. Although some of these confidence intervals are greater than 100%, emission burdens may never be negative.

In Table 3-3, selected pre-existing results from FAEED, EDMS and FOCA are shown. These results are not reported with any confidence intervals and, at least for the FOCA data, are the result of a single aircraft measurement. Data is considered valid if it falls within the 95% confidence intervals shown above. The General Electric CF34 jet is compared to ICAO data, although there is only a single aircraft measurement. For this jet, strict confidence intervals of ±50% were assumed. The following invalid existing data points are evident from Table 3-3:

1. The FOCA Lycoming O-320 HC emissions burden is too low (69 vs 258 g HC/LTO)
2. The FOCA Lycoming IO-360 CO emissions burden is too high (6988 vs 4387 g CO/LTO)
3. The FOCA Lycoming O-540 NO_x emissions burden is too low (3 vs 22 g NO_x/LTO)
4. The ICAO General Electric CF34-3A1 CO emissions burden is too low (3350 vs 7315 g CO/LTO)
5. The EDMS Lycoming O-320 HC emissions burden is too low (115 vs 258 g HC/LTO)

Of these invalid data, Item 5 is the most important. Item 5 involves an underestimate of HC emissions in EDMS/AEDT on the common Lycoming O-320 engine and, as such, will probably be used by default in any calculation GA airport emissions. The emissions are underestimated by a factor of 2.3.

Given the large variability in the emissions performance found in piston engines, it is unlikely that any of the cases found to be invalid via the comparison criteria adopted here were flawed measurements. The research results suggest that the characterization work was probably legitimate and that there is just a significant amount of variability in piston engine emissions.

Given the many repeat measurements of Lycoming O-320 family engines, the research team recommends average data from this family be substituted in current software for airport emissions estimates. Other engine families do not have the same number of replicates, and so the research team does not recommend them for substitution until additional data is available.

Copyright National Academy of Sciences. All rights reserved.

CHAPTER 4

Sensitivity Analysis on Airport Emissions

Sensitivity Analysis Using EDMS/AEDT Tools

A hypothetical GA airport's emissions were calculated before and after inclusion of the newly measured emission indices. Differences of CO: –6%, HC: 194% and NO_x: 64% were found. The effect of emissions variability is important. In fact, these seemingly large changes are not statistically different from the baseline scenario because the 95% confidence intervals for the updated scenario are very wide and the baseline scenario falls within their bounds.

Introduction and Purpose

This chapter summarizes the method used for and results of the sensitivity analysis comparing the effects of updating EDMS/AEDT database default emission indices with measured emission indices performed for ACRP Project 02-54, "Measuring and Understanding Emission Factors for GA Aircraft." The sensitivity analysis consisted of using the FAA's Emissions & Dispersion Modeling System (EDMS) modeling tool to determine the potential effect on computed emissions that may result from replacing or supplementing existing emissions indices within the EDMS/AEDT database with those measured in the field campaigns during ACRP Project 02-54. For this assessment, EDMS was used, because it produces results similar to the new AEDT.

Assessment

For ease of understanding, the analysis is divided into three steps:

1. **GA Airport Fleet**: FAA's National Tail Number Registry was used to identify the top 50% of aircraft engines within each engine category [i.e., single engine piston (SEP), multi-engine piston (MEP) and single engine turboprop (SETP)] to develop a hypothetical national GA airport fleet.
2. **Engine Substitutions**: Engine substitutions were performed to use the measured data, determine engine similarities, and provide recommendations on substitute engines for use in EDMS/AEDT modeling when no measured or database emission information is available.
3. **Sensitivity Analysis**: A sensitivity analysis was performed to compare the effects of updating EDMS/AEDT default emission indices with measured emission indices. The sensitivity analysis provides understanding of the potential effect of the research results on a hypothetical airport.

Detailed discussion of these three steps follows.

Step 1—Identifying a Hypothetical National GA Airport Fleet

FAA's National Tail Number Registry was used to select a representative fleet for a hypothetical airport.

Copyright National Academy of Sciences. All rights reserved.

FAA's National Tail Number Registry was queried to construct a representative aircraft population. The data was further summarized and ranked by number of occurrence for each aircraft engine within each engine category. The top 50% of each engine category was then used as the Hypothetical National GA Airport fleet, as shown in Table 4-1. This category break-down did not allow capture of every possible aircraft. For example, turbofan engines were excluded. The difficulty in constructing this fleet was due to the lack of data from the FAA registry about GA operations.

Step 2—Engine Matching and Substitutions

Engine substitutions were required because some engines are not available in the airport emissions simulation software AEDT and EDMS. Substitutions were done by comparing aircraft weight and engine horsepower. Flowcharts outline the required steps.

The aircraft engines from the Hypothetical Fleet (Table 4-1) were matched to the engines sampled in each field campaign for this project only if they were exact engine matches. Engines

Table 4-1. Hypothetical National GA Airport fleet.

Engine Category*	Rank**	Cumulative Percent of Engine Category*	Aircraft Make	Aircraft Model	Engine Family	Total National Occurrence	Percent of Hypothetical Fleet
SEP	1	6	CESSNA	172	O-320	10570	11
	2	12	CESSNA	182	O-470	10057	10
	3	18	CESSNA	150	O-200	9266	10
	4	22	PIPER	PA-28	O-320	7633	8
	5	26	CESSNA	172	O-300	6836	7
	6	29	PIPER	PA-28	O&VO-360	5346	6
	7	31	CIRRUS DESIGN CORP	SR22	IO-550	2854	3
	8	33	MOONEY	M20	IO-360	2704	3
	9	34	PIPER	J3C-65	A&C65	2359	2
	10	35	CESSNA	152	O-235	2254	2
	11	37	CESSNA	180	O-470	2128	2
	12	38	CESSNA	172	IO-360	2102	2
	13	39	PIPER	PA-28	IO-360	2075	2
	14	40	PIPER	PA-22	O-320	2049	2
	15	41	BEECH	35	IO-520	2021	2
	16	43	PIPER	PA-18	O-320	1940	2
	17	44	CESSNA	170	C145	1795	2
	18	45	PIPER	PA-32	TIO-540	1749	2
	19	46	CESSNA	210	TSIO-520	1725	2
	20	47	AERONCA	7AC	A&C65	1711	2
	21	48	BEECH	35	IO-470	1677	2
	22	49	CESSNA	140	C85	1468	2
	23	49	CESSNA	182	IO-540	1406	1
	24	50	MOONEY	M20	O&VO-360	1328	1
	25	51	PIPER	PA-28	O-540	1312	1

Copyright National Academy of Sciences. All rights reserved.

Table 4-1. (Continued).

Engine Category*	Rank**	Cumulative Percent of Engine Category*	Aircraft Make	Aircraft Model	Engine Family	Total National Occurrence	Percent of Hypothetical Fleet
MEP	1	6	CESSNA	310	IO-470	1169	1
	2	12	BEECH	95	IO-470	1068	1
	3	17	PIPER	PA-30	IO-320	937	1
	4	22	PIPER	PA-31	TIO-540	902	1
	5	27	PIPER	PA-23	TIO-540	899	1
	6	32	PIPER	PA-34	TSIO-360	883	1
	7	36	CESSNA	421	GTSIO-520	716	1
	8	40	CESSNA	340	TSIO-520	660	1
	9	43	CESSNA	337	IO-360	649	1
	10	47	PIPER	PA-23	O-320	597	1
	11	50	BEECH	58	IO-520	593	1
	12	53	CESSNA	414	TSIO-520	565	1
SETP	1	17	CESSNA	208	PT6A	466	<0
	2	33	PILATUS	PC-12	PT6A-67	464	<0
	3	52	EADS SOCATA	TBM 700	PT6A-66	259	<0
TOTAL						97192	100%

*Single engine piston (SEP), multi-engine piston (MEP) and single engine turboprop (SETP)
**Rank indicates the rank by number of occurrence for each aircraft engine within each engine category (e.g., SEP, MEP, and SETP).

were substituted when the engines from the Hypothetical Fleet were not present in the EDMS/AEDT databases. In these cases, the research team used one of the following methods, based on data availability:

- Simple substitution method, or
- Advanced substitution method

The simple substitution method was used when detailed data was not available. Substitutions were made based on aircraft and engine family.

The advanced substitution method involves substituting an engine based on engine/aircraft family as well as one with similar emission coefficients, horsepower, and weight. For a more conservative analysis, an aircraft/engine with higher emission coefficients and aircraft weight is chosen. Obtaining this information requires researching the sampled aircraft/engine and looking up emission coefficients and aircraft weights within the EDMS/AEDT databases. Given that the hypothetical airport is constructed from the FAA Tail Registry Database, only engine family is available, and only the simple method is required. This type of engine substitution is standard practice for firms specializing in using EDMS and AEDT software.

Figure 4-1 outlines the procedure for the simple substitution method. Engine/aircraft entries for the hypothetical airport were compared one by one to the available combinations in EDMS/AEDT. Engine matches were prioritized over aircraft matches. For example, if a Cessna 150 with an O-320 engine was sampled in the field but this aircraft/engine combination was not in the EDMS/AEDT modeling databases, the recommended substitution would be a Cessna 172 with an O-320 engine, because the engine is a match, and the Cessna 172 aircraft is comparable to the Cessna 150 in terms of weight.

Copyright National Academy of Sciences. All rights reserved.

24 Exhaust Emissions from In-Use General Aviation Aircraft

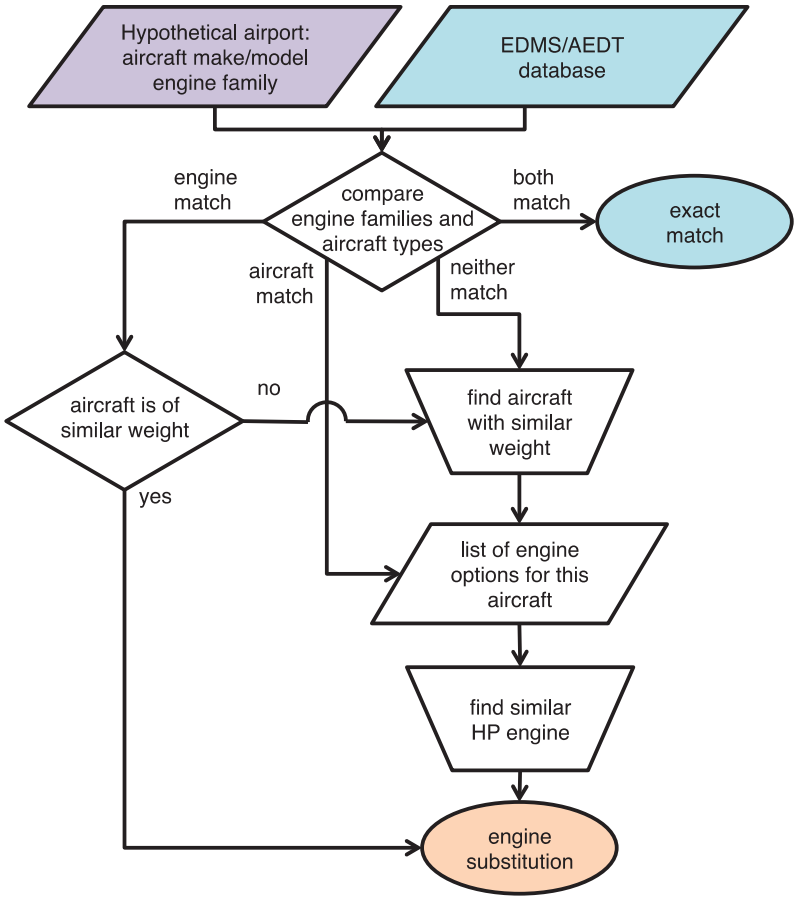

Figure 4-1. The simple substitution method for EDMS/AEDT data.

A second set of matches was constructed, substituting experimental data when available. Figure 4-2 outlines this procedure. If no experimentally measured data matches exactly, no further substitution is done and the procedure defaults to the EDMS/AEDT dataset match.

Table 4-2 shows sample mappings for the five most common SEP aircraft and lists the Hypothetical Fleet aircraft make/model and engine family, the sampled aircraft engine model, and the EDMS/AEDT aircraft make/model and engine it was matched with. Priority was given to match the aircraft engine family over the aircraft make/model. (Table L-1 in Appendix L details the full mapping for all hypothetical airport engines.)

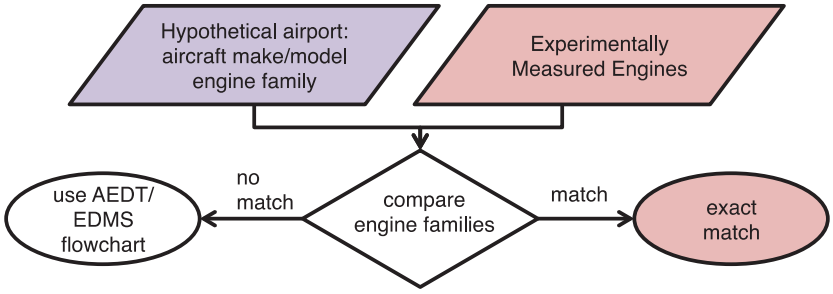

Figure 4-2. The simple substitution method for experimentally measured data.

Copyright National Academy of Sciences. All rights reserved.

Table 4-2. Example mapping of five hypothetical fleet aircraft to their equivalent engines in sampled and EDMS/AEDT datasets. (Full mapping is available in Appendix L)

Hypothetical Fleet				Sampled Engine Model	EDMS/AEDT Match			Comments
Category	Aircraft Make	Aircraft Model	Engine Family		Aircraft Make	Aircraft Model	Engine Model	
SEP	CESSNA	172	O-320	O-320	Cessna	172	0-320	Exact match with Hypothetical Fleet and sampled aircraft/engine.
	CESSNA	182	O-470	O-470	Cessna	182	IO-360-B	No O-470 in EDMS; chose IO-360 because (only option for Cessna 182) similar horsepower (hp).
	CESSNA	150	O-200	O-200	Cessna	150	O-200	Exact match with Hypothetical Fleet and sampled aircraft/engine.
	PIPER	PA-28	O-320	O-320	Piper	PA-28	O-320	Exact match with Hypothetical Fleet and sampled aircraft/engine.
	CESSNA	172	O-300	--	Cessna	172	O-320	No O-300 in EDMS; chose O-320 because similar hp.

Step 3—Sensitivity Analysis

Two emission scenarios were compared for the hypothetical airport:

- *A baseline scenario using pre-existing data and*
- *An updated scenario including experimental data.*

The variability of the experimental data was used to define limits for the updated scenario; thus one is 95% confident that the hypothetical airport emissions fall between the upper and lower confidence limits.

The baseline scenario largely fell within these confidence limits. Even though some observed changes were big (e.g., ~194% for hydrocarbon emissions), the differences were not statistically significant.

A sensitivity analysis using EDMS/AEDT was performed to determine the potential effect of replacing existing emissions indices in the EDMS/AEDT database with those derived during the ACRP Project 02-54 sampling field campaign on computed emissions. For this analysis, the research team used the latest version of FAA's EDMS (Version 5.1.4.1). The FAA released the new AEDT model in May 2015, with the current release of AEDT2b (Service Pack 2) released December 22, 2015. As detailed on FAA's website, AEDT was addressing multiple bug fixes, including known issues with user-defined aircraft and emission reports. Given current and pending updates to AEDT, ACRP Project 02-54 focused on using the EDMS model for its comparison, because the results computed would be similar to those of AEDT.

To add new aircraft to EDMS, the *User-Created Aircraft* option was invoked in EDMS. This application allows a practitioner to create a user-defined aircraft; assign it a flight profile; designate other operational characteristics that have a bearing on emissions calculation; and, most significantly, input measured carbon monoxide (CO), hydrogen carbons (HC), nitrogen oxides (NO_x), and smoke number (SN) emissions indices that are divergent from available EDMS/AEDT information. Figure 4-3 is a screenshot of a user-created menu of available options for this function within EDMS/AEDT.

Similarly, to create a user-defined aircraft in AEDT, the user must copy data from an aircraft that already exists in the AEDT database and modify the emission indices under *engine emission coefficients* (see Figure 4-4) with the new data. Detailed instructions on how to create user-defined aircraft are presented in the *AEDT 2b User Guide*, December 2015 (Koopmann et al. 2015).

The sensitivity analysis was performed at the hypothetical GA airport at an airport fleet level (i.e., the full complement of GA aircraft operating at an airport with the full level of operations assigned).

Copyright National Academy of Sciences. All rights reserved.

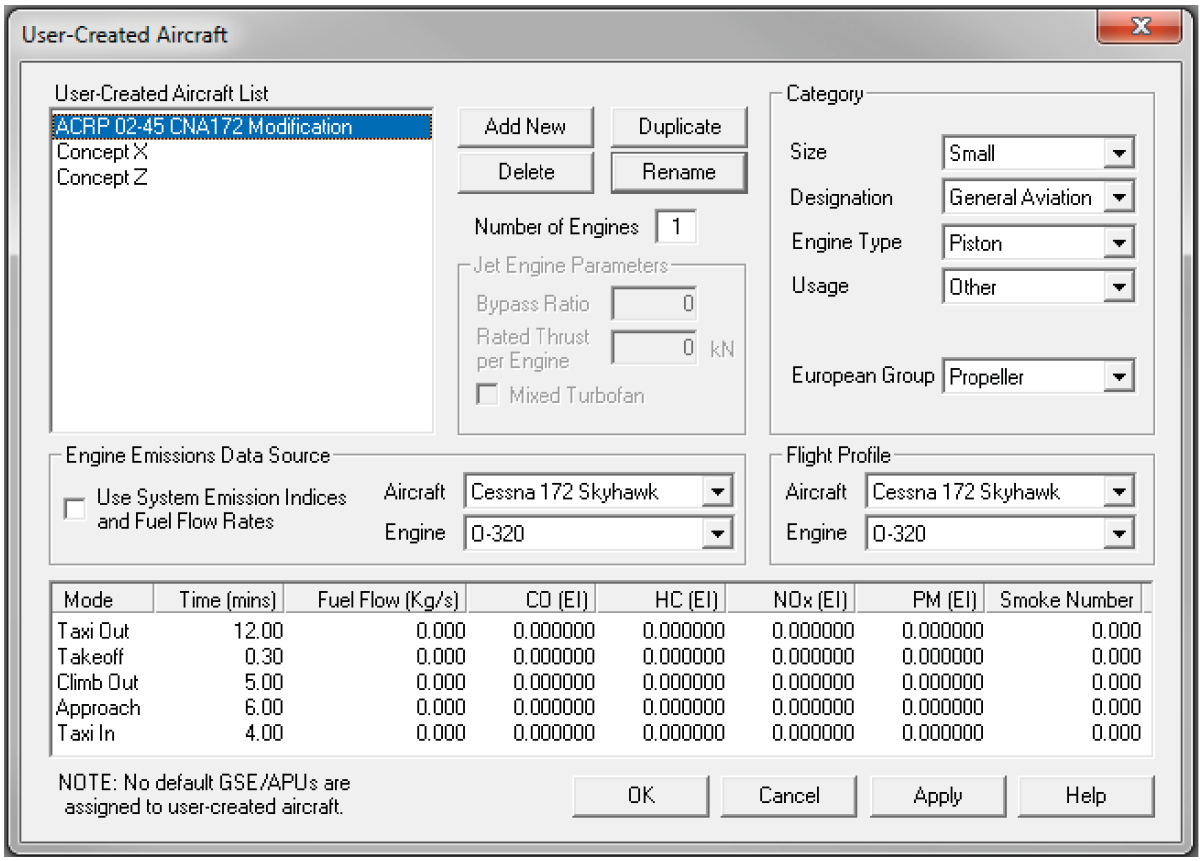

Figure 4-3. EDMS user-created aircraft modeling options.

For each aircraft replaced with a surrogate with derived emissions indices resulting from the ACRP Project 02-54 sampling field campaign, emissions were computed under three scenarios as follow:

1. **Baseline Scenario**: using EDMS/AEDT aircraft with its default/existing information,
2. **Updated Scenario (User-defined Averages)**: populating EDMS/AEDT with averages of the user-defined alternatives representing the refined data from the sampled field campaigns, and
3. **Updated Scenario (User-defined Upper Limits)**: populating EDMS/AEDT with upper limits of the user-defined alternatives representing refined data from the sampled field campaigns. For this analysis, the upper limit consisted of the 95% confidence interval estimate, which reflects a significance level of 0.05.

These emission inventories were produced and compared to assess the aggregate change in emissions on an aircraft/engine-specific level (i.e., aircraft operational modes). For example, it would be possible to disaggregate the results and attribute the change to a specific aircraft mode whose emissions indices for that specific mode substantially changed as a result of the research effort. For consistency and to focus on the effects of the new emission indices, all other standard EDMS/AEDT input data (e.g., operational times-in-mode for taxi/idle, take-off, etc.) were used. The default approach and climb-out times were based on standard ICAO/EPA data up to an altitude of 3,000 feet. Default taxi-in and out times of 7 and 19 minutes were also used.

To estimate the number of operations per aircraft in the Hypothetical Fleet, equal use throughout the year was assumed for each aircraft, because operational data is not publicly available. The total annual operations from 20 GA airports in the United States were averaged using data from FAA's Operations Network, giving an average of 97,192 operations (i.e., 48,596 landing/take-off (LTOs)) per year per airport. The number of operations of each aircraft was estimated based on its occurrence over the total averaged operations (Table 4-1) within the Hypothetical Fleet.

Copyright National Academy of Sciences. All rights reserved.

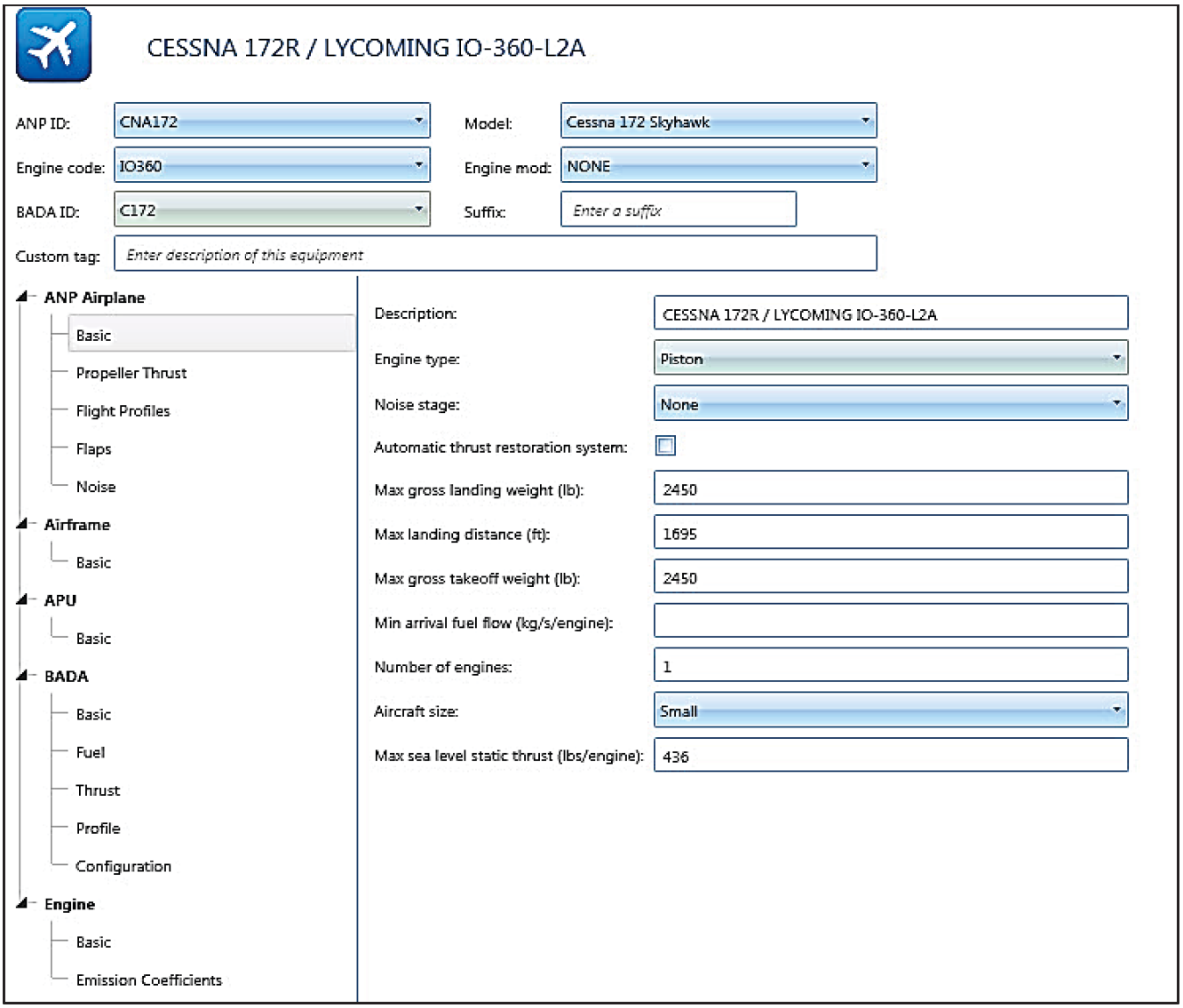

Figure 4-4. AEDT user-defined aircraft modeling options.

Baseline Scenario

Under the baseline scenario, the current EDMS/AEDT databases of GA aircraft engine emission indices were used to populate the scenario using the Hypothetical Fleet. EDMS was populated either with an aircraft/engine with an exact match to a sampled aircraft/engine or a surrogate based on similar aircraft type/weight and engine operational characteristics (i.e., emission coefficients and horsepower) from the EDMS/AEDT database. Table 4-2 (with additional values in Table L-1) lists the aircraft/engines sampled during the ACRP Project 02-54 field campaign and the corresponding surrogates used in EDMS/AEDT. Explanations for why each aircraft and engine assignment were chosen in EDMS are also listed. Substitutions were made by choosing an aircraft/engine with more conservative (i.e., higher) engine coefficients and/or higher aircraft weight.

Using surrogate GA aircraft/engines emission indices for aircraft not in EDMS databases has become the standard operating procedure (SOP) when using the model. Therefore, among the objectives of the ACRP Project 02-54 research was to show the need to expand this limited database of GA aircraft emission indices and provide model users with a greater range of aircraft/engine choices.

Copyright National Academy of Sciences. All rights reserved.

28 Exhaust Emissions from In-Use General Aviation Aircraft

Updated Scenarios

The updated scenarios examined consisted of (1) using averages of samples collected and (2) using the upper limits (within a 95% confidence interval) of samples collected:

- **Average Scenario**: Averages of each aircraft/engine sampled indices within each mode/thrust setting were entered into EDMS for comparison with the baseline scenario and
- **Upper Limit Scenario**: Upper limits were calculated as the 95% confidence interval and entered into EDMS for comparison with the baseline scenario. Some aircraft did not have sufficient data/number of samples for upper limits to be computed.

Under the updated scenarios, new GA aircraft engine emission indices derived from the ACRP Project 02-54 sampled field campaigns were added to the EDMS database using the model's User-Created Aircraft option (see Figure 4-3). Total PM mass emissions (tPMm) were the only measure of PM considered here. Additional parameters such as, but not limited to, the number of engines, aircraft/engine category, and flight profile were entered. The times in mode for each aircraft were left as EDMS default times. If a mode was not measured in the updated scenarios, the default values for that mode were kept. This process was repeated for each of the aircraft sampled in the field campaigns.

Results of the Sensitivity Analysis

Table 4-3 summarizes the emission inventory results (in short tons per year) when comparing the baseline scenario (EDMS default values) to the Updated Average and the Updated Upper Limit Scenarios, respectively. Only aircraft and ground support equipment (GSE) are reported, because auxiliary power units (APUs) are not present in the Hypothetical Fleet selected.

Table 4-3. EDMS/AEDT results comparison for baseline, average and upper limit scenarios (short tons per year).

Measure	Scenario	CO_2	CO	THC	NMHC	VOC	TOG	NOx	SOx	PM -10	PM -2.5	Fuel Consum-ption
Aircraft	Baseline	2,909	1,048	21	19	18	21	2	~1	3	3	922
	Updated Average	3,198	989	63	70	70	71	3	~1	~1	~1	1,014
	Updated Upper Limit	3,493	1,780	244	279	277	280	18	~1	2	2	1,107
GSE	Baseline	N/A	~1	N/A	0.1	0.1	0.1	0.3	<0.1	<0.1	<0.1	N/A
	Updated Average	N/A	~1	N/A	<0.1	<0.1	<0.1	0.1	<0.1	<0.1	<0.1	N/A
	Upper Limit	N/A	~1	N/A	<0.1	<0.1	0.1	0.2	<0.1	<0.1	<0.1	N/A
Totals	Baseline	2,909	1,049	21	19	18	21	2	~1	3	3	922
	Updated Average	3,198	990	63	70	70	71	3	~1	1	~1	1,014
	Updated Upper Limit	3,493	1,781	244	279	277	280	18	~1	2	2	1,107
% Difference (average)		10	-6	194	275	288	238	64	10	-66	-66	10
% Difference (upper limit)		20	70	1,046	1,391	1,447	1,235	861	20	-31	-31	20

Copyright National Academy of Sciences. All rights reserved.

When all aircraft results are averaged together, results comparing measured emission indices to the EDMS default values indicate that overall increases in emissions ranging from 10 to 288% are revealed for carbon dioxide (CO_2), total hydrocarbons (THC), non-methane hydrocarbons (NMHC), VOC, total organic carbon (TOG), nitrogen oxides (NO_x), sulfur oxides (SO_x), and fuel consumption. By comparison, CO is shown to decrease by approximately 6%, and PM by 66%. PM_{10} and $PM_{2.5}$ emissions are also shown, where PM_{10} is a measure of particulate matter mass that is smaller than 10 µm in diameter.

The results of the sensitivity analysis include more than the four emissions species input: EDMS has partitioned certain species into subcategories. For example, THC (or HC) has been used to calculate the values for NMHC, VOC, and TOG. This partitioning uses a set of factors built into EDMS that are chosen based on EPA guidance. Factors are different for turbines and for pistons. In a similar way to HC, PM_{10} emissions are used to determine $PM_{2.5}$. Investigating these factors for GA is one area for future research. In fact, as a part of this project, data was collected that would allow comparison of many different emission ratios (e.g., VOC/THC) and would help verify or redefine these partitioning factors. PM size measurements were also collected and show the partitioning of PM sizes. For example, piston engine PM sizes are typically smaller than 20 nm (0.02 µm), more than 100 times smaller than the cutoff for $PM_{2.5}$.

Figure 4-5 shows the results from this sensitivity analysis for four main emissions compounds. The solid bars are the baseline or updated scenario averages, while 95% confidence limits are shown with a thin capped line. The upper limits are significantly higher than the average values, because of the large variability of emissions for piston engines. In all cases except CO, the lower limits reach 0 (emissions cannot be negative). Figure 4-5 also demonstrates that only extreme changes in a GA airport's emissions will be statistically significant (true with 95% confidence). In fact, the large changes in the updated scenario are not statistically significant except for PM_{10}. The change in PM_{10} emissions is not surprising: the EDMS/AEDT data for piston engines all have the exact same PM emission factors, a sign that these are default values. Overall, piston engine emissions variability turns out to be much more important than the updates in individual emission factors.

The effect of emissions variability is important in a regulatory framework, because when the upper limit emission coefficients are used, all indices increase significantly, with the exception

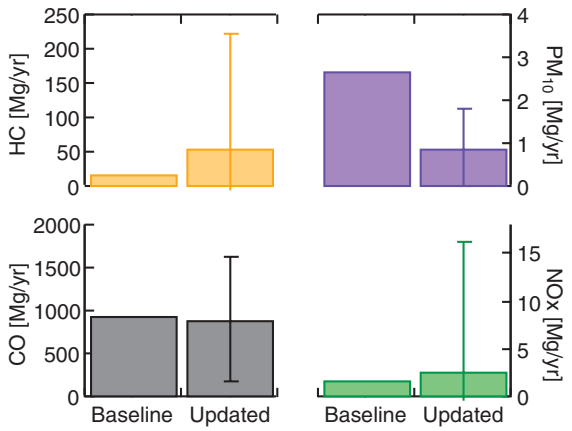

Figure 4-5. Results of the hypothetical airport sensitivity analysis showing baseline and updated results (solid bars), along with 95% upper confidence limits on the updated results. All emissions are given in mega grams per year (Mg/yr).

Copyright National Academy of Sciences. All rights reserved.

of PM, when compared to using EDMS default emission indices. The Upper Limit Scenario deliberately introduces values much higher than the Average Scenario and would overestimate results in 97.5% of cases. For example, VOCs increase by 1,447% when using the upper limits as compared to the default EDMS values.

These 95% confidence intervals are undesirably wide. They are also taken assuming a Gaussian distribution of emitters. As shown in Chapter 3, except for CO, those distributions are not Gaussian. The following section will investigate a more sophisticated approach toward getting confidence intervals on this sensitivity analysis. This approach aims to shrink these confidence limits and incorporate knowledge on the distribution shapes.

Overall, the results of this sensitivity analysis indicate that the effect of piston engine variability is much larger than the effect of updated emission indices. EDMS/AEDT aircraft/engine selections and default aircraft engine indices are representative, within our confidence intervals, of measured aircraft engine emission indices for many pollutants. This is despite seemingly large differences in total yearly emissions. The wide confidence limits highlight the need to improve and better use knowledge about the distribution of emitters, either through advanced statistical methods or with high numbers of repeat measurements of commonly used piston engines. The extensive engine mapping required to perform this analysis for a hypothetical GA airport further demonstrates the need to expand this limited database of GA aircraft and provide model users with a greater range of aircraft/engine choices.

Using Monte Carlo Methods to Improve Airport Emissions Estimates

The emissions at a hypothetical airport were simulated by sampling from the measured emission indices. This "Monte Carlo" approach is different from simply using the average indices for each aircraft and allows the variability of the results to come into play. The confidence limits in the final airport emissions were shrunk significantly.

Monte Carlo methods are a promising tool for pinning down yearly emissions burdens, as long as the input data (e.g., time in mode, large number of emission indices) are sufficient. Despite a large variability in emission indices, it is possible to constrain an airport's emissions tightly over time.

The sample of GA engine emissions produced in this research exhibits variability. It is difficult to forecast the overall uncertainty in using the average emission indices to compute a burden at an airport; traditional assumptions about normal distributions do not necessarily apply to this limited sample of engines coupled with their variable EIs. Here, the research team describes a Monte Carlo (MC) simulation that pits the variability in the EI data against the number of operations at the hypothetical GA airport. The basis of the Monte Carlo simulation will be to draw on the pool of EI data for each engine type described in Table L-1. To compute the airport emissions burden, the annual number of operations for each engine type will be summed with each LTO by drawing a random aircraft test point. In this way, all ACRP, EDMS, ICAO and FOCA data types are sampled. Figure 4-6 illustrates the procedure.

In the base case MC simulation, the variance of the fuel flow is considered to be Gaussian or normally distributed. The base times in mode are common for all operations and all engine/airframe types (see times in Figure 4-3). The base time in mode is modified by a factor from 0.5 to 2.0, using an asymmetric distribution centered on 1, so as to induce additional variability in the emissions burden. The simulation case "EDMS" uses only the EDMS engine types and a tabulation of those engine substitutions. The simulation case "EDMS + FOCA, FAA Aircraft Engine Emissions Database (FAEED), ACRP" combines all test data in the pool of emissions data to draw from, including the fuel flow rate data.

Copyright National Academy of Sciences. All rights reserved.

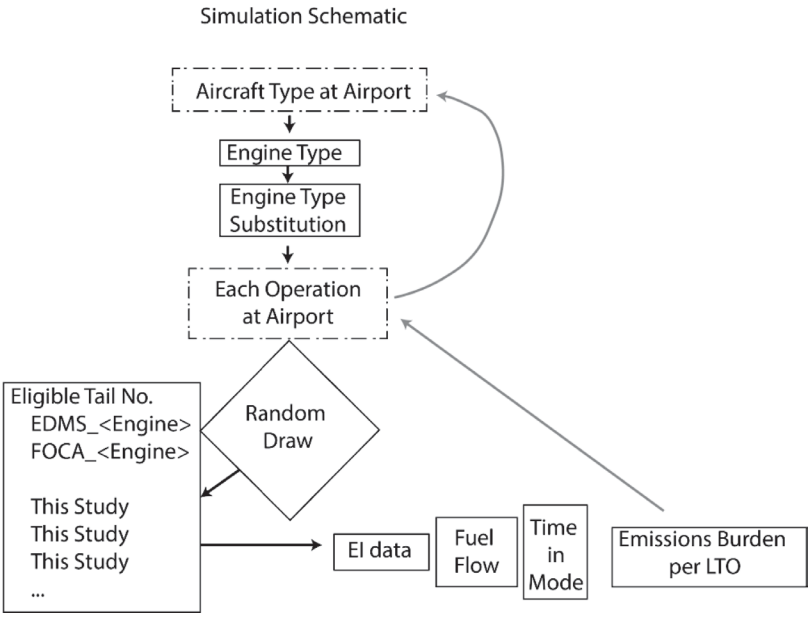

Figure 4-6. Schematic representation of the Monte Carlo simulation of total emissions burden at the airport. Many of these "annual" simulations are performed to deduce the distribution of emissions.

Figure 4-7 illustrates the differences observed in the net distributions of CO emissions per LTO. This figure is constructed by repeatedly drawing from the sample pool of emission indices until the results converge. The total CO burden to the airport is shown in grey for the baseline (left) and updated (right) scenarios. The individual contributions of the power states are shown in color. In this case, although the size of the sample pool has gone up by an order of magnitude, there is little change in the central value of the distribution (grey). This similarity means that the n = 2 CO emissions data points in AEDT/EDMS are representative of the larger n = 22 sample pool measured here. This result is expected because CO emissions are found to be Gaussian distributed (see Figure 3-6). Results from the emissions species HC and NO_x do not show this same

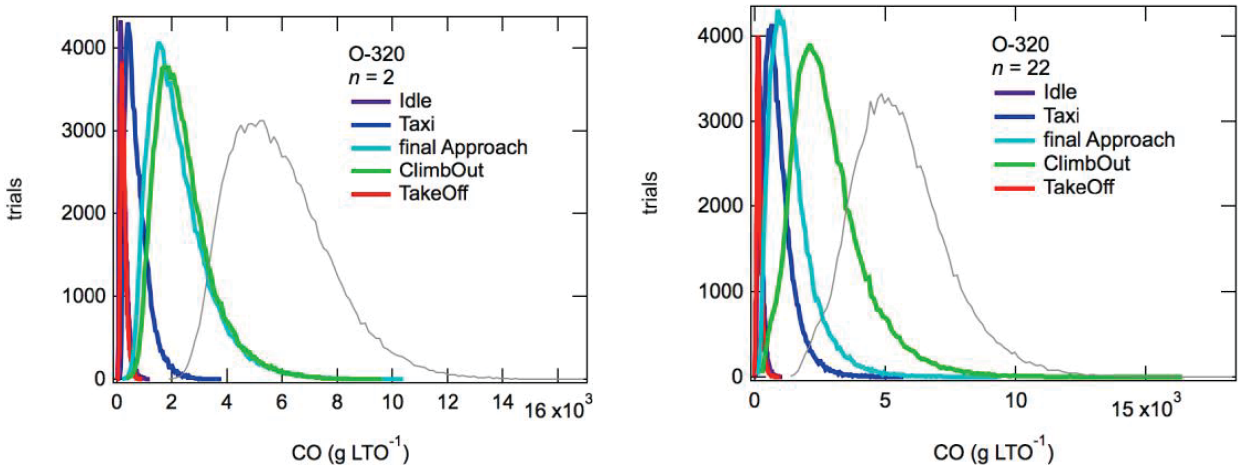

Figure 4-7. Distribution of CO emissions burden per LTO. The left hand panel is the EDMS only simulation result for numerous synthetic LTOs. The right hand panel includes EDMS with the test data from this project. The grey line is the distribution resulting from the sum of the LTO phases.

Copyright National Academy of Sciences. All rights reserved.

trend. Figure 4-7 also suggests the climb-out phase of the LTO is responsible for the greatest share of emissions.

Generating distributions of emissions by LTO state (and total) was repeated for the two engine lists used in the sensitivity analysis. Employing MC simulations this way does not account for any usage profile bias—all engines in the sample pool are sampled equally, which is unrealistic. The distribution of individual LTOs is likely dominated by professional activity at the airport (e.g., planes owned by flight schools). Nor will this MC simulation analysis account for potential ambient temperature or summer/winter fuel blend effects. The advantage of using this simulation approach is that it should empirically arrive at a distribution of emissions burdens indicative of the uncertainty in the source data. At this hypothetical airport, the large number of operations over the course of a year will tend to narrow the uncertainty in overall burden, approaching the mean value over the course of the year. For this reason, the weekly emissions were tabulated to retain some of the parent variability.

Figures 4-8 through 4-10 show the results for CO, HC and NO_x for the baseline EDMS and combined data scenarios.

The central values of these MC results can be compared to the results of the EDMS/AEDT analysis presented earlier. The same trend in CO emissions was observed in the AEDT-based sensitivity analysis, where total annual CO emissions burdens decreased slightly.

The comparison of the HC emissions trend observed in this analysis was also observed in the AEDT-based sensitivity analysis. There, the factor increase was about 3-3.3 depending on the particular class of hydrocarbons, which agrees with this alternative approach.

The NO_x comparison is not as good as either the CO or HC results. In that analysis, the baseline EDMS result of 2 short tons per year (st yr^{-1}) increased 50% to 3 st yr^{-1}. The MC analysis sees a much greater increase of 277%, when including all of the engine data. The underlying reasons for this disagreement are unclear.

Figure 4-11 shows the individual contributions of different power states to the total burdens for the updated scenario. These graphs reflect the trends discussed in Chapter 3: low power states like taxi and idle contribute most to HC emissions; high-power states like take-off and climb-out

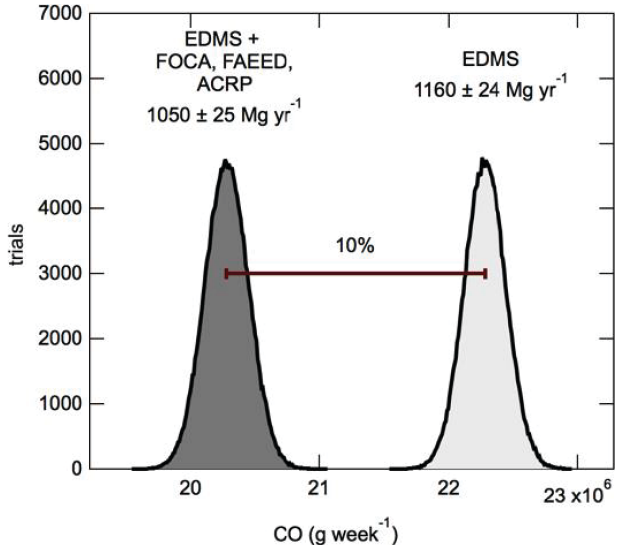

Figure 4-8. CO emissions burden change between the two scenarios.

Copyright National Academy of Sciences. All rights reserved.

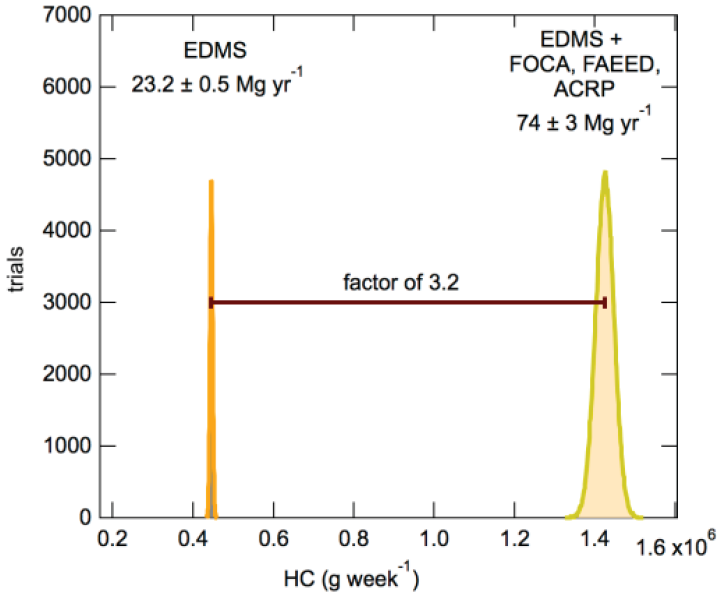

Figure 4-9. HC emissions burden change between the two scenarios.

contribute most to NO_x emissions. The pie chart for CO emissions looks similar to the pie chart for fuel burn, again reflecting the observation that CO emissions are relatively constant at all powers.

Although the trends in results are expected to be similar to the EDMS/AEDT approach, the MC method should yield significantly different results for the uncertainties. Figure 4-12 compares the emissions burdens for the two approaches. The EDMS/AEDT approach uses simple 95% confidence limits. These limits are many times larger than the converged MC uncertainties.

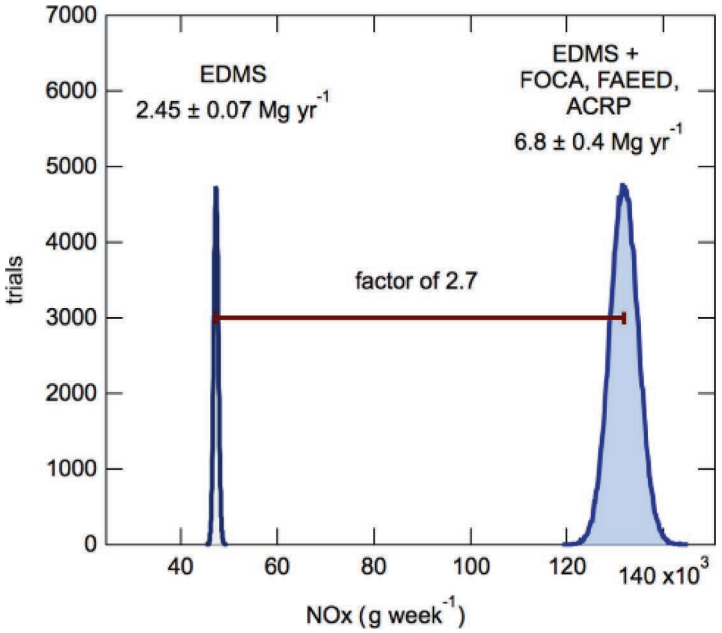

Figure 4-10. NO_x emissions burden change between the two scenarios.

Copyright National Academy of Sciences. All rights reserved.

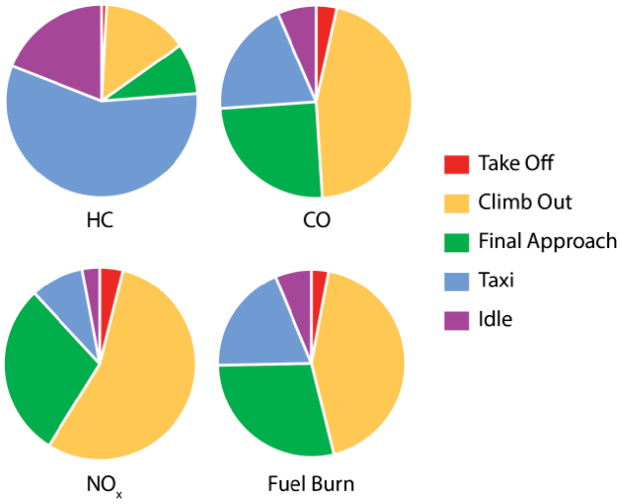

Figure 4-11. Partitioning of emissions burden by power state.

Indeed, one of the reasons why the MC results have such small confidence limits is due to the large number of operations at the hypothetical airport. Even when running a mere week's worth of operations, the variability in the EIs for the datasets is statistically collapsed.

This significant shrinking of the confidence limits is very promising. It means that, despite a large variability in emission indices, it is possible to constrain an airport's emissions tightly over time. There are important caveats to this method, however—the test pool of emission indices must be representative of the airport's fleet. The more measurements available, the more certain that the MC method is converging to a real answer. In this case, even the large number of measurements done (e.g., 15 separate Lycoming O-320 engines) is not very big compared to the

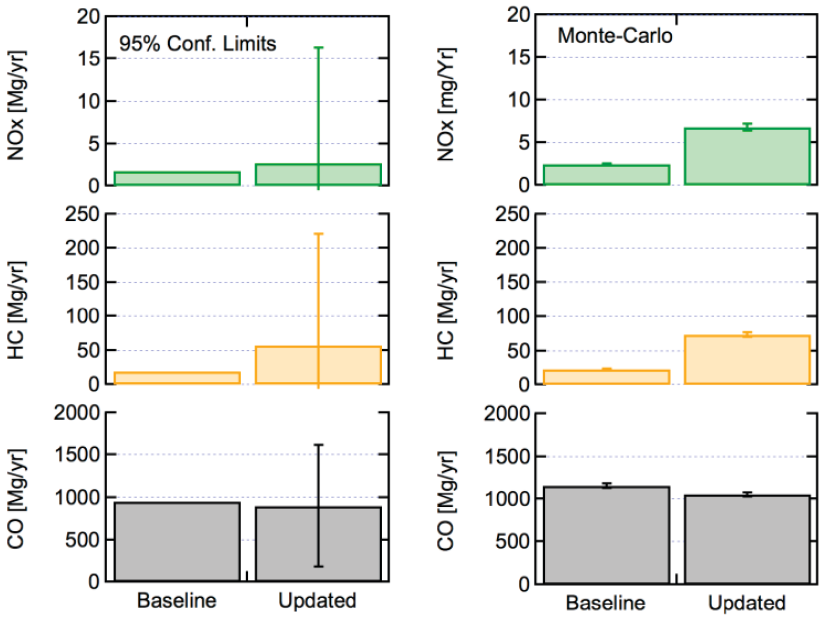

Figure 4-12. Comparison between EDMS/AEDT and Monte-Carlo estimates of a hypothetical airport's emissions. Quantities of pollutant are reported in mega grams per year (Mg/yr).

Copyright National Academy of Sciences. All rights reserved.

number of operations to be simulated (e.g., over 20,000 operations). Times in mode may also introduce a significant bias if they are considerably different from the defaults, and it would be valuable to have real operational data to verify this assumption.

The results of this analysis suggest measuring additional emission indices and constructing representative distributions of emitters would be valuable. Such measurements would need to sample large numbers of aircraft (thousands, not dozens) in an automated way in the course of their normal operations. Getting a better handle on the true shapes of the emissions distributions will result in more certainty in the accuracy of airport emissions estimates. Monte Carlo methods are well suited to use such distributions of emitters and assess their effect on airports.

Copyright National Academy of Sciences. All rights reserved.

CHAPTER 5

Other Parameters Affecting Emissions

Previous chapters have discussed the observed variability in emission indices between repeat measurements of the same engine. In doing these measurements, the research team discovered a complex landscape of conditions and variables that all affect the measured emissions from GA aircraft. Because these conditions generally get lost as the data is rolled into the averaged emission indices tables, in this chapter, the research team examines some of these parameters in detail. These conditions account for some of the variability between measurements. More important, such knowledge enhances understanding of GA aircraft and can highlight places where EDMS/AEDT-style emission inventories may gloss over details.

Pilot Mindset on Fuel Mixture

During the engine tests, pilots were asked to operate their engines as they usually would. Two "schools of thought" became apparent regarding fuel/air mixture in carbureted piston engines:

- Full-rich at all times
- Lean it out whenever possible

The full-rich at all times mindset was common among many of the mechanics and pilots who operated their aircraft during the test. The mixer is pushed all the way forward, giving a maximally rich fuel/air mixture, known as "full-rich." Advantages and disadvantages are presented below.

Advantages:

- **Engine remains cooler at all times**. Excess fuel leads to incomplete combustion, which produces less heat. Overheating was of particular concern during the ground tests (where there was reduced air flow for cooling). The engine is kept cool by deliberately reducing the efficiency/adding more fuel than needed. The theoretical engine temperature eventually begins to decrease again with extremely lean operation, and some aircraft manuals recommend operation in this region (FOCA 2007a, b) (none of the aircraft that the research team encountered).
- **Simple**. For beginner pilots or those not used to operating a given aircraft, full-rich operation requires less fiddling back and forth between the throttle (propeller RPM) and mixer (fuel/air mixture) to achieve a stable combustion state with no cylinder misfires.
- **Safe**. An engine running full rich will not stall. Pilots may not want to take risk stalling, even at cruise altitudes.

Disadvantages:

- **Inefficient**. A significant amount of fuel goes unburned.
- **High CO and HC emissions**. The research team estimates that at least 8% of the potential thermodynamic efficiency is not being converted to heat to move the piston and generate work.

Copyright National Academy of Sciences. All rights reserved.

The lean it out whenever possible mindset was usually held by pilots with newer training, and particularly pilots operating aircraft with gauges showing the exhaust gas temperature (EGT) and cylinder head temperature (CHT) for one or all of the engine cylinders. When available, EGT can be used to determine the optimal mixture for efficiency. One 1970s era aircraft had even been retrofitted with an EGT gauge and sensors for this purpose. The research team also worked with a flight school that focused on retraining pilots wishing to increase their fuel economy.

Pilots of both mindsets run the engine at full rich during take-off and final approach, when the aircraft is close to the ground and stalling can be disastrous. Although the pilots may consider a given state "lean," the true stoichiometry of the fuel mixture is likely still rich compared to the ideal mixture.

Advantages:

- **Longer engine life**. Operating with a lean mixture will prevent deposits in the engine.
- **Better fuel economy**. Lean combustion consumes less fuel for the same power.
- **Lower emissions of HC and CO**. More fuel is converted all the way to CO_2.

Disadvantages:

- **Requires more pilot experience**. EGT and CHT gauges must be monitored, if available, and the throttle/mixer adjusted accordingly. If no such instruments are available, the pilot must be able to "feel" when the mixture is getting too lean by the sound and vibrations of the engine.
- Too lean a mixture will cause misfires in the engines and the **aircraft will eventually stall**.
- **Higher NO_x emissions**. Higher combustion temperatures produce more NO_x.
- Requires that **all cylinders have comparable combustion properties**. If cylinders do not follow the same EGT temperature trends for the same mixtures, running lean on cylinder 1 could cause overheating in cylinder 6, and so on. This can decrease engine lifetime.

These approaches largely determined the richness/leanness of the measured mixing states, because pilots and mechanics were, for the most part, averse to changing the mixture for concern about the risk (real or perceived) of engine health. Given that cruise is not considered in airport LTO emissions calculations and that take-off and final approach are performed at full rich by all piston engine pilots, taxi and idle emissions probably will be the most affected by these differences in aircraft operation. Most older piston engine aircraft, lacking fuel injection or EGT/CHT technology, probably will be operated at or near to full-rich mixtures at all times, given the challenges and risks involved in lean operation.

CO_2 Carbon Fraction as an Indicator of Combustion

CO_2 carbon fraction is the most direct indicator of engine operation. CO_2 carbon fraction describes how much fuel carbon is completely converted into CO_2. In Equation 5-1, TotalC = CO_2 + CO + THC, and this ratio is computed directly as a side effect of computing the emission index. A CO_2 carbon fraction of 1 indicates ideal combustion where all fuel carbon is converted into CO_2.

$$CO_2 \text{ carbon fraction} = \frac{CO_2}{TotalC} \qquad \text{Eq. 5-1}$$

In Figure 5-1, CO_2 carbon fractions for individual test points are plotted as a function of the percent of maximum achieved propeller RPM. Individual aircraft are shown as different marker types and colors, with common engines having the same label in the legend. Figure 5-1 shows the great range of measured fractions. Very few data points exceed CO_2 carbon fractions of 0.8.

Copyright National Academy of Sciences. All rights reserved.

38 Exhaust Emissions from In-Use General Aviation Aircraft

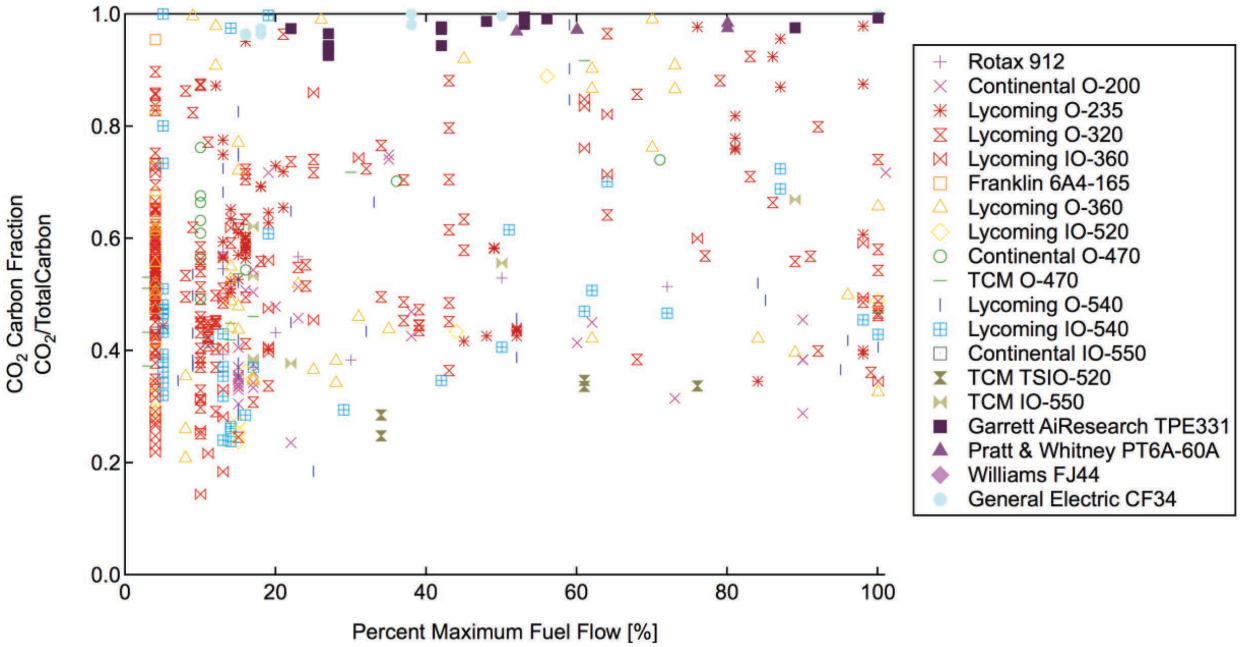

Figure 5-1. CO_2 carbon fraction vs. % maximum RPM for individual test points.

Of those data points, most belong to turbofan engines: the Garrett AiResearch, Pratt & Whitney Canada, Williams and General Electric engines.

Earlier the research team showed that piston engines produce a significant amount of CO in all engine states. A measure of fuel oxidation can be devised to include both CO_2 (complete oxidation of fuel carbon) and CO ("halfway" oxidation of fuel carbon). Plotting this oxidized carbon fraction vs. percent max RPM (Figure 5-2) results in higher fractions than in Figure 5-1, indicating that the cause of the low CO_2 carbon fractions is the high amount of CO. With this

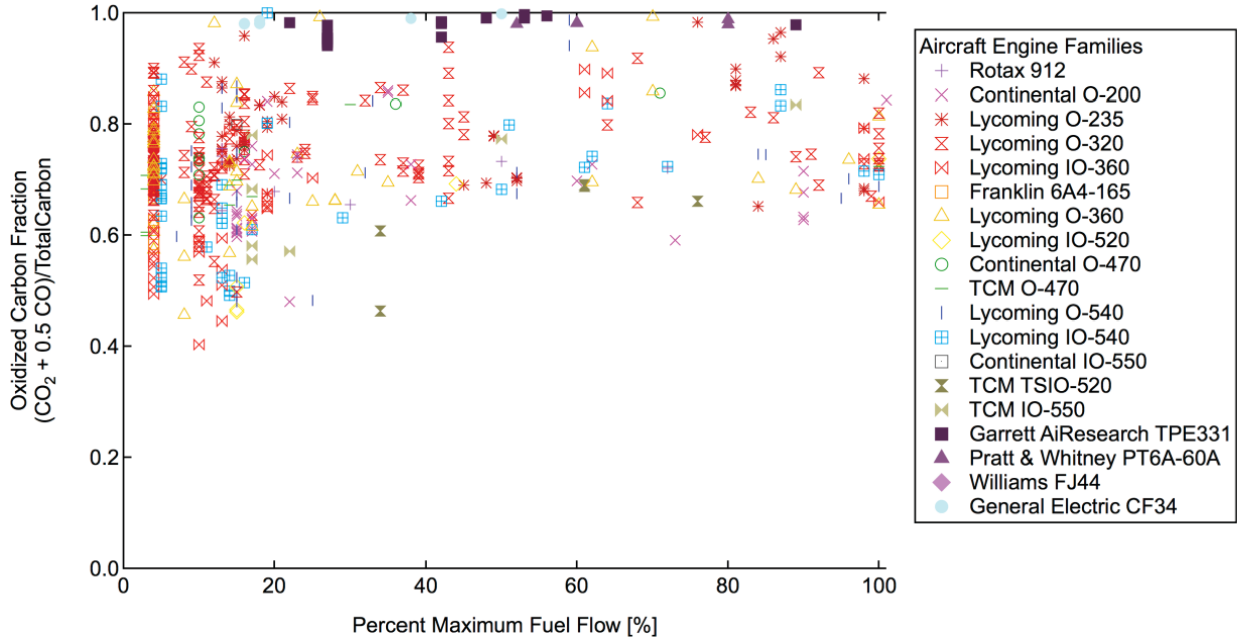

Figure 5-2. A measure of carbon oxidation vs. % max RPM for individual test points.

Copyright National Academy of Sciences. All rights reserved.

Table 5-1. Comparative loss of thermal potential from combusting to CO instead of CO_2.

	CH_2 +	O_2	->	CO	$+H_2O$	
$\Delta H_f(298)$	93	-		-26.4	-57.8	-177 kcal/mole
$\Delta S_f(298)$	46.3	49		45.1	47.3	-2.9 cal/mole/K
$\Delta G_{rxn}(298)$						=-176 kcal/mole
	CH_2 +	3/2 O_2	->	CO_2	$+H_2O$	
$\Delta H_f(298)$	93	-		-94	-57.8	-244.8 kcal/mole
$\Delta S_f(298)$	46.3	49		45.1	47.3	-23.6 cal/mole/K
$\Delta G_{rxn}(298)$						= -237.7 kcal/mole

figure, one starts to recover a curved shape to the data, with very low and very high-powered engine states operating at generally reduced conversion efficiencies of fuel carbon to oxidized carbon and intermediate engine states operating at higher conversion efficiencies.

One key difference between the emissions from aviation piston engines and turbofan engines is the ratio of carbon monoxide to carbon dioxide (CO/CO_2). With the turbofan engine, aside from the near-idle engine condition, the thermodynamic efficiency is very high. With aviation piston engines, the observed carbon monoxide emission index is ~ 500 – 1200 g CO/kg fuel. Relative to the CO_2 EI of 3160 g/kg, this is a more significant portion of the combustion carbon than is typical of turbofan engines. (Aviation piston engines are operated differently from ground vehicle engines, with only the former having highly elevated CO emissions.)

Using the combustion of CH_2 as a proxy fuel, one can evaluate the loss of potential thermal energy by producing CO instead of CO_2. In Table 5-1, the net loss of heat energy potential from the combustion inefficiency is bounded at ~25% on a per carbon basis. Thus, when one quantifies an emission index of CO of ~ 1000 g/kg fuel, this equates to ~30% of the combusted carbon not going to CO_2 and the combined effect is a basic inefficiency of ~ 8%.

Thermal NO_x and Rich vs. Lean Combustion

In urban photochemistry, the NO_x species (predominantly NO and NO_2) undergo transformations that lead to the production of ozone. At lower altitudes, ozone is a direct health hazard and is the key component associated with the observation of modern smog. NO_x compounds are only part of the system of reactions that lead to ozone production. In many regimes, the balance of various trace level chemical species is termed, "NO_x limited." This prompts the adoption of NO_x control or emissions limits to mitigate degraded air quality.

The ACRP Project 02-54 research sought to quantify the emissions rate using two factors: (1) fuel flow rate (commonly expressed as gallons per hour) and (2) the fuel-based emission index (determined by the observed enhancement of the pollutant in the exhaust relative to the sum of all forms that fuel carbon can take). Combustion of fossil fuel hydrocarbons in the engine produces no change in number of carbon atoms, but changes the molecules in which they are found. The research team used this conservation principle in determining the emission index.

The three elements that describe the flame characteristic of the combustors that are subject of this research are typically piston driven, aviation gas burning, and pre-mixed fuel to air. This is in contrast to the commercial aviation engine type, commonly a high-bypass ratio turbine engine. The emissions characterization framework, with engine states in the landing take-off cycle (LTO) exhibits large contrasts in *both* the fuel flow rate and the fuel-based EI values. **The NO_x emission indices in general aviation have relatively less sensitivity to the engine state**

Copyright National Academy of Sciences. All rights reserved.

40 Exhaust Emissions from In-Use General Aviation Aircraft

(or named LTO mode) and greater dependence on the air-to-fuel ratio (or rich vs. lean combustion). Although this is a broad generalization, the contrast is drawn from the differences seen between piston motors and turbofans.

This section illustrates this point by examining a measurement of the NO_x emissions at a named engine state at two different fuel-to-air ratios. However, the basis for this comparison requires a brief discussion of the actual combustion properties that lead to the production of thermal NO_x during combustion.

Combusting fossil fuel produces heat and gas expansion in the piston manifold to produce work. Ideally, combustion runs to completion and the only products are CO_2 and H_2O. This is shown in the chemical reaction sequence below, where the consumed number of molecular oxygen (n) is dictated by the carbon-to-hydrogen ratio in the fuel (expressed here as x and y).

$$C_xH_{2y} + n\,O_2 \rightarrow\rightarrow\rightarrow x\,CO_2 + y\,H_2O$$

The idealized chemical schematic holds that the yields of CO_2 and H_2O are matched to the fuel content of carbon and hydrogen. In reality, combustion does not match the ideal reaction scheme because it does not account for other forms of fuel carbon. When combustion does not proceed to the ideal completion, the stable product carbon monoxide, CO, is created. As a result, a useful metric for evaluating the combustion efficiency of the system is the CO/CO_2 ratio observed in the exhaust gas. The less-ideal expression is depicted in the chemical scheme below that now accounts for some combustion efficiency "slip" of ideal CO_2 emerging as CO and HC (sum of all other fuel hydrocarbons).

$$C_xH_{2y} + n'\,O_2 \rightarrow\rightarrow a\,CO_2 + b\,CO + c\,\Sigma\,HC + y'\,H_2O$$

NO_x is functionally defined as the sum of reactive oxides of nitrogen, which in the context of emissions is adequately approximated as the sum of NO and NO_2. Molecular oxygen is the needed oxidant to carry the combustion, but it is only present by volume in air at ~20%. Most of the air volume is composed of molecular nitrogen (N_2). NO is produced at high temperature combustion when there is enough energy to break the strong triple bond present in N_2 (Zeldovitch 1946). There is very little organic nitrogen in the fossil fuel source and the effective combustion temperature and time spent at high temperature are the drivers for producing NO_x.

During the engine test depicted in Figure 5-3, the pilot operated the engine according to the test protocol. The test sequence was defined by the canonical named engine states (e.g., idle, taxi, take-off). The final test condition, however, involved a repeat of the engine revolution speed and fuel flow rate associated with cruise, but with additional air added to the combustion mixture. Leaning the fuel mixture is anecdotally known to result in greater EGT. This is the symptom of elevated combustion temperature in the various pistons. In Figure 5-3, the CO/CO_2 observed in the lean-cruise test is lower than in the rich-cruise (the black and red tracers are on top of each other in the rich-cruise, but black, CO, is lower than red, CO_2, in the lean-cruise). This suggests that the combustion is proceeding more efficiently. With the increase in efficiency, the temperature is also increasing, thereby producing more NO_x.

Transient Emissions Are Negligible

In this research, a transient of a GA engine is defined as a deliberately included variation of engine operation from one steady-state condition (e.g., idle or approach) to another. The accurate quantification of the steady-state conditions of engine operation and emissions is necessary

Copyright National Academy of Sciences. All rights reserved.

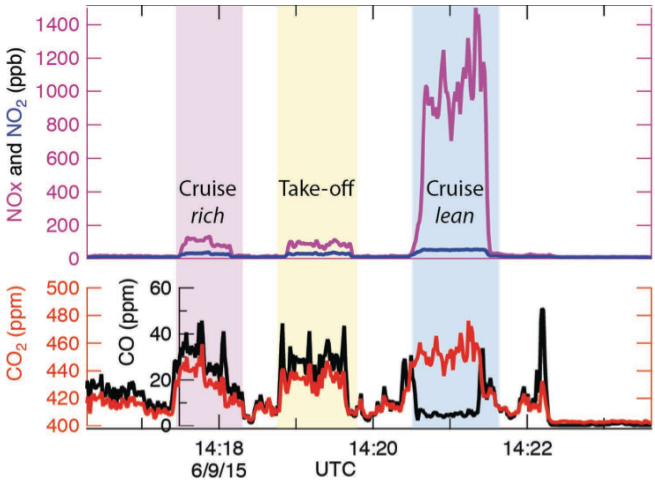

Figure 5-3. NO_x and combustion carbon time series. The upper panel depicts the total NO_x and specific NO_2 in parts per billion by volume during an engine test. The lower panel charts the matching time series of CO_2 and CO. Three particular engines states are identified in the pastel time periods: rich-cruise, take-off and lean-cruise.

for the investigation on GA emissions. The aviation industry has recognized that the operating conditions within each component also need to be understood when moving between steady-state conditions. The determination of gas and PM emissions at engine transient conditions may involve different methods of instrumentation and analysis from the steady-state measurements.

During field measurements, the research team observed engine transient events as the pilots were adjusting engine operating parameters such as fuel/air ratio and engine throttle. Inspection of the time series in such engine tests reveals that both NO_x and THC emissions are sensitive to transient events in the engine. This section aims to evaluate the sensitivity of the total LTO burden to transient emissions.

A sample aircraft (Unique ID 6, Continental O-200-A) was examined to assess the magnitude and effect of transient emissions. The first and most important transient observed was the startup transient during engine start (Figure 5-4). The transient was most evident as an increase in PM emissions (e.g., APC and EEPS traces, pink and brown) along with a slight increase in HC compared to the steady-state idle condition. The effect of startup emissions on commercial aviation was investigated in the research that resulted in *ACRP Report 63* (Herndon et al. 2012).

Other transients were observed for this aircraft. A transient from take-off to idle showed emissions of NO_x dropping significantly during the transient, with slight increases in acetylene and other hydrocarbons (including HC). A transient from approach to idle, on the other hand, showed increases in EI for all species, except NO_x. These and other transient observations show that the exact nature of transient emissions is highly dependent on initial conditions.

To assess the burden of these transient emissions, LTO emissions were calculated. Figure 5-5 shows two LTO emissions burdens graphs, where the colored area under the rectangles indicates the relative contributions of each state to emissions. Times in mode were chosen as in Table 3-1 with each transient lasting 10 seconds, except for the startup transient, which lasted 30 seconds. The left-most graph shows emissions without transients; the right-most graph shows emissions

Copyright National Academy of Sciences. All rights reserved.

42 Exhaust Emissions from In-Use General Aviation Aircraft

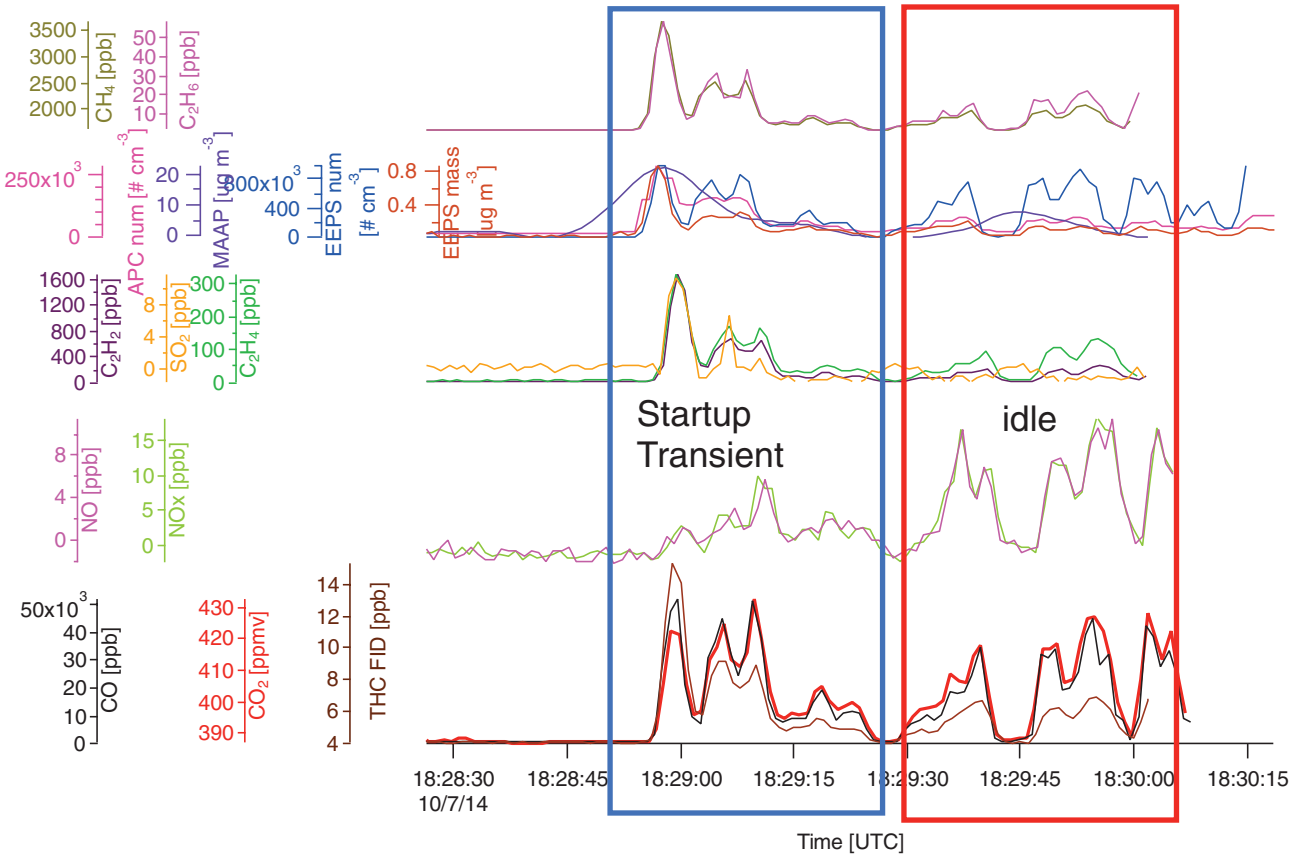

Figure 5-4. Changes in emission signatures between the startup transient and the* idle *state.

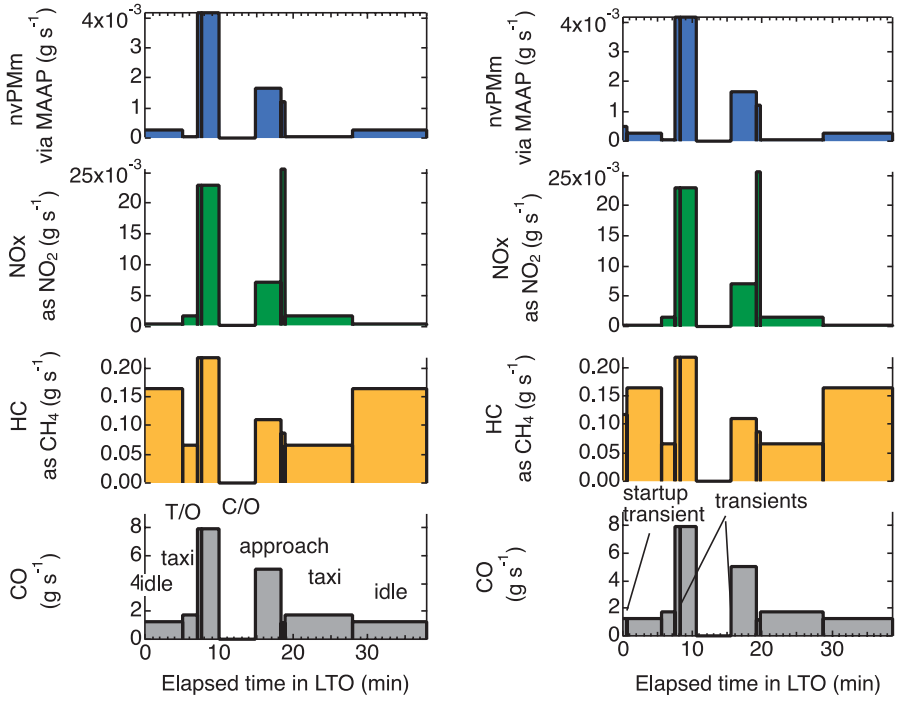

Figure 5-5. Emissions burdens for a sample LTO cycle with* (right) *and without* (left) *the effect of transient emissions.

Copyright National Academy of Sciences. All rights reserved.

Table 5-2. Impact on LTO burden of aircraft N7482G from transient emissions.

		HC	CO	NOx	nvPMm (MAAP)
		g/LTO	g/LTO	g/LTO	g/LTO
N7482G	Continental O-200-A	255	4735	7.43	1.391
Increased emissions due to transients		+1	+14	+0.01	+0.006

with the addition of transients. Examination of these figures shows that the effect of transient emissions on the LTO burden is negligible. In fact, the duration of the transients were so short that only the startup transient is visible. Table 5-2 summarizes the magnitude of these transient emissions and compares them to the total burden without transients. The contribution to the total is negligible, only 0.3% of the totals at most.

Ambient Conditions

The research team investigated the influence of ambient temperature variation on HC emissions by plotting emission indices versus temperature. Measurements were made in spring and autumn to limit the effect of temperature variations. The lowest ambient temperature observed during a piston engine test was 283.6 °K and the highest was 297.0 °K; the ambient barometric pressure was between 100.4 and 102.7 kPa.

Within the small range of barometric pressures, no effect on EI was observed. Ambient temperature varied somewhat more widely. Figure 5-6 presents correlation plots of CO and HC emission indices from measured piston aircraft engines vs. ambient temperature. Red markers correspond to measurements at idle condition and blue markers to measurements at T/O. A linear fit was performed to the data, and the slope (m), intercept (b), and coefficient of correlation (R^2) are reported. Note the poor correlation observed for all cases, with coefficients of correlation of $R^2 < 0.18$; a "good" correlation would have an $R^2 > 0.75$. These R^2 values mean that temperature effects are not important within the observed temperature range. This is due to the dual effect of variability in emission indices and the limited temperature range

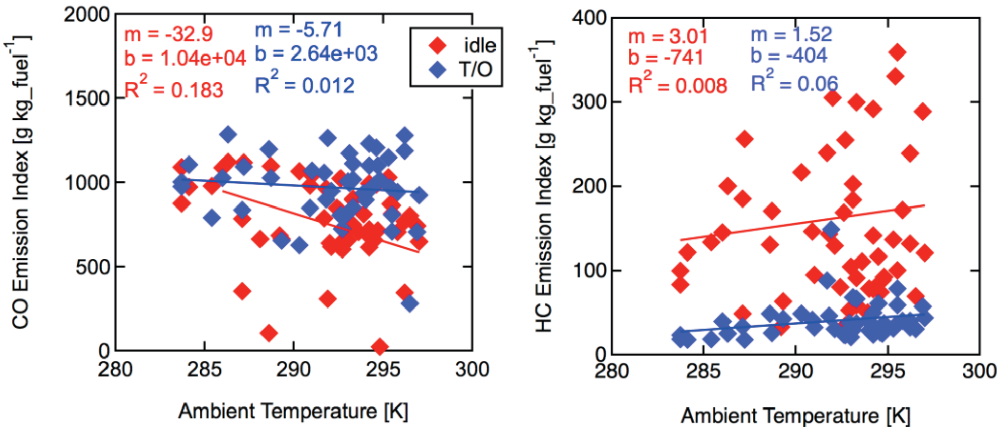

Figure 5-6. Correlation between emission index and temperature for piston engine CO and HC emissions. The slope (m), intercept (b) and coefficient of correlation (R^2) are shown for each fit. Idle and T/O power states are shown.

Copyright National Academy of Sciences. All rights reserved.

44 Exhaust Emissions from In-Use General Aviation Aircraft

sampled. A change in emission indices for measurements taken at more extreme temperatures or barometric pressures would be expected.

Previous studies also investigated the effect of ambient temperature. Appendix 3 of the FOCA report (FOCA 2007b) states that hotter ambient temperatures result in richer running engines. Though correlation is very poor for the research team's results, this is consistent with the data in Figure 5-6. Furthermore, FOCA recommends using temperature effects of 0.016 g HC per kg fuel per K and 3.1 g CO per kg fuel per K to correct emission indices taken at non-ambient temperatures (FOCA 2007c). These FOCA values are taken from data spanning a 30 Kelvin temperature difference, much larger than the ~13 degree difference sampled here. Studies have also been done on the effect of ambient conditions on jet engine emissions, both for PM (Gleitsmann and Zellner 1998) and for HC emissions (Herndon et al. 2012).

Fuel Additives

Numerous aircraft tested exhibited unusually high toluene emissions and their fuel also revealed elevated levels of toluene compared to fuel samples pulled from fixed-base operator (FBO) supplies.

Figure 5-7 compares the burden of HC per LTO cycle to the burden of toluene only. Points are marked with the unique ID of the aircraft. Several high-toluene aircraft populate the upper part of the graph (e.g., aircraft 26) while most aircraft are clustered at modest toluene burden levels. The presence of toluene does not correlate to higher total HC burdens.

The observation of toluene in both fuel and exhaust suggests that the aircraft owners were using a non-traditional fuel such as premium unleaded (Mogas) or a commercially available fuel additive. Mogas can be eliminated because it contains a mixture of aromatic compounds (i.e., benzene, toluene, xylene). The research team believe the source of the toluene can be traced to a fuel additive called Alcor TCP. TCP or tricresyl phosphate is used to help alleviate the condensation (fouling) of lead onto the spark plugs and valves of older low-compression piston aircraft engines. The only commercial AVGAS is 100 Low Lead, which uses tetraethyl lead to achieve its octane rating. Combustion of tetraethyl lead produces lead oxide, which is not volatile at normal

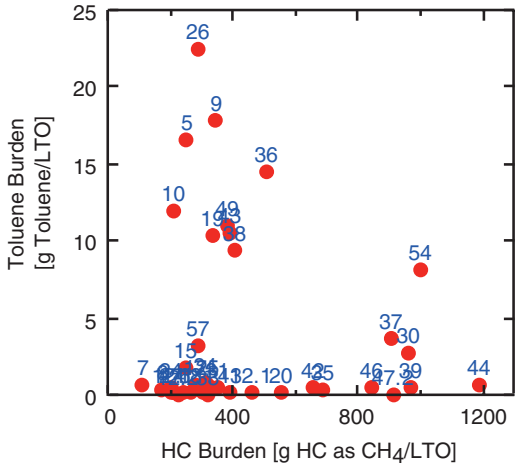

Figure 5-7. Toluene emissions burden per LTO compared to hydrocarbons emissions burden per LTO for measured aircraft.

Copyright National Academy of Sciences. All rights reserved.

Table 5-3. MSDS composition information for Alcor TCP fuel additive.

3. COMPOSITION/INFORMATION ON INGREDIENTS		
Chemical Name	**CAS No**	**Weight-%**
Toluene	108-88-3	35-45
Petroleum Distillate	64742-88-7	35-45
Tricresyl Phosphate	1330-78-5	10-20
Isopropyl alcohol	67-63-0	0-10

engine exhaust temperatures. To combat this problem, dibromoethane is added to 100 LL. During combustion, the lead reacts with the bromine, thereby forming $PbBr_2$, which is volatile and passes through the exhaust system before it condenses. The aerosol mass spectrometer confirmed the presence of lead and lead bromide in the particle phase.

Based on information found on the Internet (http://www.pipercubforum.com/marvel.htm), older low-compression piston aircraft engines at taxi/idle speeds have engine exhaust temperatures below the volatility limit of lead bromide and suffer lead fouling. Two products, Marvel Mystery Oil and Alcor TCP, show up on pilot forums as products that can minimize lead fouling. Analysis of a sample of 100 LL doped with Marvel Mystery Oil using the PTR-MS did not result in any apparent change in the amount of toluene observed. Marvel Mystery Oil contains a small amount of chlorinated hydrocarbon, which could produce lead chloride, a product that is more volatile than lead bromide. A sample of Alcor TCP was not available for analysis, but the material safety data sheet (MSDS) for this product lists toluene as a major ingredient (Table 5-3). All pilots and other aircraft operators were asked about fuel additives. All reported no such use. The research team cannot explain the high levels of toluene observed if no fuel additives were present. This discrepancy underscores the importance of determining how widespread the use of fuel additives is in the GA sector.

Hydrocarbon Emissions from GA Are Primarily Unburned Fuel

The exhaust gas composition of GA engines is expected to reflect the effects of operating under excess fuel (rich combustion) conditions. Because these engines operate far from their stoichiometric fuel-to-air limit, it is logical to assume that a significant fraction of the HC measured by the flame ionization detector instrument consists of unburned fuel. In this section, the research team examines this assumption by examining the fraction of the fuel carbon that can be accounted for by the individual species that were directly measured (e.g., CH_4, C_2H_2, C_2H_4, C_2H_6, HCHO, CH_3CHO, acetone, C_6H_6, C_7H_8, C_8H_{10}, and $C_{10}H_{8)}$. With the exception of toluene (C_7H_8), which is present as a fuel additive (previous section), all of these components are combustion byproducts. Although this analysis cannot definitively identify the HC components that were not directly measured, one can conclude through comparison with automotive piston engine exhaust studies that the unidentified portion of the exhaust is primarily composed of unburned fuel.

Figure 5-8 shows histograms of the fuel carbon accounted for by the individual components measured, one representing the total and another with the total excluding the toluene contribution, which is present at considerable quantities only when it is present in the fuel. Figure 5-8 illustrates several important observations. First, the measured components only account for a small fraction (10 to 20%) of the total. Second, the measured fraction is highly variable, with at least some of the variability arising from the presence of the toluene fuel additive. The influence of toluene provides direct evidence that unburned fuel exists in significant quantities within the exhaust. Automotive piston engine exhaust studies (Schauer et al. 2002) without emission control systems show that the exhaust composition is strongly correlated to the fuel composition, where

Copyright National Academy of Sciences. All rights reserved.

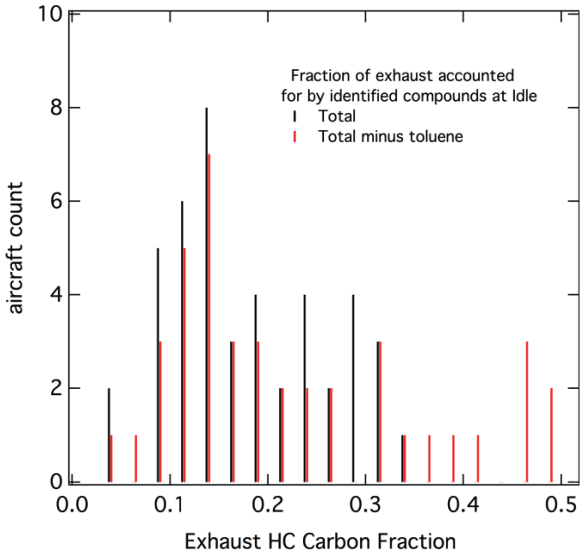

Figure 5-8. Fraction of exhaust UHC accounted for by the individual measured components under idle power condition.

approximately 80% of HC exhaust consists of the same compounds present in the fuel in nearly the same distribution. The remaining 20% of the HC exhaust consists of decomposed fuel in the form of small hydrocarbons such as acetylene and partially oxidized material like formaldehyde. Tallying the five most prevalent non-fuel components, formaldehyde, acetylene, ethylene, methane and acetaldehyde in Schauer's study accounts for 12.5% of the total HC exhaust carbon, which is comparable to the results observed in Figure 5-8 for most of the aircraft studied here. This result is not surprising, given that GA and vehicle engines both employ spark-initiated piston engines. It therefore stands to reason, by comparison, that the composition of the bulk of the unidentified GA HC resembles that of AVGAS 100LL fuel.

In assessing the effect of HC emissions at a GA airport, composition information is useful because not all hydrocarbon species affect local air quality and human health equally. Yet here again the research team observed significant variability in the composition of HC emissions among piston engines. Statistical tools that use the measured distribution of compositions presented here can help bound speciated hydrocarbon emission burdens and enable informed decisions at airports.

New Measures of PM to Replace "Smoke Number"

The current ICAO database for large commercial gas turbine engines quantifies emissions for NO_x, CO, Unburned Hydrocarbons (UHCs, equivalent to HCs elsewhere in this document), and smoke number (ICAO 2013). The latter was instituted to provide a quantity for visible smoke that could be regulated and that could be used to control the smoke particle emissions through the metric of that smoke number. PM science has progressed tremendously since the 1970s, when SN was introduced, and the international aviation community is active in developing a new standard for aviation non-volatile PM (nvPM) emissions. Rather than just a measure of the visible obscuration like the SN, the new standard will report nvPM mass and number, quantities that are directly connected to environmental and human health impacts. For aviation PM, like many other combustion-generated PM, the particles' sizes are small enough to be considered part of existing PM10 (PM smaller that 10 μm) and PM2.5 (PM smaller that 2.5 μm)

Copyright National Academy of Sciences. All rights reserved.

regulations, and any likely future regulations with a smaller cutoff (for particles smaller than 1 or 0.1 μm, for instance).

ICAO's Committee on Aviation Environmental Protection (CAEP) is developing a regulatory standard for non-volatile PM (nvPM) number and mass-based emissions from civil aviation aircraft engines to replace the standard of smoke number measurement. The standardized sampling and measurement method that will be used for this future regulation has been defined in the Aerospace Information Report (AIR) 6241, developed by the Society of Automotive Engineers (SAE) Aircraft Exhaust Emissions Measurement Committee (SAE E31). This standard method will become normative once it is converted into a certification document, which will then be used by engine manufacturers in certifying aircraft engines for nvPM emissions. The system defined in AIR6241 is designed to operate in parallel with existing sampling systems for gaseous emissions and smoke certification defined in ICAO Annex 16. The system specifications in AIR6241 build on the work conducted in previous research to evaluate sampling and measurement methods for aircraft engine nvPM emissions measurements.

The primary measurement instruments in the AIR6241 systems report nvPM number and mass-based emissions. The nvPM number can be measured using an AVL particle counter (APC), which includes a volatile particle remover (VPR) consisting of a two-stage dilution with a rotary diluter and a catalytic stripper, and an *n*-butanol-based condensation particle counter (CPC) TSI 3790E, which has a 50% cutoff diameter, D_{50}, at 10 nm. During the research, an APC owned by United Technologies Research Center (UTRC) was deployed to each of the three field measurement campaigns. The reported number emissions of non-volatile PM (nvPMn) were determined based on the APC measurements in compliance with the AIR6241 recommendations.

For nvPM mass measurements, two real-time, high-resolution instruments that satisfied the performance specifications were recommended: the Artium Laser Induced Incandescence LII-300 and the AVL Micro Soot Sensor (MSS). However for this research, due to the lack of an available MSS or LII instrument, the research team used the conventional filter-based multi-angle absorption photometer (MAAP) to measure the nvPM mass emissions. The MAAP instrument has been widely applied to determine nvPM mass for many field measurements on commercial aircraft engine emissions [e.g., Experiment to Characterize Aircraft Volatile Aerosol and Trace-Species Emissions (EXCAVATE), Aircraft Particle Emissions eXperiment (APEX) I-III, and Alternative Aviation Fuel Experiment (AAFEX) I-II].

ACRP Research Report 164 reports these nvPM quantities of mass and number, but goes further in reporting the total mass and number, as well. The total quantities represent the sum of the nvPM quantities plus the volatile contributions to mass and number, respectively. The total mass and number become important once the exhaust mixes with cooler ambient air and volatile PM condenses and will certainly be the PM quantities emitted to the atmosphere.

PM Volatility Is High for Piston Engines

A typical GA piston engine shows a particle signature where high-volatility particles dominate. This trend is particularly obvious for particulate matter number (PMn) where the total particle count (volatile + non-volatile) exceeds the non-volatile count by an order of magnitude or greater. Figure 5-9 compares the emissions burden per LTO cycle (times-in-mode as shown in Table 3-1) for several engine families. These trends agree with the research team's understanding of piston engine operation.

Total PM mass (tPMm) is reported by the EEPS, however, this value is not appropriate for direct comparison to non-volatile PM mass (nvPMm) reported by the MAAP. The EEPS reports mass by calculation from the measured size distribution, assuming a particle density of 1.0. The

Copyright National Academy of Sciences. All rights reserved.

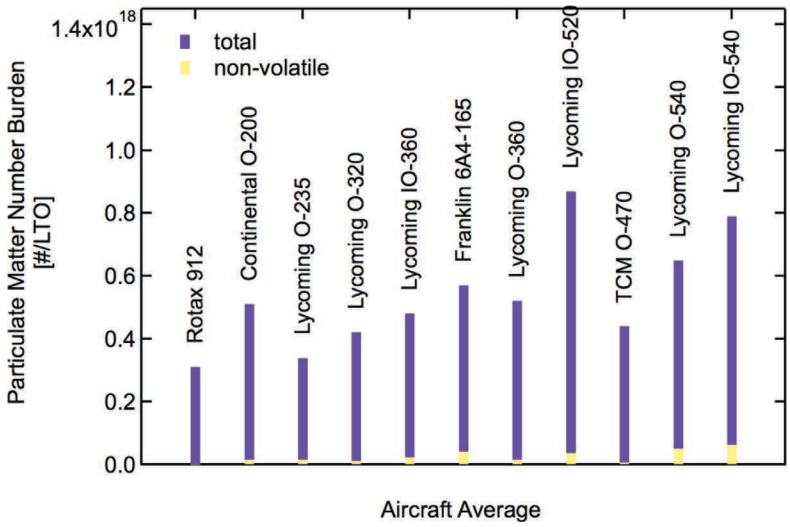

Figure 5-9. Comparison of total and non-volatile particulate matter number (tPMn vs. nvPMn).

EEPS measures total particle number, which ensures that black carbon particles are weighted to a larger size due to coating by volatiles. Given that the uncertainty in the EEPS counting efficiency increases at larger particle size, and the larger particles contribute most to mass, comparison to the MAAP is, at best, approximate.

PM Size Is Small, < 20nm, for Piston Engines

Piston engines emit particles as lognormal particle size distributions (PSD). A TSI engine exhaust particle sizer (EEPS) was used to measure a PSD at 1Hz so that all engine operating conditions could be observed as well as the transition between operating points. The difference between ambient and engine PSDs is obvious as shown in Figure 5-10, where the ambient signature is shown on the left and the engine on the right. The yellow line in the left-hand plot represents the lower bound of instrument detection ("zero") and the red line on the right-hand plot represents the upper bound ("saturation"). Besides the relatively random size distribution, the ambient concentration on the left is < 4E3 cm^{-3}, whereas the engine emission of primary particles is significantly larger (>1E7 cm^{-3}) and lognormal.

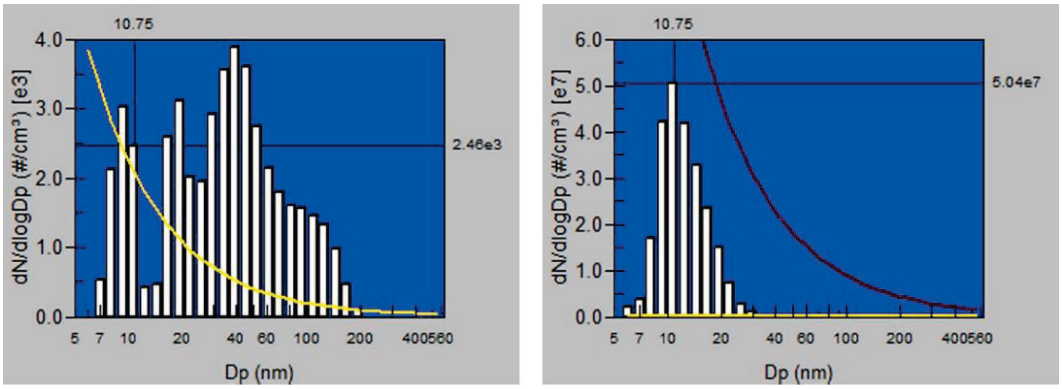

Figure 5-10. Typical ambient* (left) *and piston engine* (right) *particle size distributions.

Copyright National Academy of Sciences. All rights reserved.

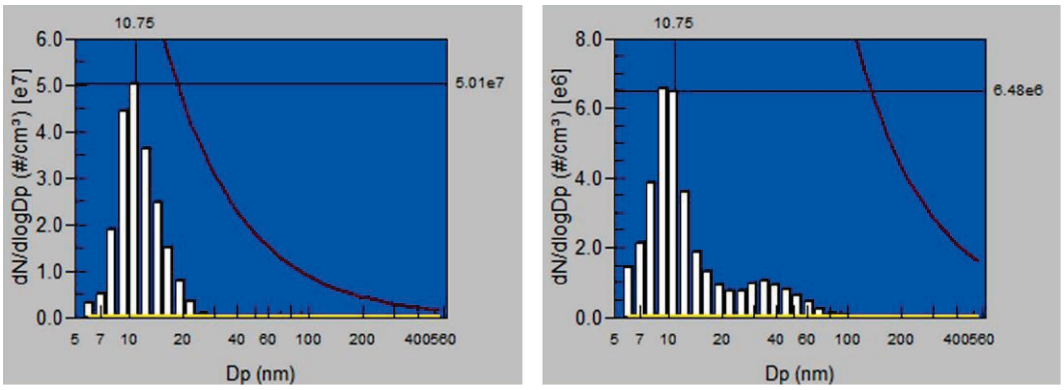

***Figure 5-11. Typical engine PSD at a stable operating power* (left) *and the PSD during the transition to another stable point* (right).**

For almost all of the engines in the measurement database from this project the emitted particles were observed to have a geometric mean diameter (GMD) that is small (<20 nm); therefore, most of particles are in the nucleation mode (i.e., newly formed particles). Particles in this size range were found to dominate the emitted PSD at all engine operating conditions. However, during transitions from low to high or high to low power, a soot mode (20 – 100 nm) was often observed (see Figure 5-11). Because the soot mode contributes to the engine PM mass emission more significantly than the nucleation mode because of particle size, the presence of the soot mode was also indicating lower overall combustion efficiency. In that respect, the overall width of the PSD, even in the nucleation mode, was reflecting the ratio of fuel-to-air mixture the engine was burning.

Although the GMD is somewhat invariant vs. engine power, the particle size concentration increases as engine power increases as shown in Figure 5-12. The number concentration data in this figure is not corrected for dilution in the plume, but wind conditions were steady during this test series. This response of increasing PM emissions with increasing power was expected

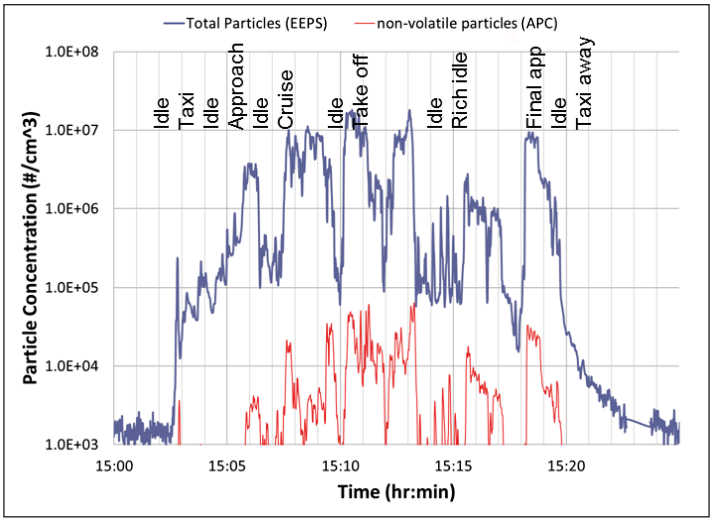

Figure 5-12. Typical variation in the particle concentration distribution vs. engine operating condition (blue = total particle concentration, red = non-volatile particles only).

Copyright National Academy of Sciences. All rights reserved.

50 Exhaust Emissions from In-Use General Aviation Aircraft

because the combustion process was the same for each stroke of the piston engine, unlike a gas turbine where the fuel air mixing is modulated vs. engine power. The piston engine increases power by simply increasing the frequency of the piston movement.

The red curve in Figure 5-12 is a measurement of non-volatile particles only as made by the APC. To use the EEPS (total particle number) and the APC (non-volatile only) data to assess the partitioning of solid and volatile particles, the APC must be corrected for sample conditioning losses from the catalytic stripper and other losses. These losses were about a factor of 3 and were applied to the APC data in the plot. Differences between the two curves represent the volatile particle concentration, which is seen to be significant. The large fraction of volatile particles is due to the lower combustion efficiency of the piston engine compared to a gas turbine and supports richer operating conditions. The lower efficiency is supported by the higher levels of carbon monoxide and unburned hydrocarbons previously noted. Another contributor of particles to the nucleation mode could come from lead in the AVGAS used in these engines. The lead is emitted as lead bromide ($PbBr_2$) in the combustion process of GA piston engines. $PbBr_2$ is a volatile species that can contribute to the formation of new particles in engine exhaust.

GA Turbofan Engines

The research team measured PM emissions in mass and number as well as particle size distributions from engine exhaust plumes from two gas turbine aircraft engines: a CF34-3A1 turbofan engine made by GE Aviation and a TPE331-6-252B turboprop engine, initially developed by Garrett AiResearch and made by Honeywell at present.

The research team observed both nucleation and soot particles from the EEPS measurements for the CF34-3A1 engine from engine idle to take-off (see Figure 5-13). Soot mode is dominant

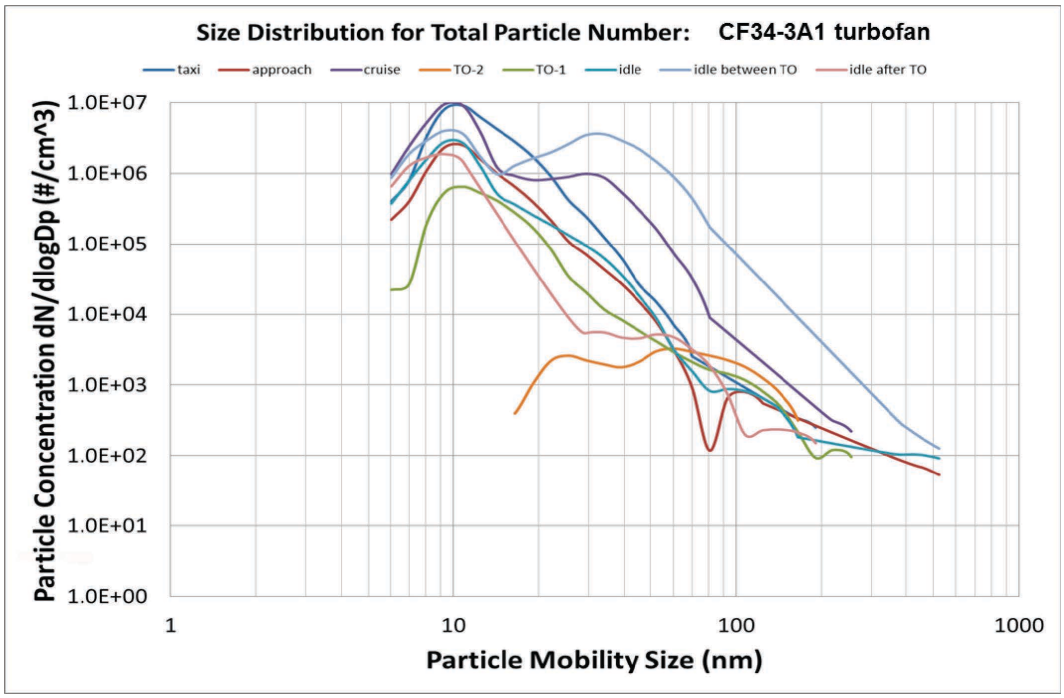

Figure 5-13. Particle size distributions for the CF34-3A1 turbofan engine. Individual test points are shown in different colors.

Copyright National Academy of Sciences. All rights reserved.

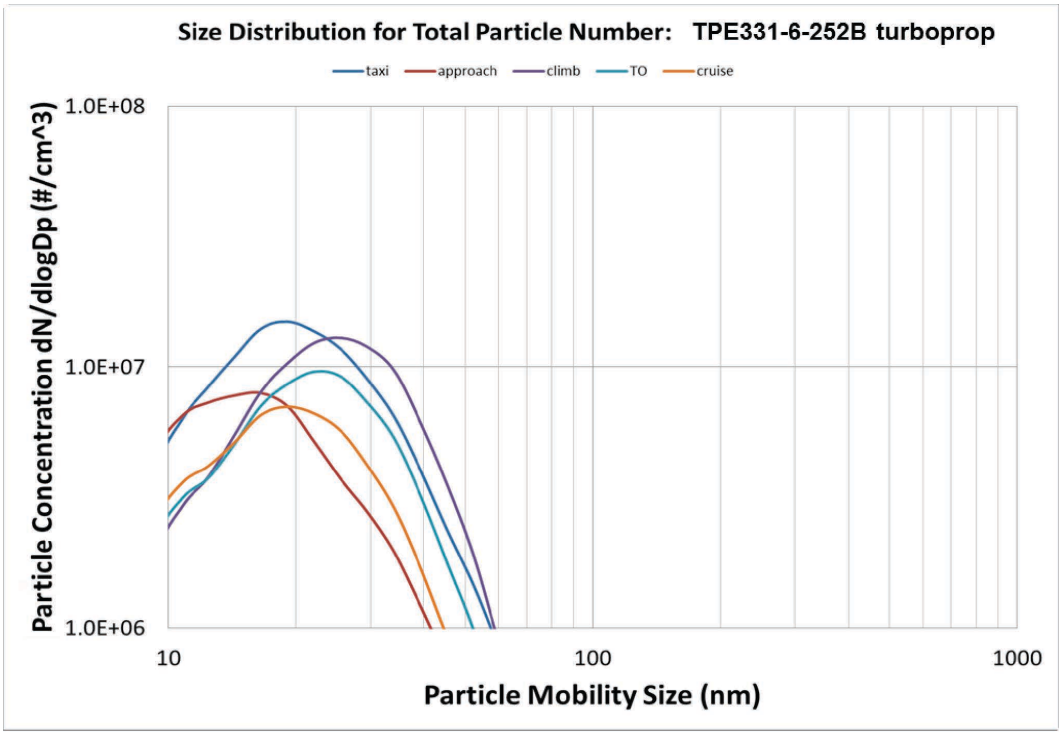

Figure 5-14. Particle size distributions for the TPE331-6-252B turboprop engine. Individual test points are shown in different colors.

at high-power condition, while nucleation mode becomes more important in number count at low power. However for the TPE331-6-252B engine, only one mode around 35 nm was observed, as demonstrated in Figure 5-14. Nucleation and mode become indistinguishable in the engine exhausts from the TPE331-6-252B turboprop engine. The non-volatile and volatile PM compositions are probably internally mixed to generate an individual particle mode.

PM emissions indices of the TPE331-6-252B engine are larger than those of the CF34-3A1 engine due to the lower temperature of its engine exhausts. For both gas turbine engines, medium power conditions (40-60% of thrust) yield the lowest PM emissions in number and mass. PM emission indices for the CF34-3A1 engine are shown in Figure 5-15. This observation of low emissions at cruise condition is in agreement with previous field measurements on commercial aircraft engines and implies that gas turbine aircraft engine performance is optimized at the cruise condition, which consumes the most fuel and provides the best energy efficiency.

Copyright National Academy of Sciences. All rights reserved.

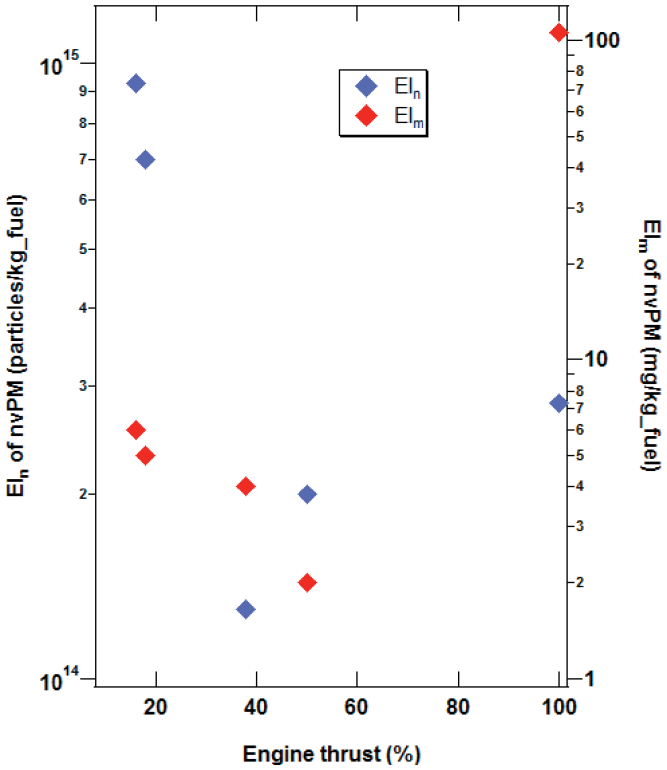

Figure 5-15. Emission indices of nvPM in number and mass for the CF34 turbofan engine.

Copyright National Academy of Sciences. All rights reserved.

CHAPTER 6

Conclusions

In this report, emission indices are listed for 47 full engine tests. A thorough analysis of trends and variability in these EIs is presented, with emphasis on the statistical comparison of the research team's results with existing data. A sensitivity analysis shows how substituting experimentally determined EIs and fuel flows into EDMS/AEDT leads to differences in reported airport emissions. Parameters affecting emissions are investigated and discussed. The inherent variability in piston engine emissions is quantified and explored.

This report achieves all three major goals of ACRP Project 02-54:

(1) Verify sample data sets that exist:
   a. Replicate measurements of several tested engines were used to perform a statistical validation of existing data.
   b. Given the large degree of inherent variability in piston engines, most of the existing data was validated, even if it differed a lot from results from this research.
   c. Several invalid data points were found. The most important of these data points is the 2.3-times underestimation of the hydrocarbon emissions data for the very common Lycoming O-320 engine by the FAA-mandated software used for calculating airport emissions (EDMS/AEDT).
   d. The research team recommends that the Lycoming O-320 engine data in EDMS/AEDT be substituted with engine family average results from this research. This data is provided at the beginning of the Emission Index Data Tables in Appendix P.

(2) Supplement the most commonly used aircraft engine data that does not exist in EDMS/AEDT or other emission databases:
   a. Forty-seven unique engines were fully sampled in all engine states as a part of this research. This included coverage of 10 engines from a list of the top 20 national piston engines. Existing EDMS/AEDT databases include only eight piston engines.
   b. Ten new engine families that are not included in EDMS/AEDT databases were measured. Many different subtypes of engines were also measured.
   c. The assumption underlying this goal of supplementation is that one engine type yields one set of well-defined emission indices. This assumption is not valid due to the flexible way in which piston engines are operated and the resulting variability in their emissions.
   d. Repeat measurements are particularly important given this variability. All of the emission indices collected as part of this project thus serve to supplement existing data and construct a database of piston engine emissions measurements.

(3) Develop recommendations for determining substitution for aircraft not in existing emission databases:
   a. As part of the sensitivity analysis, a method for choosing an engine substitution from within the current bounds of the EDMS/AEDT software has been described and displayed in flowchart form.

Copyright National Academy of Sciences. All rights reserved.

54 Exhaust Emissions from In-Use General Aviation Aircraft

b. The assumption underlying this goal of substitution is that one engine type yields one set of well-defined emission indices. This assumption is not valid, given the large variability in piston engine emissions.
c. The two sensitivity analyses were performed using different methods; both use the substitution method described in Item a. The research team propose future research on determining the best way to treat variability for GA airports, including substitution methods.

GA emissions, in particular those from piston engines, present a significant challenge to airports and others wanting to perform inventory and air quality calculations. An understanding of the observed trends in GA emissions, combined with a characterization of the confidence intervals inherent to any calculated emissions estimate, will enable airports and policymakers to make decisions based on sound science and an understanding of the real-world operation of GA aircraft.

Future Research

Suggested topics for future research follow.

- **Research the best way to include the effects of variability in GA airport inventories**. The concepts of variability and 95% confidence intervals are crucial for GA airports. A confidence interval consists of an upper limit and a lower limit such that one is 95% sure that the true average emission falls between them. Variable data have wide confidence intervals. A GA airport inventory should have confidence intervals that reflect the range of possible emissions, given the inherent variability of its fleet's emissions. Two possible ways to include this variability have been explored here. Monte Carlo methods that use random sampling show significant promise over standard methods using FAA-mandated tools. Other methods could be investigated. One such method might group all piston engine aircraft together and assign a single set of representative emission factors and confidence limits for the whole piston fleet. Broad horsepower subcategories could also be considered. This method could simplify airport emissions calculations by reducing the number of individual aircraft types chosen as part of a sensitivity analysis.
- **High-volume automated measurements for improved GA airport inventories**. Each method that the research team explored to deal with aircraft variability relies on a large number of aircraft measurements. Although we have 47 full engine tests, including hundreds of individual test points, this may not be enough data to fully quantify distributions of piston engine emitters, particularly those relatively rare high-emitting points. High-volume automated measurements of hundreds of aircraft would be an ideal way to expand this dataset. An automated measurement system could be set up at an airport, downwind of a taxi area and a runway. Data during normal airport operations could be collected for a matter of months, and then analyzed. The distribution of piston engine emitters would then be well defined and could be used to determine representative emission values and confidence intervals. This measurement topic is complementary to the three topics about fleet characteristics, fleet use, and representative times-in-mode.
- **Fleet characteristics of a representative GA airport**. Significant work was done in this research to construct a hypothetical GA airport that is representative of a U.S. national fleet. However, limitations in the FAA Tail Registry Database hampered this effort, particularly for small GA jets. Further research in this area would include surveys of fleet characteristics and number of operations at GA airports across the country.
- **Fleet use at a representative GA airport**. Even with accurate knowledge of the fleet characteristics of GA airports, it is still important to understand how that fleet is used day-to-day. For example, flight school aircraft are expected to account for a disproportionate number of operations compared with based aircraft. How does the list of most-used aircraft differ from the list of most common aircraft constructed from the FAA tail number registry? Knowing the characteristics of the in-use fleet can help focus future measurements on the aircraft of highest importance.

Copyright National Academy of Sciences. All rights reserved.

- **Researching real airport operations to determine times-in-mode that are more representative of true GA operations**. Throughout this research, the default values for time spent in taxi (taxi and idle are often clumped together) were used. However, these default times were designed for commercial airports with significantly more traffic than at many GA airports. Taxi/idle times in particular are expected to be shorter than the EDMS/AEDT defaults of 26 minutes total. Research on the real times-in-mode of a subset of GA airports would improve the accuracy of airport emissions calculations using these newly developed emission indices.
- **Engine leaning practices**. The fuel-to-air ratio in piston engines has a significant effect on the resulting emissions. This fuel-to-air ratio is dictated by a propeller plane's mixer setting and pilot preference for a "rich" mixture (excess fuel) or a "lean" mixture (less excess fuel). What proportion of pilots routinely run full-rich in all engine states except cruise? What causes this preference? Full-rich operation significantly increases the emissions of both CO and HC (but decreases NO_x).
- **Fuel additive use and impact**. During the field measurements, aircraft exhaust and fuel samples unusually high in toluene were observed. The presence of toluene significantly affects the hydrocarbon emission signatures of these aircraft. The most likely source of toluene was a fuel additive designed to reduce spark plug fouling. Further investigation of the actual use rates of fuel additives and the point at which they were added to the fuel is needed to pin down the extent of this activity.
- **Realistic partitioning of emissions in EDMS/AEDT**. The emissions software programs EDMS and AEDT output not only results for the main emissions species (i.e., HC, CO, NO_x, and PM), but also partition those species into different classes. For example, HC emissions are broken into the categories of non-methane hydrocarbons (NMHC), VOC, and total organic carbon (TOG). PM emissions are broken into size categories of PM_{10} and $PM_{2.5}$. The auxiliary data collected during this research project could be used to verify and improve these partitions. This could have a significant effect on airports because certain subcategories of HC and PM emissions are of more concern to human health than others.

Policy Implications of This Research

One potential policy implication relates to the flexibility in piston engine operation. Hydrocarbon and carbon monoxide emission factors are highest in idle and taxi, the two power states that occur on the ground, and decrease precipitously with leaner fuel mixtures. **A policy encouraging pilots to run leaner could be researched**, particularly during taxi and idle where accidentally stalling the engine poses no safety issue. Such a policy could reduce airport emissions of hydrocarbons and carbon monoxide, but comes with a potential increase in NO_x emissions.

A second policy implication relates to the large inherent variability observed in piston engine emissions. **This variability must be taken into account to perform realistic assessments of an airport's emissions**.

Any GA airport's emissions will have upper confidence limits many times higher than the average, depending on the pollutant. Monte Carlo methods have great potential to shrink these confidence limits when combined with the large number of operations at an airport over the course of a week (or year). These methods depend on having access to large datasets of emissions and times in mode that are representative of the GA airport being simulated.

The research team's recommendation for dealing with this variability is to push for high-volume measurements of piston engine emissions, coupled with advanced statistical methods. Such high-volume measurements could be done simply, with unattended automated systems installed at airports, and without impact on operations. **In the interim, GA airport environmental impact statements should be produced with confidence intervals, even if they are very wide**. This type of result gives airport managers and policymakers the power to make informed decisions based on the true weight of evidence.

Copyright National Academy of Sciences. All rights reserved.

APPENDIX A

Engine Prioritization List

The prioritized list of engines below was used in the planning stages of the research to prioritize the engines measured. The rank of the aircraft engine is based on the FAA registry of the national GA fleet for piston engines and turbofan engines in 2014. Those rows highlighted in yellow show engines that were measured experimentally in all engine states.

Category	Engine Make	Engine Family	RANK	FOCA Data Exists	EDMS Data Exists	Full Engine Tests	Partial Engine Tests
MEP	CONT MOTOR	TSIO-520 SERIES	1	yes		1	
SEP & MEP	LYCOMING	O-320 SERIES	1	yes	yes	16	4
MEP	CONT MOTOR	TSIO-360 SERIES	2	yes	yes		
MEP	CONT MOTOR	IO-470 SERIES	3				
SEP	CONT MOTOR	O-200 SERIES	3	yes		4	1
SEP	LYCOMING	O&VO-360 SERIES	4			6	
SEP	CONT MOTOR	O-470 SERIES	5			1	1
SEP & MEP	LYCOMING	TIO-540 SERIES	5	yes	yes		
MEP	LYCOMING	IO-320 SERIES	6	yes	yes		
SEP	CONT MOTOR	O-300 SERIES	6				
SEP & MEP	LYCOMING	IO-360 SERIES	7	yes	yes	4	
SEP	CONT MOTOR	A&C65 SERIES	8				
SEP & MEP	CONT MOTOR	IO-550 SERIES	12	yes			2
SEP	LYCOMING	O-235 SERIES	13			3	
SEP & MEP	LYCOMING	IO-540 SERIES	14	yes		4	1
MEP	CONT MOTOR	GTSIO-520 SERIES	15				
SEP	CONT MOTOR	C145 SERIES	17				
MEP	P & W	R-985 SERIES	18				
SEP & MEP	CONT MOTOR	IO-520 SERIES	18			1	
MEP	LYCOMING	O-540 SERIES	19	yes		3	
SEP	CONT MOTOR	C85 SERIES	19				
SETP	P & W	PT6A-67 SERIES	1				
SETP	P & W	PT6A SERIES	2				
SETP	P & W	PT6A-66 SERIES	3				
SETP	P & W	PT6A-SERIES	4				
SETP	P & W	PT6A-42 SERIES	5				
SETP	P & W	PT6A-114	6				
SETP	P & W	PT6 SERIES	8				
SETP	P & W	PT6A-34	10				
SETP	P & W	PT6A-6 SERIES	12				
SETP	P & W	PT6A-60A	14				1
SETP	P & W	PT6A-64	16				
SETP	P & W	PT6A-140	17				
SETP	P & W	PT6A-60 SERIES	18		yes		1
SETP	P & W	R1340 SERIES	20				

Copyright National Academy of Sciences. All rights reserved.

APPENDIX B

Test Matrix

The test matrix reproduced here was used by the cockpit observer to direct the engine tests and note all relevant conditions.

Copyright National Academy of Sciences. All rights reserved.

Date _____ Time (Local) _____ Pilot _____

Time (UTC) _____

Tail Number _____ Max HP _____

Aircraft Make _____ Max Propellor RPM _____ Notes

Aircraft Model _____ Engine Hrs _____

No. engines _____ Direct Drive _____ Variable Pitch _____

Engine Make _____ Run-Up Times/Settings _____

Engine Model _____ Fuel/Additives _____

Nominal Condition	Time (Local)	Engine Parameters (enter n/a if required)		% of Max. Power	Cockpit Notes
Run Up		Propellor RPM	Throttle/Manifold Pressure or %		
		Engine RPM	Fuel Mixture % of full rich		
		Oil Temp	Engine Cyl. Head T/ EGT		
		Oil Pressure	Fuel Flow		
			Air/Fuel Ratio		
Idle		Propellor RPM	Throttle/Manifold Pressure or %		
		Engine RPM	Fuel Mixture % of full rich		
		Oil Temp	Engine Cyl. Head T/ EGT		
		Oil Pressure	Fuel Flow		
			Air/Fuel Ratio		
Taxi		Propellor RPM	Throttle/Manifold Pressure or %		
		Engine RPM	Fuel Mixture % of full rich		
		Oil Temp	Engine Cyl. Head T/ EGT		
		Oil Pressure	Fuel Flow		
			Air/Fuel Ratio		
Idle					
Approach		Propellor RPM	Throttle/Manifold Pressure or %		
		Engine RPM	Fuel Mixture % of full rich		
		Oil Temp	Engine Cyl. Head T/ EGT		
		Oil Pressure	Fuel Flow		
			Air/Fuel Ratio		
Idle					
Cruise		Propellor RPM	Throttle/Manifold Pressure or %		
		Engine RPM	Fuel Mixture % of full rich		
		Oil Temp	Engine Cyl. Head T/ EGT		
		Oil Pressure	Fuel Flow		
			Air/Fuel Ratio		

Copyright National Academy of Sciences. All rights reserved.

Approach		
Idle		
Climb Out	Propellor RPM	Throttle/Manifold Pressure or %
	Engine RPM	Fuel Mixture % of full rich
	Oil Temp	Engine Cyl. Head T/ EGT
	Oil Pressure	Fuel Flow
		Air/Fuel Ratio
Approach		
Idle		
Take off	Propellor RPM	Throttle/Manifold Pressure or %
	Engine RPM	Fuel Mixture % of full rich
	Oil Temp	Engine Cyl. Head T/ EGT
	Oil Pressure	Fuel Flow
		Air/Fuel Ratio
Approach		
Idle		
Full Power	Propellor RPM	Throttle/Manifold Pressure or %
	Engine RPM	Fuel Mixture % of full rich
	Oil Temp	Engine Cyl. Head T/ EGT
	Oil Pressure	Fuel Flow
		Air/Fuel Ratio
Approach		
Idle		
Final	Propellor RPM	Throttle/Manifold Pressure or %
Approach	Engine RPM	Fuel Mixture % of full rich
	Oil Temp	Engine Cyl. Head T/ EGT
	Oil Pressure	Fuel Flow
		Air/Fuel Ratio
Idle		
Other	Propellor RPM	Throttle/Manifold Pressure or %
(optional)	Engine RPM	Fuel Mixture % of full rich
	Oil Temp	Engine Cyl. Head T/ EGT
	Oil Pressure	Fuel Flow
		Air/Fuel Ratio
Idle		
Run Down or Taxi Away		

Copyright National Academy of Sciences. All rights reserved.

APPENDIX C

ICAO vs. FOCA Databases

The ICAO maintains a database of turbofan engine emission indices, with the operational states defined based on a percentage of available thrust. The Swiss Federal Office of Civil Aviation (FOCA) maintains a database of piston engine emission indices, with the engine states defined by percentage of maximum propeller horsepower, inferred based on fuel flow measurements.

Table C-1. Comparison of operational states for turbojets (ICAO) and piston-powered propeller aircraft (FOCA).

Engine State based on Landing Take-Off cycle (LTO)	ICAO definition % available thrust (turbofan)	FOCA definition % max propeller horse power
Take-off	100	100
Climb	85	85
Cruise	-	65
Approach	30	45
Taxi	7	Operator's manual

Copyright National Academy of Sciences. All rights reserved.

APPENDIX D

Method for Calculating Emission Ratios

Emission ratios are the first step in calculating emission indices from time series data. This appendix details methods of determining emission ratios.

A time series is the measured concentration of a species of interest plotted as a function of time. Figure D-1 shows a selection of the many time series measured during the ACRP Project 02-54 field campaigns. The colored brackets at the bottom of the graph indicate the engine states during this test (red = idle, cyan = T/O, etc.). In this graph, many different species of interest are plotted, including combustion products (e.g., CO_2 and CO) and speciated hydrocarbons and aromatics (e.g., methane (CH_4) and toluene).

The standard method for determining the emission ratio uses the plot of the species of interest versus total carbon (e.g., NO_x vs. Total C). The time offset between the two traces is optimized and a linear fit of the data is taken. The slope (m) of this fit gives the emission ratio, while the coefficient of correlation (R^2) gives an indicator of data quality. An example of this type of analysis is shown for the plume in the middle of Figure D-1, with the workup summarized in Figure D-2. Appendix E outlines the calculation of the emission index from an emission ratio.

An improved algorithm for determining emission ratios has been developed to deal with non-ideal experimental data. Previously, some tests points were simply thrown out due to a poor R^2. In the advanced algorithm, clean background periods are manually defined and used in determining individual emission ratios.

Figure D-3 shows an example of two improved emission ratio determination methods. Figure D-3 (A) shows concentrations of a select few species of interest versus time for the "climb-out" state of the N62480 engine. Although the time traces for CO and total hydrocarbons (THC) match the time trace for total carbon (Total C), the traces for NO_x and the PM mass signal (MAAP) are not as well correlated. Examining Figure D-3 (C) shows that a simple correlation of the raw data (blue circles, red fit line) yields a ratio of 4.35 ppb NO_x/ppm Total C, but with a coefficient of correlation of 0.11, far below the data quality threshold of 0.75. This data point would previously have been rejected due to poor correlation.

Figure D-3 (B) shows how periods of clean background are appended to either side of the time series of interest. The emission ratio is then computed via one of two methods: the corrected slope method or the corrected area method. The standard method is also shown for comparison (blue circles, red fit line in Panel C). The corrected slope method [Figure D-3(C), cyan crosses and cyan fit line] yields a slope (m) of 6.6 ppb NO_x/ppm Total C, and an R^2 of 0.49, still below the data quality threshold. For some data, this corrected slope method improves the fit sufficiently. The corrected area method [Figure D-3 (B), filled areas] yields a ratio of 7.5 NO_x/Total C and will be the ratio used in the final determination of the emission index for this data point.

Copyright National Academy of Sciences. All rights reserved.

62 Exhaust Emissions from In-Use General Aviation Aircraft

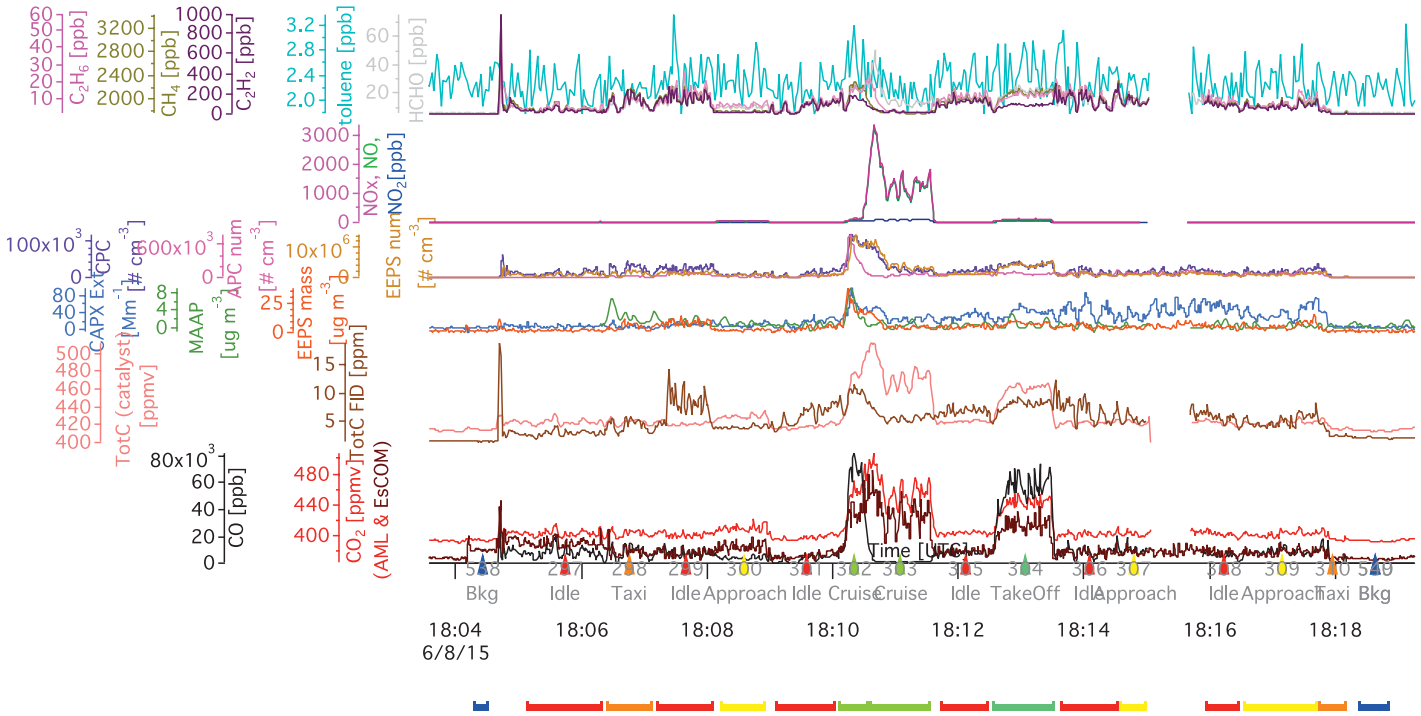

Figure D-1. Time series for many measured species for aircraft N6453H.

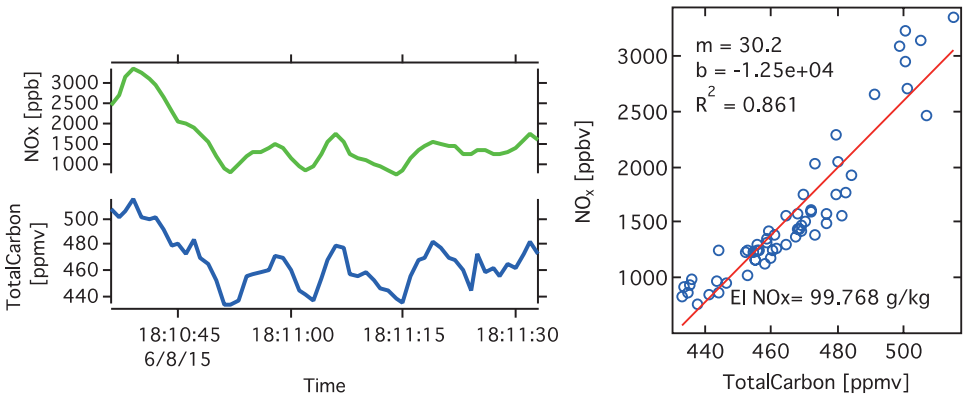

Figure D-2. Determination of the emission ratio for NO_x (green) vs Total C (blue). The time traces in the left plot have been plotted against one another on the right hand plot (blue circles). The red line shows the best fit, with the resulting slope (m), intercept (b) and coefficient of correlation (R^2) shown on the plot. The corresponding EI is also shown (EI NO_x).

Copyright National Academy of Sciences. All rights reserved.

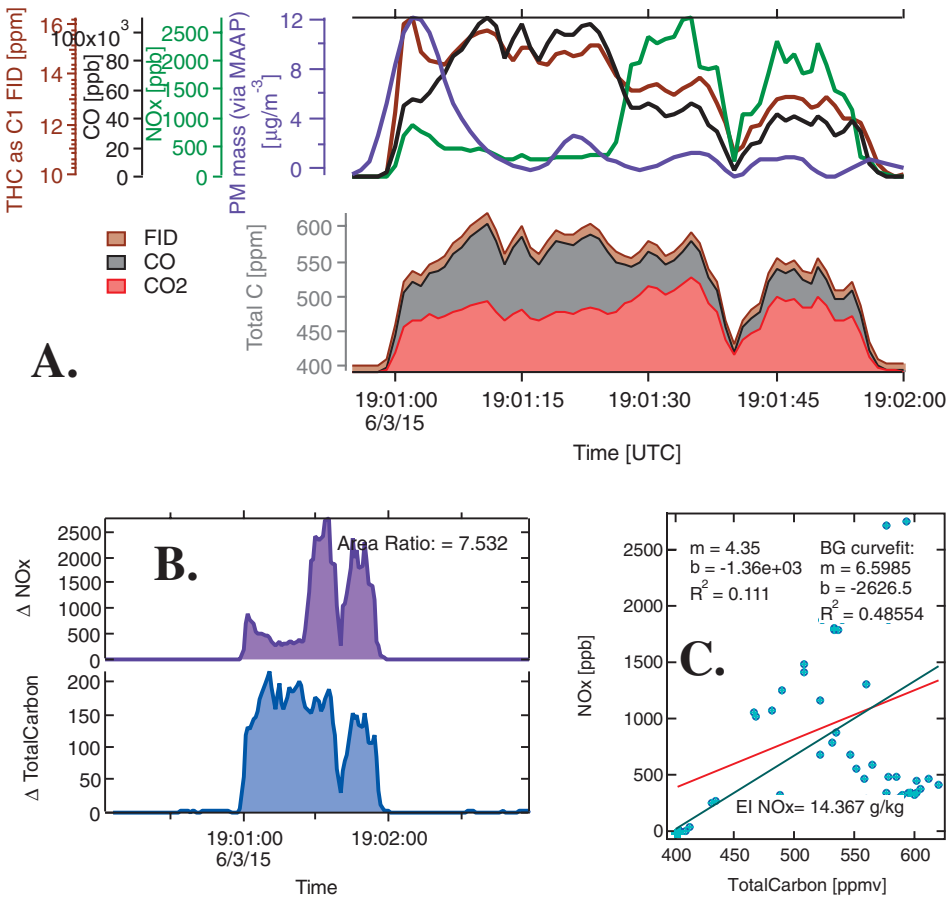

Figure D-3. Example plume analysis showing updated methods that include periods of manually defined "background" signal. Panel A shows 4 time traces for species of interest, including NO_x (green). In Panels B and C, emission ratios for NO_x are determined via three methods (see text). Periods of manually defined background have been added to the data in Panels B and C, as indicated by the extended baseline in Panel B, and the locus of points (cyan + signs) in the lower left of Panel C.

Copyright National Academy of Sciences. All rights reserved.

APPENDIX E

Method for Calculating Emission Indices

Emission ratios are the first step in calculating emission indices from time series data. Emission indices are in units of grams of compound per kilogram of fuel (e.g., g X/kg fuel). Raw data gives the emission ratio: the concentration enhancement of the compound of interest over the concentration enhancement of carbon dioxide ($\Delta C_X/\Delta C_{CO2}$). Emission indices are calculated knowing the carbon content of the fuel and performing a unit conversion. This standard procedure assumes that the major carbon-containing combustion product is CO_2, with negligible amounts of other carbon-containing compounds (e.g., CO and methane). This is not true for the piston engines that the research team measured, with carbon monoxide (CO) constituting a significant portion of the exhaust. For this reason, the concentration enhancement of total carbon (ΔC_{TotC}) is used in lieu of CO_2 in the emission ratio. This ensures proper accounting when CO is not negligible. The equation below is a simplified conversion from the emission ratio versus the total carbon ($\Delta C_X/\Delta C_{TotC}$) to the emission index (EI_X) (Timko et al. 2010, Herndon et al. 2010). MW_X is the molar mass of the compound of interest; F_{CO2} is the fuel carbon content, expressed in grams of CO_2 per kilogram of fuel, and is 3160 for Jet A and 3067 for AVGAS 100 LL; and 44 is the molar mass of CO_2 in g/mol. All unit conversions are rolled in.

$$EI_X\left[\frac{gX}{kg\ Fuel}\right] = \frac{\Delta C_x}{\Delta C_{TotC}} MW_X \frac{F_{CO_2}}{44} \qquad \text{(Eq. E-1)}$$

A similar method is used for the particulate mass measurements (Timko et al. 2010), substituting grams of compound with number of particles or other measures as necessary. Slightly different equations are required for $EI_{m,X}$, the particulate mass emission index, than for $EI_{n,X}$, the particulate number emission index, due to differences in the units of the measurements. In the equations below, ΔM_x is the concentration enhancement of a particle of type X in the exhaust relative to ambient, in $\mu g\ m^{-3}$. ΔN_x is a particle count: the concentration enhancement of particle type X relative to ambient, in units of $\#\ cm^{-3}$. ΔC_{CO2} is the corresponding enhancement in CO_2, in ppm. The particulate inlet had its own CO_2 monitor, and this measure is used to ensure that the timing of the particle inlet matches up with the gas-phase measurements of ΔC_{TotC}. The temperature (T, Kelvin) and pressure (P, Torr) are those that define the condition for the particulate measurement flow calibration and correspond to 293.15 K and 760 Torr, respectively for the MAAP instrument (Multi Angle Absorption Photometer). For example, 0.06236 is the ideal gas constant in units of $m^3\ Torr\ K^{-1}\ mol^{-1}$.

$$EI_{m,X}\left[\frac{gX}{kg\ Fuel}\right] = \frac{\Delta M_x}{\Delta C_{TotC}} \frac{T}{P} \cdot 0.06236 \cdot \frac{F_{CO_2}}{44} \qquad \text{(Eq. E-2)}$$

$$EI_{n,X}\left[\frac{\#X}{kg\ Fuel}\right] = \frac{\Delta N_x}{\Delta C_{TotC}} \frac{T}{P} \cdot 0.06236 \cdot \frac{F_{CO_2}}{44} \cdot 10^{12} \qquad \text{(Eq. E-3)}$$

Copyright National Academy of Sciences. All rights reserved.

APPENDIX F

Variability in Emissions Results from Variability in the Engine

Before examining the question of data validation and comparison of these results with prior test data, it is important to gain confidence that the source of apparent variability is not due to instrumental noise. The appendices and other sections of the report demonstrate the explicit formula and analysis protocols used in this project. **The discussion here demonstrates that the emissions characterization procedure is accurate, relatively free from systematic error, and diagnostic of the true combustion taking place in the engine**. The case is made by examining two time series and the signal correlations for two different engine states. These two test conditions are compared and contrasted in the larger context of the whole dataset to support the statement that **the variability observed in these emission indices results from actual variability in the engine**.

In the time series shown in Figure F-1, the engine is operating at ~87% of maximum fuel flow. The relative proportions of CO_2, CO, and hydrocarbon species can be evaluated via the relative proportions of their color in the stacked time series (left). On the right, several observations about the correlation can be made. First, the slope of the correlation gives the emission ratio for carbon monoxide, which is used to calculate the emission index for this engine state. Two alternative analysis methods are depicted. In the first, only data during the test point are considered. This is shown as the dark blue circular data points. The molar ratio in this analysis is 112 ppb CO per ppm of total carbon (TotC). For the alternate analysis, data points from the ambient sample, prior to and following the test (light blue crosshairs) are added and the slope re-computed. In this second procedure, the resulting slope, m = 104 ppb CO per TotC, is 7% lower. The specific conditions associated with selecting the correlation factor are described in Appendix E. This plume example suggests that the correlation method is highly precise when sufficient modulation of the exhaust signal is sampled during a test condition.

In Figure F-2, the same engine is operating at ~11% of maximum fuel flow. The raw difference index is almost fourfold greater at this lower engine power state than the engine state in the simulated cruise test condition.

Figures F-1 and F-2 show CO emission indices that differ by approximately a factor of 4. In Figure F-3, the NO_x emission index for these two points is anti-correlated by a large factor (upper panel). Additionally, the specific production of methane kicks in with the greater production of CO (lower panel). The production of methane at low power has been observed before in aircraft engines (Santoni et al. 2011). A specific hydrocarbon, produced only via combustion, is a useful diagnostic of the conditions in the cylinder. The bulk unburned hydrocarbon emission index includes unburned fuel, which provides less insight into combustion temperature.

Figure F-3 plots the current dataset of NO_x, CO, and specific methane emission indices for all engines from the second field campaign and all engine states. The coloring of the data point is associated with the likely extent of fuel to air. Most of the engines tested do not allow for a precise quantification of the fuel-to-air ratio; this is set by the "feel" and "sound" of the rumbling engine

Copyright National Academy of Sciences. All rights reserved.

66 Exhaust Emissions from In-Use General Aviation Aircraft

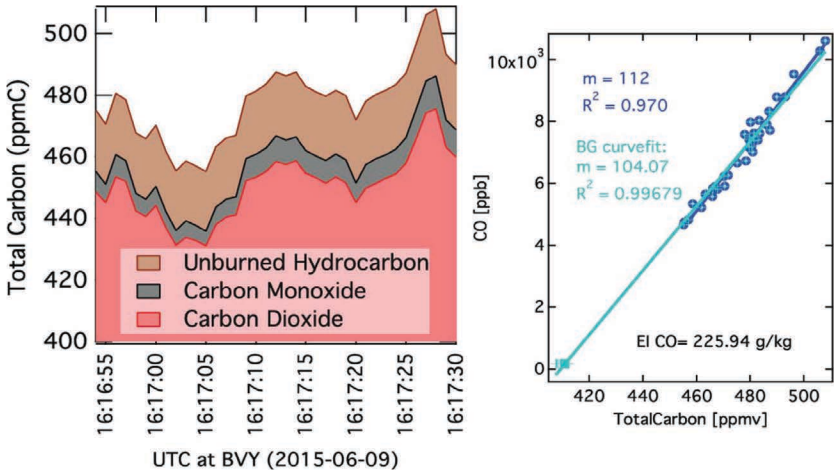

Figure F-1. Time Series and Emission Ratio N9184Y, Lycoming O-320-D3G, Engine RPM = 2300. The left hand panel is a time series of HC, CO and CO_2. The time series data is stacked to indicate the relative contribution to the total carbon signal. The right hand panel is a correlation plot of the specific carbon monoxide (CO) data with total carbon. Correlations are taken with and without inclusion of background data (BG) as described in Appendix D with the calculated slope (m) and coefficient of correlation (R2) reported. See text for additional discussion.

by the pilot (as discussed in the section "Pilot Mindset on Fuel Mixture"). To collect data on real-world engine states, pilots were encouraged to run the engine they way they would typically operate.

For engine states that would be characterized as lean and/or higher combustion temperature, the emission index of CO decreases while the NO_x emission index increases. In general, this relationship is found in the NO_x emission index (see the region of the upper panel where EI CO is less than ~ 400 g/kg), but this is not as strong as the relationship between the emission indices observed in the turbofan combustor. In the case of the piston engine, each cylinder represents

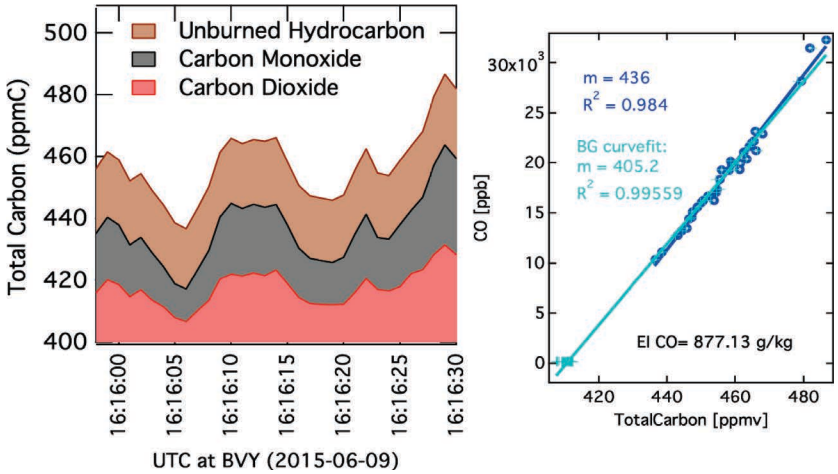

Figure F-2. Time Series and Emission Ratio N9184Y, Lycoming O-320-D3G, Engine RPM = 850. The data is colored the same as the previous figure but is for a different engine state.

Copyright National Academy of Sciences. All rights reserved.

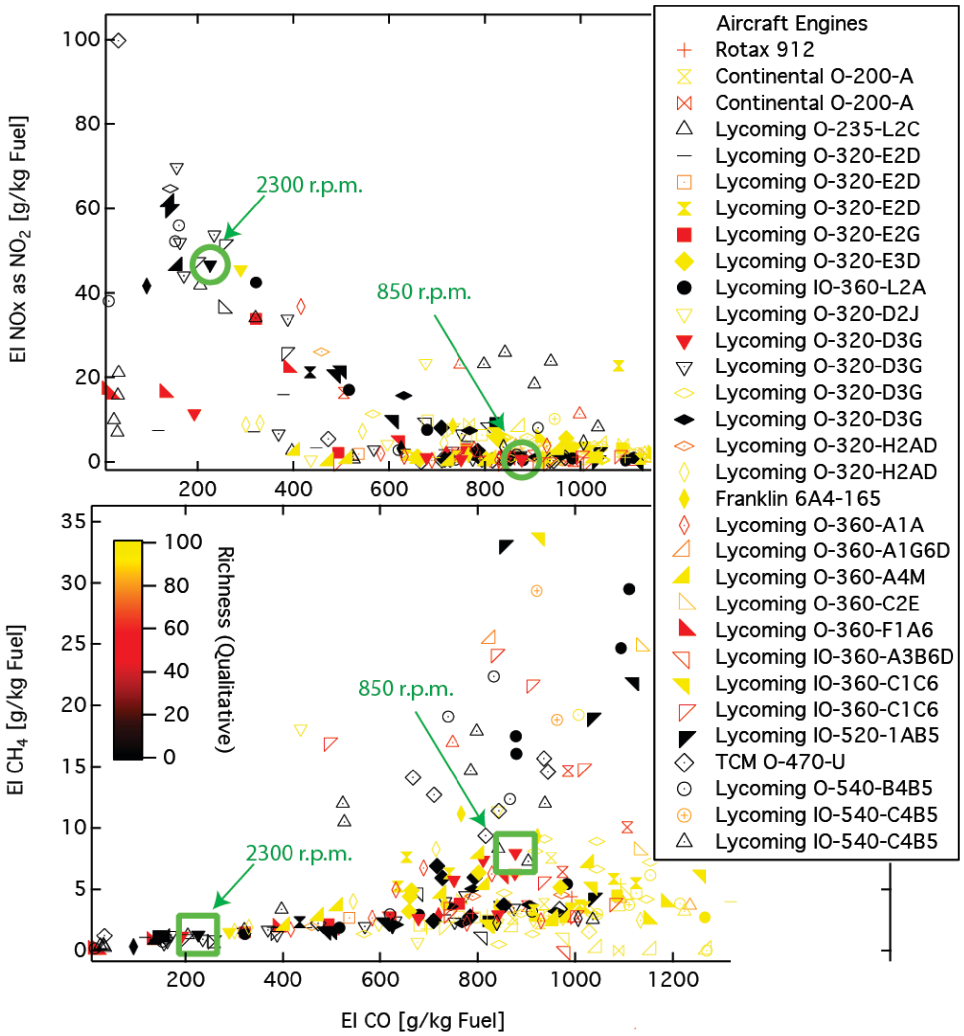

Figure F-3. EI NO_x and EI HC vs EI CO. All test data are depicted for all engine states. In the upper panel, the NO_x emission index is plotted vs the CO emission index. In the lower panel the specific methane emission index emission index is plotted vs EI CO. The marker style is the motor and the coloring is a qualitative estimate of how fuel-rich the motor was being operated. The data points called out as 2300 and 850 are the two engine states depicted in Figures F-1 and F-2 respectively.

a discrete combustor with potentially different temperatures that are mixed into the exhaust manifold.

The two example test conditions, shown in Figures F-1 and F-2, have emissions of CO, NO_x, and CH_4 that are chemically consistent with what is known about thermal NO_x (DuBois and Paynter 2006, Kerrebrock 1992) and the production of methane during low-temperature combustion (Santoni et al. 2011). Taken together, these demonstrate that the EI quantification methods used in this work are diagnostic of the engine combustion characteristics.

Copyright National Academy of Sciences. All rights reserved.

APPENDIX G

Gas-Phase Measurement Instruments

The gas-phase instruments used during the ACRP Project 02-54 research are listed in Table G-1. This instrument manifest includes a carbon dioxide (CO_2) analyzer (LI-COR), two NO_x monitors (NO_x Box, Thermo Scientific) for the separate detection of nitric oxide (NO) and nitrogen oxides ($NO + NO_2$), a cavity-attenuated phase shift spectrometer for nitrogen dioxide detection (CAPS-NO_2, Aerodyne Research, Inc.), and a heated flame ionization detector for hydrocarbon detection (HFID, California Analytical Instruments). A tunable infrared laser direct absorption spectrometer measured carbon monoxide, nitrous oxide, and water vapor (TILDAS N_2O-mini, Aerodyne Research, Inc.). These instruments are sufficient to measure the three main gas-phase emission indices: carbon monoxide, NO_x, and hydrocarbons.

To better characterize and understand the aircraft exhaust, additional gas-phase measurements were performed. Most of these were focused on characterizing the mix of hydrocarbons emitted. Three additional TILDAS instruments were included to measure additional trace gases, the carbon-containing species methane (CH_4), ethane (C_2H_6), formaldehyde (HCHO), acetylene (C_2H_2), and ethene (C_2H_4). A proton-transfer-reaction mass spectrometer (PTR-MS) measured acetaldehyde, acetone, benzene, toluene, sum of xylenes and ethylbenzene, and naphthalene.

Routine zeroing of instruments was performed by overblowing the gas-phase inlet with a cylinder of ultra-zero-air before, during, and after each engine test. Routine calibrations were also performed with a set of calibration tanks to assess instrument performance. Zeroed and calibrated data was used to compute all emission ratios.

Copyright National Academy of Sciences. All rights reserved.

Table G-1. Gas phase instrument manifest.

Instrument	Full name or description	What is being measured?
CO_2 LI-COR	Non-dispersive infrared gas analyzer for carbon dioxide	Carbon dioxide (gas phase inlet)
TILDAS (N_2O-Mini)	Tunable infrared laser direct absorption spectroscopy	Nitrous oxide, carbon monoxide, water
TILDAS (CH_4-Dual)	Tunable infrared laser direct absorption spectroscopy	Methane, methane isotopes, sulfur dioxide, acetylene
TILDAS (C_2H_6-Mini)	Tunable infrared laser direct absorption spectroscopy	Ethane
TILDAS (HCHO-Dual)	Tunable infrared laser direct absorption spectroscopy	Formaldehyde, ethene
NO_x Box	Thermo Scientific chemiluminescence NOx analyzer	Nitrogen oxides (NO_x = NO + NO_2)
NO_x Box	Thermo Scientific chemiluminescence NO_x analyzer In NO mode only	Nitric oxide (NO)
CAPS-NO_2	Cavity attenuated phase shift spectroscopy	Nitrogen dioxide (NO_2)
HFID	Heated flame ionization detection of hydrocarbons	unburned and partially combusted hydrocarbons (HC)
PID	Photoionization detector for volatile organic hydrocarbons	Volatile organic hydrocarbons (VOC)
PTR-MS	Proton-transfer-reaction mass spectrometry	Acetaldehyde, 1,3-butadiene, acrolein, propanal, benzene, toluene, sum of xylenes and ethylbenzene, naphthalene, other VOCs

Copyright National Academy of Sciences. All rights reserved.

APPENDIX H

PM Measurement Instruments

The particle measurement instruments used during this research are listed in Table H-1 and include a MAAP (Model 5012, Thermo Scientific), a CAPS-based particle extinction monitor (PM_{ex}) (Aerodyne Research Inc.), an AVL particle counter (APC, AVL), and an engine exhaust particle sizer (EEPS) (Model 3090, TSI). These instruments provided information about particle absorption and extinction, number density, and mobility-based size distribution. A High-Resolution Time-of-Flight Aerosol Mass Spectrometer (HR-ToF-AMS, Aerodyne Research, Inc.) was also used to provide information about the possible presence of any semi-volatile coatings on the soot. A Teflon-coated aluminum cyclone (Model URG-2000-30ED) with a 2.5-micron-diameter cutoff was used to remove large particles. Carbon dioxide concentration measurements were provided by a LI-840A CO_2 analyzer (Li-Cor Biosciences) to provide for 1-s time resolution.

The MAAP is a filter-based particle light absorption measurement instrument. It uses multiple light-emitting diodes (LEDs) centered at a wavelength of 640nm to determine particle light absorption via carefully correcting the influence of light scattering at several scattering angles. The obtained light absorption is linearly proportional to non-volatile soot mass. A mass absorption coefficient of 6.4 m2/g is normally used to determine non-volatile particle mass (nvPMm). Given the lack of alternate instrumentation, the MAAP instrument was used instead of the SAE E-31 recommended instruments (MSS or LII) for the measurement of nvPMm.

Table H-1. Particulate matter instrumentation manifest.

Instrument	Full name or description	What is being measured?
EsCOM	Engine soot and carbon dioxide optical monitor	Carbon dioxide, particle sizing, extinction
SP-AMS	Soot particle aerosol mass spectrometer	Particle size and chemical composition
CAPS-PM-SSA	Cavity attenuated phase shift spectroscopy of particle single scattering albedo and total extinction	Particle single scattering albedo, total extinction
MAAP	Multi-angle absorption photometer	Black carbon mass loading/ non-volatile particulate matter mass (nvPMm)
APC	AVL model particle counter	Non-volatile particulate matter number concentration (nvPMn)
EEPS	Engine exhaust particle sizer	Particle size distribution and total particulate matter mass and number (tPMm* and tPMn)
CO_2 LI-COR	Non-dispersive infrared gas analyzer for carbon dioxide	Carbon dioxide (particle inlet)

*see the Engine Exhaust Particle Sizer material provided later in this appendix.

Copyright National Academy of Sciences. All rights reserved.

The CAPS technique, similar in nature to cavity ring-down spectroscopy, relies on the use of a sample cell employing high reflectivity mirrors. In this particular application, square-wave modulated red light (~635 nm) from an LED is directed through one mirror and into the sample cell. The distortion in the square wave caused by the effective optical path-length within the cavity (~1 km) is measured as a phase shift in the signal as detected by a photodiode located behind the second mirror. The presence of particles in the cell causes a change in the phase shift, which is related to the total extinction (the sum of scattering and absorption), ε_{part}, by the following relationship:

$$\cot\theta - \cot\theta_0 = \frac{c}{2\pi f}\varepsilon_{part} \qquad \text{(Eq. H-1)}$$

where

θ_0 is the phase shift measured in the absence of particles,
c is the speed of light, and
f is the modulation frequency.

The CAPS PM_{ex} extinction monitor has a detection level of less than 0.3 μg m-3 with a time response of 1 second.

Total particle mass and number (tPMm and tPMn), including both volatile and non-volatile particles were measured using a TSI model 3096 engine exhaust particle sizer (EEPS). This instrument uses multiple electrometers to measure particle size distributions 10 times a second. The size range is 5.6 to 560 nm with a resolution of 16 channels per decade for 32 channels in total. The instrument consists of a cyclone at the inlet to remove particles >1 μm. The sample flow is mixed with ions generated using a corona discharge to produce a predictable particle charge level vs. particle size. The charged particles then flow between a charged central rod and an outer cylinder consisting of a series of individual electrometers. The electrometers nearer the sample inlet detect the smaller particles, whereas those nearer the outlet detect the larger particles, thereby providing an electrical mobility-based particle size distribution.

Non-volatile PM number (nvPMn) was measured using an AVL particle counter (APC), in compliance with the AIR6241 recommendations (SAE International). The APC reports particle number concentration as the number of particles per cubic centimeter. To eliminate contributions of volatile particles, the device uses a two-stage dilution process coupled with a volatile particle remover (VPR). The sample is first diluted with air heated to 150°C using a chopper diluter. The sample then flows through a VPR consisting of a catalytic stripper at 350°C to convert gaseous hydrocarbons to carbon dioxide. The sample is then cooled to <35°C before entering a TSI 3790E condensation particle counter (CPC), which uses a light-scattering detector to count the non-volatile particles in the flow.

At present, AMS is the only available instrument capable of simultaneously providing quantitative size and chemical mass loading information in real time for non-refractory sub-micron aerosol particles. It uses an aerodynamic lens to focus the particles into a narrow beam that is then introduced into a high vacuum chamber while the air is differentially pumped. Volatile and semi-volatile species in/on the particles as well as non-volatile black carbon composition are vaporized via optical pumping from a high-power continuous-wave Nd:YAG laser at 1064 nm. The vaporized species are then ionized by the impact of energetic electrons (70 eV). The ions formed are analyzed by a time-of-flight mass spectrometer (Tofwerk, Thun, Switzerland). Particle aerodynamic size is determined via particle time-of-flight.

The Engine Exhaust Particle Sizer™ (EEPS™) spectrometer is a fast-response, high-resolution instrument that measures the size distribution and number concentration of engine exhaust particle emissions in the range of 5.6 to 560 nanometers. It offers the fastest time resolution available—10 times per second—which makes it well suited for dynamic and transient tests. The EEPS

Copyright National Academy of Sciences. All rights reserved.

spectrometer operates at 10 L/min, which greatly reduces particle sampling losses due to diffusion. Additionally, it operates at ambient pressure to eliminate any concern about evaporating volatile and semi-volatile particles.

An EEPS spectrometer (Model 3090 from TSI Inc.) was used in this research to determine particle size distribution from the GA aircraft engine exhausts. It measures particle count from 5.6 to 560 nanometers, reporting a total of 32 channels (16 channels of size per decade). Integrating over the 32 channels, the research team obtained total particle concentration from the particle size distribution. In addition, once an effective density, weightings for surface area, volume, and mass (PM) are entered into the EEPS data analysis software, the software will report the calculated statistics via numerical integration over the 32 channels. The calculated properties include median diameter, geometric mean diameter, and total particle surface, volume and mass. In this report, total particle concentration and mass were obtained via the EEPS measurements.

Compared to the direct measurement of non-volatile black carbon mass from the MAAP, the EEPS results on particle mass are calculated values, which are based on assumed input parameters (e.g., particle effective density and shape).

Copyright National Academy of Sciences. All rights reserved.

APPENDIX I

PM Line Losses

Instrument Considerations

Given that nvPM mass emissions from modern combustion engines are now often near the limit of detection for practical instrumentation that measures mass, particle number concentration is being used to provide a more sensitive measurement of engine emissions. The AVL Advanced Particle Counter (APC) for aircraft applications is a real-time non-volatile particle number counting instrument that reports particle number concentration values in units of particles per cubic centimeter. By measuring solid particles, the dependence on the sampling system is reduced and the sample is more stable over time. To eliminate contributions of volatile particles, the device employs a two-stage dilution process coupled with a volatile particle remover (VPR). During first-stage dilution, dilution air heated to 150°C is added to the exhaust sample with a chopper diluter. Then the sample is transported to a catalytic stripper or VPR, maintained at 350°C. Material present as homogeneous volatile particles or volatile coatings on particles are eliminated by vaporization and subsequently oxidation, leaving only solid particles. After volatile removal in the catalytic stripper, second-stage dilution cools the sample before it enters a condensation particle counter (CPC). In the CPC, butanol is condensed on the particles, which causes them to grow, thereby enabling light scattering of a laser beam to be used to count particles.

Several factors affect the value reported by the APC. Measurement of particles is always subject to losses in the sample line. In the APC, significant losses also occur in the VPR, which is a catalytic stripper containing many small-diameter passages. The losses are measured in the laboratory as a function of particle size and reported for each individual instrument by the vendor. Typical losses in an AVL APC are ~50%. In addition to the losses, the reported number concentration depends on the counting efficiency curve of the CPC. The APC has a counting efficiency of ≥50% at 10 nm and ≥90% at 15 nm. A CPC with a different counting efficiency curve would report a different concentration. If particle concentrations are to be compared, it is important to understand the instrument cut offs, counting efficiency curve, and line losses associated with the measurements.

Inlet/Sample Line Losses

The particle instruments that perform measurements on samples extracted from a flow are dependent on the sampling system used to make the measurement. Particles, by definition, have a minimum size of nanometers and, therefore, do not have molecular properties. Unlike molecules, particles do not necessarily follow the streamlines of a flow. Particle transport is susceptible to physical mechanisms that result in particle loss by changing the trajectory of the particle such that the particle deposits on the wall of the transport tubing. Except for thermophoresis, the particle losses are size dependent. Thermophoretic loss occurs when the temperature of the

Copyright National Academy of Sciences. All rights reserved.

74 Exhaust Emissions from In-Use General Aviation Aircraft

wall is less than the gas, which is often the case when engine exhaust is sampled. Particle loss due to turbulent diffusion is the largest size-dependent loss where the loss is highest for the smallest particles. Other size-dependent losses are due to inertia, gravity, bending of the tubing, and electrostatics. Particle sizes of combustion-generated particles as they exit the device are generally less than 500nm; therefore, losses due to thermophoresis and diffusion dominate.

In recognition of the importance of particle loss in sampling systems, in 2008 a spreadsheet model was developed at United Technologies Research Center (UTRC) to predict particle transport as a function of particle size. This model could then be used to assess the performance of various sample line configurations (Liscinsky et al. 2010). The resulting Excel-based tool assumes steady-state flow and calculates particle losses using standard equations taken from Yook and Pui (Yook and Pui 2005) and Willeke and Baron (Baron and Willeke 2001). Although Baron created a very powerful and widely used spreadsheet tool called Aerocalc (Baron 2001) that contains many of the same particle transport calculations, Aerocalc treats each loss mechanism as a separate calculation. The UTRC tool simplified the analysis of a sample line by integrating the effect of five different particle loss mechanisms over ten different sample line sections. The UTRC tool predicts transport efficiency for particles over a range of sizes, based on characteristics of the flow, the transport line, and ambient conditions.

The UTRC model was validated in laboratory testing during development. Subsequently, it has been found that experimental data taken on practical sampling systems at campaigns sponsored by NASA APEX and AFFEX and EPA VARIAnT have agreed better than expected with the modeling predictions. Given that the measurement of particle loss is tedious and prone to error, the use of a predictive tool for line loss has evolved to become a recommended practice. SAE E-31 is developing an Aerospace Information Report, AIR6504, which details the entire theory of line loss in the standard sampling system used to measure nvPM from aircraft engines as described in AIR6241 (SAE International). When published, the tool will expand on the UTRC tool, include losses in the VPR, and account for CPC counting efficiency.

Figure I-1 is a schematic of the particle sampling system used during the first campaign (October 2014). The total sample flow rate was 18 SLPM, with a line length of 40ft from the tripod collection probe to the instrument trailer interface. The setup for the second campaign (June 2015) has a similar instrument setup but the third campaign (October 2015) used a longer line length (140ft) from the tripod collection probe to the trailer interface. Figure I-2 shows the losses as a function of particle size predicted by the UTRC line loss tool as a function of loss mechanism. The plots show that the shorter line had higher transport as expected; however, the smallest particles have the highest losses and below 20 nm ~50% of the particles are not transported in the shorter line compared to ~30% in the longer line. Also the losses increase dramatically when the particles are less than 20nm and, in the longer sample line, the losses of 10nm particles are 95%. Given that the measured particle size distributions indicate that most of the particles are less than 20nm, comparison of data among the different sampling systems requires a correction for line loss. Furthermore, to use the particle measurements as input to models of particulate emissions requires a correction for particle number that is at least a factor of 2.

Copyright National Academy of Sciences. All rights reserved.

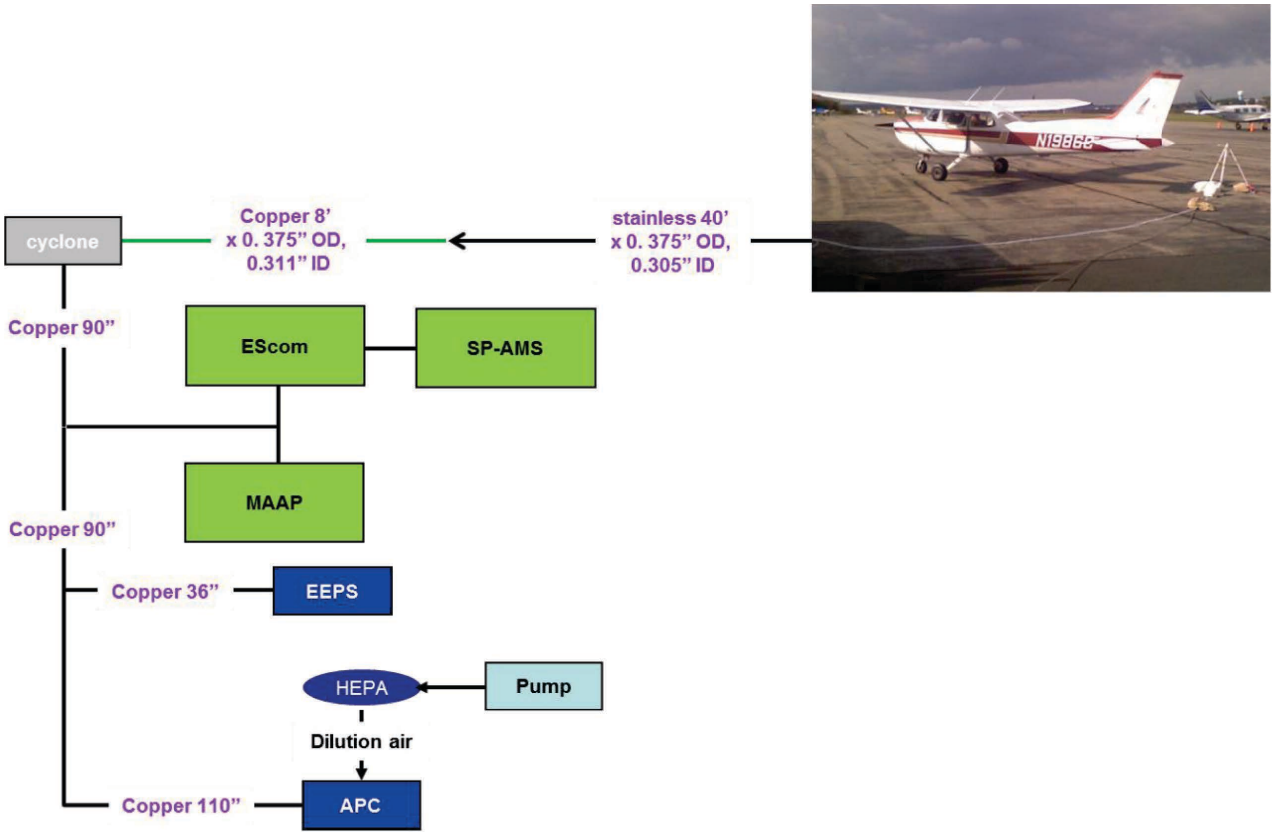

Figure I-1. Layout of the Particle Sampling System for Campaign 1.

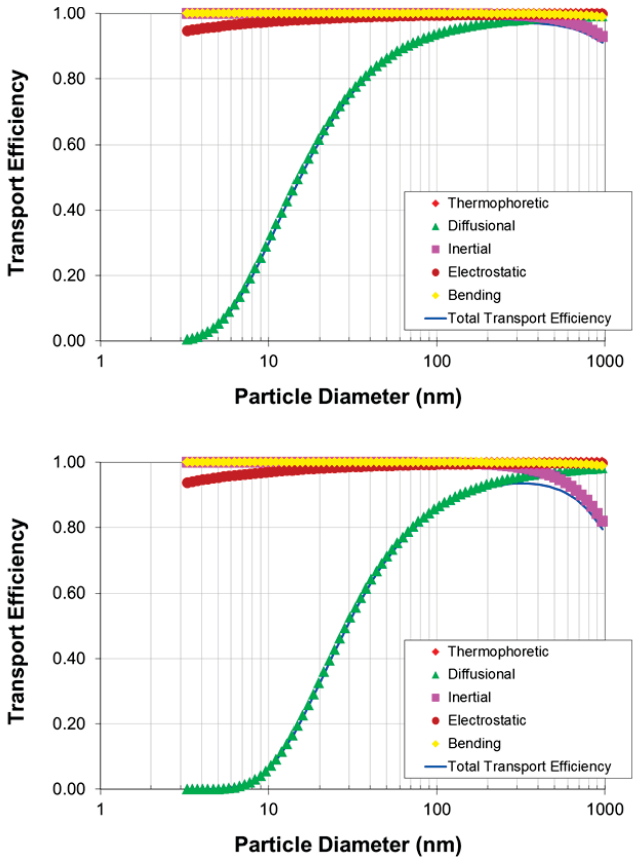

***Figure I-2. Predicted Particle Losses for Campaign 1 and 2* (top plot) *and 3* (bottom plot).**

Copyright National Academy of Sciences. All rights reserved.

APPENDIX J

Estimating Fuel Flows for Piston Engines

Many of the aircraft measured for ACRP Project 02-54 engine tests had no fuel flow gauge. Furthermore, aircraft with analog fuel flow gauges as opposed to digital gauges often do not register fuel flow at idle (dial is below the lowest mark). In these cases, other methods must be used to estimate a fuel flow for the engine state of interest.

Aircraft engine operating manuals typically display some sort of plot or a combination of plots that allow the pilot to relate engine RPM to fuel flow. These plots typically start at 50% power and above and tend to be for a mixture full-rich setting. For aircraft with constant speed propellers (i.e., variable pitch propellers), the manifold pressure for a given RPM is required to estimate a fuel flow. In these cases, a limited set of engine states, propeller RPM, and manifold pressures were chosen based on the pilot's operation of the test aircraft and the manual's description of sample operating conditions. For example, many aircraft manuals state the fuel flow for a representative cruise state with 24 inches of manifold pressure and 2400 RPM.

None of the operating manuals investigated for this report mention fuel flow at taxi and/or idle. A data point for fuel flow at low power states is important, however, in anchoring the fuel flow estimate. Thus, when available, the manual fuel flows were supplemented with FOCA data for the taxi state, which is a measured value. FOCA defines the taxi state as whatever the operating manual states. The RPM for the taxi state is set at 1000 RPM for most aircraft, based on pilot's actual use. When no FOCA data was available for the aircraft in question, the closest engine type was chosen, taking into account the maximum fuel flow, the engine horsepower, and the compression ratio. In some cases, the engine manual specifies enough operational points that a fuel flow at taxi is not required to anchor a fit of these data points.

Combining the data described above produces plots that relate the fractional fuel flow (fuel flow/max fuel flow) to the fractional engine RPM (RPM/max RPM). An exponential fit to this data is found to be more appropriate than multiple polynomial fits because an exponential fit allows fitting the entire RPM space with a single function. This fit then allows for the fuel flow for any given engine RPM to be estimated. A different plot is generated for distinct engine types, with some engine subtypes grouped as in the engine manuals (e.g., Lycoming O-320-A, -E are grouped separately from Lycoming O-320-B, -D).

Figure J-1 plots the equations used to estimate fuel flows when no appropriate cockpit data was available. Fractional fuel flows for a great variety of engine types follow a similarly shaped curve when the data is put in these relative terms. 95% confidence limits for the average of these curve fits are shown as the shaded grey region. Uncertainties are greatest at low engine states (0.2 – 0.6 fractional engine RPM). At these fractional engine RPMs, the fractional fuel flow 95% confidence limits are ± 0.05 (or 5%).

This method of determining fuel flow can be verified with engines for which fuel gauges are installed [e.g., aircraft with a Lycoming O-360-A4M engine (Figure J-2)]. The measured fuel

Copyright National Academy of Sciences. All rights reserved.

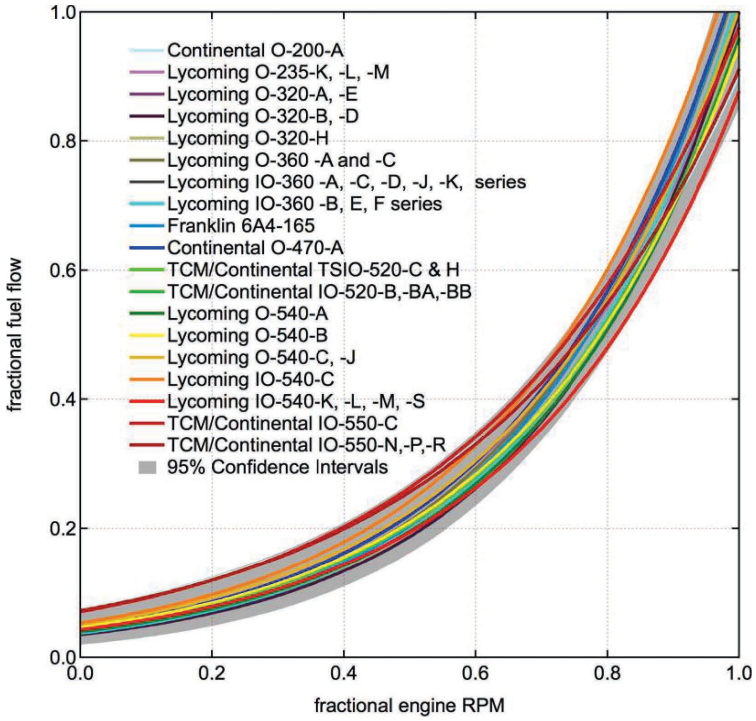

Figure J-1. Plot of exponential equations used to estimate fuel flows for various engine types.

flows in this aircraft agree well with the exponentially modeled fuel flows, with the exception of the cruise engine state—The pilot executed a rich-cruise state which shows a fuel flow better aligned with the modeled flows. The cruise engine state is typically a leaned state, which differs from the mixture full-rich data used in creating the modeled fuel flows.

In cases where no cockpit fuel flow is available, this method of estimating fuel flow produces numbers that agree with experienced pilots' best guesses for fuel flow, even at idle and taxi. For

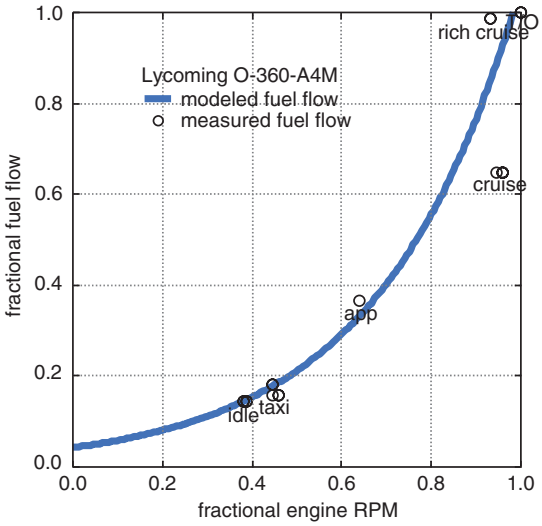

Figure J-2. Measured fuel flow vs exponentially modeled fuel flow for a Lycoming O-360-A4M engine.

Copyright National Academy of Sciences. All rights reserved.

78 Exhaust Emissions from In-Use General Aviation Aircraft

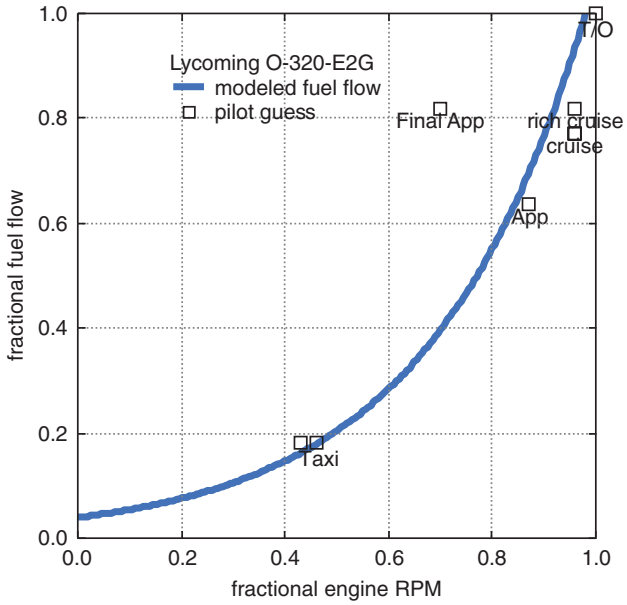

Figure J-3. Pilot guess at fuel flow vs exponentially modeled fuel flow.

example, for the aircraft with a Lycoming O-320-E2G engine (Figure J-3), the pilot's guess for fuel flow for all states is within 10% of the simulated value for all but the final approach engine state. This discrepancy is attributed to a bad guess on the part of the pilot.

All of the above is taken into consideration in the protocol for assigning a fuel flow to a test point. Figure J-4 illustrates this protocol.

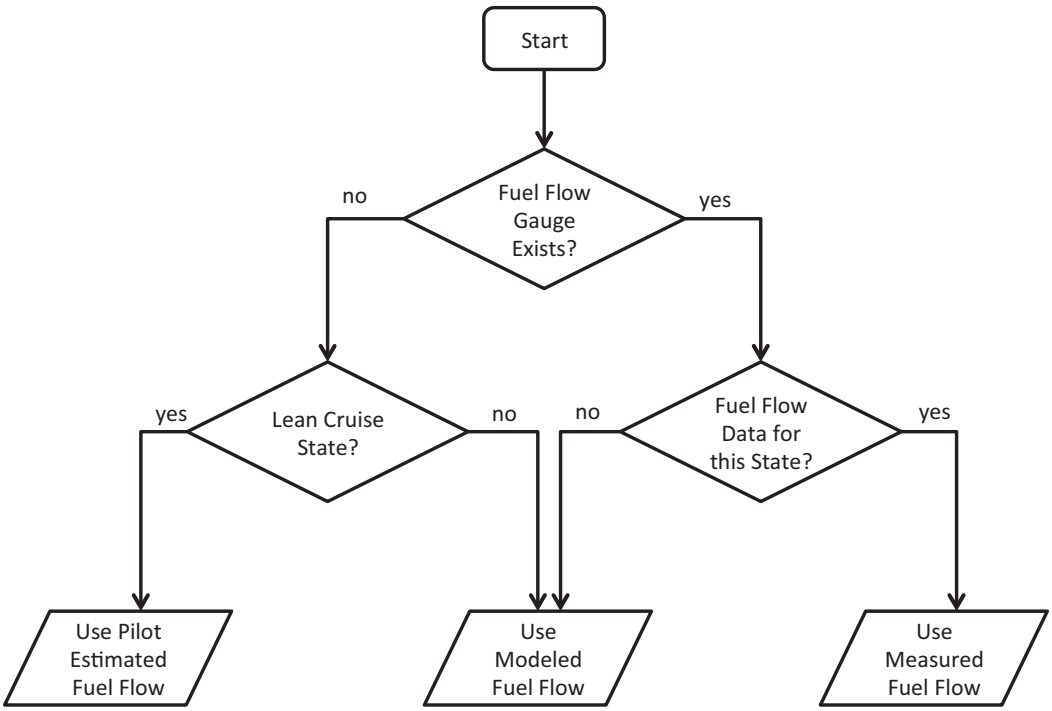

Figure J-4. Flow chart for determining best fuel flow to use for a given test point.

Copyright National Academy of Sciences. All rights reserved.

APPENDIX K

Carbon Content of AVGAS 100 LL

The carbon content of aircraft fuel is essential in calculating accurate emission indices. The usual carbon content used in aircraft emissions work is 3160 g CO_2/kg fuel, which assumes a hydrogen/carbon ratio, or α, of 1.9. Although carbon content is appropriate for kerosene-based Jet A fuel, it is not necessarily appropriate for AVGAS 100LL. FOCA uses a carbon content of 3118 g CO_2/kg fuel ($\alpha = 2.086$) based on hydrocarbon information from the fuel supplier Chevron (FOCA 2007b). Table K-1 lists the manufacturer's information available for the AVGAS 100LL fuel present at one of the test airports. No carbon content information was available.

To verify the carbon content of the AVGAS used in these engine tests, two fuel tests were done on collected samples. Under-wing samples (directly from the aircraft's fuel reservoir) were taken from each tested aircraft, and additional samples were taken from each airport's fuel dispensaries. However, carbon content testing was performed on only two samples due to the high cost of testing. The two samples sent for testing were

1. **FBO Mix**: A mix of equal volumes of fuel from three separate FBOs,
2. **High Aromatics**: An under-wing sample from an aircraft showing high amounts of aromatics in the fuel.

Two standardized tests from the American Society for Testing and Materials (ASTM) were requested:

1. ASTM D5291: Determination of Carbon and Hydrogen in Petroleum Products and Lubricants and
2. ASTM D5769: Benzene, Toluene and Total Aromatics in Finished Gasoline by GCMS

Results are shown in Table K-2. The fuel from the mix of FBOs has a somewhat lower carbon content than either the Jet A (3.0% lower) or the FOCA AVGAS results (3.4% lower). The high-aromatics fuel sample is similarly lower in carbon content. The research team use 3067 g/kg fuel as the carbon content of AVGAS 100LL in all results presented in this report and 3160 g/kg fuel for Jet A. This comparison of carbon contents shows only small differences between samples that should not significantly affect the calculated emission indices: errors in EIs are less than ~3.4%.

Although differences in carbon content between different fuels are small, the differences in aromatics may be large. The ASTM D5769 method used in the detection of aromatics cannot detect levels below 10%, and so the difference between the FBO mix sample and the high aromatic sample may be anywhere between 4.5% and 14.5%. The presence of aromatics, specifically toluene, in a subset of fuel samples is investigated in more detail in the section on fuel additives.

Copyright National Academy of Sciences. All rights reserved.

80 Exhaust Emissions from In-Use General Aviation Aircraft

Table K-1. Manufacturer's specification sheet for AVGAS 100LL.

Shell AVGAS Specification	Max Value	Min Value
Knock Rating, Lean Mixture (Motor Method) Octane Number		99.5
Knock Rating, Rich Mixture (Supercharge Method) Performance Number		130
Freezing Point C	-58	
Distillation end point °C	170	
Reid Vapour Pressure @ 38 °C kPa	49	38
Sulphur content %m	0.05	
Tetraethyl lead content g Pb/L		
Avgas 100	0.85	
Avgas 100LL	0.56	
Colour Avgas 100 Avgas 100LL	Green Blue	

Table K-2. Carbon content of aircraft fuel.

Specification	Jet A	AVGAS 100LL FOCA	AVGAS 100LL FBO Mix	AVGAS 100LL high aromatics
mass % H (m/m)	13.8%	8.03%	16.3%	14.9%
α (H/C ratio)	1.901	1.857	2.320	2.086
Fuel C (g/kg Fuel)	862.4	865.2	837.0	851.0
Fuel CO_2 (g/kg Fuel)	3160	3170	3067	3118
Aromatics (v/v)			<10%	14.50%

Copyright National Academy of Sciences. All rights reserved.

APPENDIX L

Hypothetical Airport Engine Mapping

An important task in computing an airport's emissions burden is to map the aircraft to emissions data available in various databases. In Table L-1, the hypothetical airport used for the sensitivity analysis is mapped to engines from

1. The set of experimentally sampled planes
2. Data available in EDMS/AEDT

The comments column explains how these mappings and substitutions were done.

Table L-1. Hypothetical fleet matched with sampled engines.

Hypothetical Fleet				Sampled Engine Model	EDMS/AEDT Match			Comments
Category	Aircraft Make	Aircraft Model	Engine Family		Aircraft Make	Aircraft Model	Engine Model	
SEP	CESSNA	172	O-320	O-320	Cessna	172	O-320	Exact match with Hypothetical Fleet and sampled aircraft/engine.
	CESSNA	182	O-470	O-470	Cessna	182	IO-360-B	No O-470 in EDMS; chose IO-360 because (only option for Cessna 182) similar horsepower (hp).
	CESSNA	150	O-200	O-200	Cessna	150	O-200	Exact match with Hypothetical Fleet and sampled aircraft/engine.
	PIPER	PA-28	O-320	O-320	Piper	PA-28	O-320	Exact match with Hypothetical Fleet and sampled aircraft/engine.
	CESSNA	172	O-300	--	Cessna	172	O-320	No O-300 in EDMS; chose O-320 because similar hp.
	PIPER	PA-28	O&VO-360	O-360	Piper	PA-28	IO-360-B	No O-360 in EDMS; chose IO-360 because similar hp.
	CIRRUS DESIGN CORP	SR22	IO-550	IO-550	Cirrus Design Corp	SR22	TIO-540-J2B2	No IO-550 in EDMS; chose TIO-540-J2B2 because (only option for SR 22) similar hp.
	MOONEY	M20	IO-360	IO-360	Cessna	337	IO-360-B	Exact Engine match; matched to Cessna 337 because M20 engine hp too high and Cessna 337 has correct engine and is similar aircraft.

(continued on next page)

Copyright National Academy of Sciences. All rights reserved.

Table L-1. (Continued).

Hypothetical Fleet					EDMS/AEDT Match			Comments
Category	Aircraft Make	Aircraft Model	Engine Family	Sampled Engine Model	Aircraft Make	Aircraft Model	Engine Model	
	PIPER	J3C-65	A&C65	--	Piper	PA-23	TIO-540-J2B2	No A&C65 in EDMS; no Piper J3C-65 in EDMS; chose Piper 23, as this was the closest Piper.
	CESSNA	152	O-235	O-235	Cessna	150	O-200	No O-235 in EDMS; no Cessna 152 in EDMS; chose Cessna 150 because similar weight; chose O-200 because (only option for Cessna 150) similar hp.
	CESSNA	180	O-470	O-470	Cessna	182	IO-360-B	No O-470 in EDMS; No Cessna 180 in EDMS; chose Cessna 182 because similar weight; chose IO-360 because (only option for Cessna 182) similar hp.
	CESSNA	172	IO-360	IO-360	Cessna	172	IO-360-B	Exact match with Hypothetical Fleet and sampled aircraft/engine.
	PIPER	PA-28	IO-360	IO-360	Piper	PA-28	IO-360-B	Exact match with Hypothetical Fleet and sampled aircraft/engine.
	PIPER	PA-22	O-320	O-320	Piper	PA-28	O-320	No Piper 22 in EDMS; matched with PA-28 because similar weight and power.
	BEECH	35	IO-520	IO-520	Beech	36	TIO-540-J2B2	No IO-520 in EDMS; no Beech 35 in EDMS; Beech Bonanza 36 is similar aircraft; chose TIO-540 because (only option for Bonanza 36) similar hp.
	PIPER	PA-18	O-320	O-320	Piper	PA-28	O-320	Exact engine match; no Piper 18 in EDMS; matched to Piper 28 because similar weight.
	CESSNA	170	C145	--	Piper	PA-28	O-320	No C145 in EDMS; no Cessna 170 in EDMS; matched to Piper 28 because similar weight; matched to O-320 because C145 is similar to O-300, which is similar to O-320.
	PIPER	PA-32	TIO-540	--	Piper	PA-32	TIO-540-J2B2	Exact match with EDMS.
	CESSNA	210	TSIO-520	TSIO-520	Cessna	210	TIO-540-J2B2	No TSIO-520 in EDMS; matched to TIO-540-J2B2 because (only option for 210) similar hp.
	AERONCA	7AC	A&C65	--	Piper	PA-23	TIO-540-J2B2	No A&C65 in EDMS; no Aeronca 7AC in EDMS; chose Piper 23, as Piper J2C and Aeronca 7AC are similar, and this was the closest to Piper J2C.

Copyright National Academy of Sciences. All rights reserved.

Table L-1. (Continued).

Hypothetical Fleet					EDMS/AEDT Match			Comments
Category	Aircraft Make	Aircraft Model	Engine Family	Sampled Engine Model	Aircraft Make	Aircraft Model	Engine Model	
	BEECH	35	IO-470	--	Beech	36	TIO-540-J2B2	No IO-470 in EDMS; no Beech 35 in EDMS; matched to Beech 36 because similar aircraft; matched to TIO-540 because (only option for Beech 36) similar hp.
	CESSNA	140	C85	--	Cessna	150	O-200	No C85 in EDMS; no Cessna 140 in EDMS; matched to Cessna 150 because similar aircraft; matched with O-200 because similar hp.
	CESSNA	182	IO-540	IO-540	Piper	PA-32	TIO-540-J2B2	No IO-540 in EDMS (only TIO-540); matched to Piper 32 because similar weight aircraft which had comparable engine; matched with TIO-540 because similar engine; Cessna 182 only had IO-360-B in EDMS which is not a comparable engine to the TIO-540.
	MOONEY	M20	O&VO-360	O-360	Mooney	M20	TSIO-360C	No O-360 in EDMS; chose TSIO-360C because (only option for M20) similar hp.
	PIPER	PA-28	O-540	O-540	Piper	PA-24	TIO-540-J2B2	No O-540 in EDMS; matched with Piper 24 because similar weight to the Piper 28 and has IO-540 engine.
MEP	CESSNA	310	IO-470	--	Cessna	310	TIO-540-J2B2	No IO-470 in EDMS; matched with Cessna 310 with TIO-540 because similar hp.
	BEECH	95	IO-470	--	Cessna	310	TIO-540-J2B2	No IO-470 in EDMS; no Beech 95 in EDMS; Matched with Cessna 310 because similar aircraft; matched with TIO-540 because (only option for 310) similar hp.
	PIPER	PA-30	IO-320	--	Piper	PA-28	IO-320-D1AD	Exact match with EDMS.
	PIPER	PA-31	TIO-540	--	Piper	PA-31	TIO-540-J2B2	Exact match with EDMS.
	PIPER	PA-23	TIO-540	--	Piper	PA-23	TIO-540-J2B2	Exact match with EDMS.
	PIPER	PA-34	TSIO-360	--	Piper	PA-34	TSIO-360C	Exact match with EDMS.
	CESSNA	421	GTSIO-520	--	Cessna	421	TIO-540-J2B2	No GTSIO-520 in EDMS; matched to TSIO-540 because (only option for 421) similar hp.

(continued on next page)

Copyright National Academy of Sciences. All rights reserved.

Table L-1. (Continued).

Hypothetical Fleet					EDMS/AEDT Match			Comments
Category	Aircraft Make	Aircraft Model	Engine Family	**Sampled Engine Model**	Aircraft Make	Aircraft Model	Engine Model	
	CESSNA	340	TSIO-520	TSIO-520	Cessna	340	TIO-540-J2B2	No TSIO-520 in EDMS; matched to TIO-540-J2B2 because (only option for 340) similar hp.
	CESSNA	337	IO-360	IO-360	Cessna	337	IO-360-B	Exact match with Hypothetical Fleet and sampled aircraft/engine.
	PIPER	PA-23	O-320	O-320	Cessna	172	O-320	Exact engine match; matched to Cessna 172 because Piper 23 did not have O-320 option in EDMS (only TIO-540) which was a much more powerful engine; Cessna 172 is a more comparable aircraft to Piper 23 than Piper 28 is (which also had O-320, but was lighter aircraft).
	BEECH	58	IO-520	IO-520	Beech	58	TIO-540-J2B2	No IO-520 in EDMS; matched to TIO-540 because (only option for Beech 58) similar hp.
	CESSNA	414	TSIO-520	TSIO-520	Cessna	414	TIO-540-J2B2	No TSIO-520 in EDMS; matched to TIO-540 because (only option for Cessna 414) similar hp.
SETP	CESSNA	208	PT6A	PT6A-60A	Cessna	208	PT6A-114	Exact match with Hypothetical Fleet and sampled aircraft/engine.
	PILATUS	PC-12	PT6A-67	--	Pilatus	PC-12	PT6A-67	Exact match with EDMS.
	EADS SOCATA	TBM 700	PT6A-66	--	EADS Socata	TBM 700	PT6A-60	No PT6A-66 in EDMS; matched to PT6A-60 because similar hp.

Copyright National Academy of Sciences. All rights reserved.

APPENDIX M

Terminology and Abbreviations

APC:	Aircraft Particulate Counter. An instrument that measures non-volatile PM number
CAPS PM_{EX}:	Cavity-attenuated phase shift PM extinction monitor.
CH_4:	methane, the smallest hydrocarbon.
CHT:	Cylinder head temperature.
CO:	carbon monoxide, a combustion product.
CO_2:	carbon dioxide, a combustion product.
EEPS:	Engine Exhaust Particulate Sizer. An instrument that measures mobility-based particle size distribution
EGT:	Exhaust gas temperature
EI:	Emission index. A measure of the emissions of a given type from an engine. Expressed as grams of the species of interest per kilogram of fuel consumed.
FID:	Flame Ionization Detector. The instrument that measures total hydrocarbon (HC).
FOCA:	Swiss Federal Office of Civil Aviation. This organization has produced an extensive report on piston engine aircraft emissions, along with emission indices for a selection of piston engines.
HC:	Total hydrocarbons (also THC), a class of emission species that includes methane, ethane, longer chain alkanes, alkenes, aromatics, etc. The mass used in calculating HC emissions is that of CH_4 (methane), by convention.
HP:	Horsepower
HR-ToF-AMS:	High-resolution time-of-flight aerosol mass spectrometer.
ICAO:	International Civil Aviation Organization. This US-based organization has compiled an extensive database of emission factors for turbofan engines (aka jet engines).
MAAP:	Multi-Angle Absorption Photometer. The instrument that measures non-volatile PM mass
Mixer:	controls the mixture in a normally aspirated (non-fuel-injected) piston engine
Mixture:	the mix/proportion of fuel/air in an engine
NO_x:	Oxides of nitrogen, a side-product of combustion. NO_x includes both NO and NO_2. The mass used in calculating NO_x emissions is that of NO_2, by convention.
nvPMm:	non-volatile PM mass
nvPMn:	non-volatile PM number
PM:	Particulate matter.
PTR-MS:	Proton-Transfer-Reaction Mass Spectrometry. The method used to measure many of the component hydrocarbons in exhaust such as benzene and toluene.

Copyright National Academy of Sciences. All rights reserved.

RPM:	rotations per minute
SN:	Smoke number. Outdated measure of PM.
Throttle:	controls the airflow to the engine and is used to set the propeller RPM in a piston engine.
tPMn:	Total PM number (includes volatile and non-volatile particles)
tPMm:	Total PM mass (includes volatile and non-volatile particles)
UHC:	Total unburned hydrocarbons (used interchangeably with HC)

Copyright National Academy of Sciences. All rights reserved.

APPENDIX N

References

Anderson, B. E., et al. 2006. *APEX Report*, NASA/TM—2006-214392. National Aeronautics and Space Administration. Cleveland, OH.

Baron, P. A., 2001. *Aerocalc* (3-Nov-01). http://aerosols.wustl.edu/AAARworkshop08/software/AEROCALC-11-3-03.xls.

Baron, P. A., and Willeke, K. 2001. *Aerosol Measurement: Principles, Techniques, and Applications*. 2 ed: Wiley.

DuBois, D., and Paynter, G. C. 2006. ""Fuel Flow Method2" for Estimating Aircraft Emissions." *SAE Technical Paper Series*. 2006-01-1987:14.

EPA. 1989. *AP-42: Compilation of Air Pollutant Emission Factors*. Environmental Protection Agency. Washington, D.C. http://www.epa.gov/oms/ap42.htm.

FOCA. 2007a. *Aircraft Piston Engine Emissions Summary Report*, 0 / 3/33/33-05-003.022. Switzerland: Federal Office of Civil Aviation FOCA.

FOCA. 2007b. *Aircraft Piston Engine Emissions. Appendix 3: Power Settings and Procedures for Static Ground Measurements*, 0 / 3/33/33-05-003 ECERT. Switzerland: Federal Office of Civil Aviation FOCA.

FOCA. 2007c. *Aircraft Piston Engine Emissions. Appendix 5: Calculation of Emission Factors*, 0 / 3/33/33-05-003 ECERT. Switzerland: Federal Office of Civil Aviation FOCA.

Gleitsmann, G., and Zellner, R. 1998. "The Effects of Ambient Temperature and Relative Humidity on Particle Formation in the Jet Regime of Commercial Aircrafts: A Modelling Study." *Atmos. Environ.* 32 (18): 3079–3087.

Heiken, J. 2015. *ACRP Report 133: Best Practices Guidebook for Preparing Lead Emission Inventories from Piston-Powered Aircraft with the Emission Inventory Analysis Tool*, ISBN 978-0-309-30862-5. Transportation Research Board of the National Academies. Washington, DC. http://onlinepubs.trb.org/Onlinepubs/acrp/acrp_rpt_133.pdf.

Herndon, S., et al. 2012. *ACRP Report 63: Measurement of Gaseous HAP Emissions from Idling Aircraft as a Function of Engine and Ambient Conditions*, ISBN 978-0-309-21401-8. Transportation Research Board of the National Academies. Washington, DC.

ICAO. 2013. "ICAO Engine Exhaust Emissions Databank, Issue 19." International Civil Aviation Organization, Last Modified 04/15/2013 Accessed 01/07/2013.

Kerrebrock, J. L. 1992. *Aircraft Engines and Gas Turbines*. Cambridge, Massachusetts: The MIT Press.

Koopmann, J., et al. 2015. *Aviation Environmental Design Tool (AEDT) Version 2b User Guide*. USDOT, FAA. Washington, D.C. https://aedt.faa.gov/Documents/UserGuide.pdf (accessed 03/17/2016).

Liscinsky, D. S., et al. 2010. *Effect of Particle Sampling Technique and Transport on Particle Penetration at the High Temperature and Pressure Conditions Found in Gas Turbine Combustors and Engines*, NASA/CR-2010-NNC07CB03C. Center, Glenn Research, National Aeronautics and Space Administration. Cleveland, OH.

Lobo, P., et al. 2015. "Measurement of Aircraft Engine Non-Volatile PM Emissions: Results of the Aviation-Particle Regulatory Instrumentation Demonstration Experiment (A-PRIDE) 4 Campaign." *Aerosol Sci. Technol.* 49 (7):472–484. DOI: 10.1080/02786826.2015.1047012.

SAE International. "Air 6241 Procedure for the Continuous Sampling and Measurement of Non-Volatile Particle Emissions from Aircraft Turbine Engines." Available from SAE International, 400 Commonwealth Drive, Warrendale, PA 15096-0001, Tel: 877-606-7323 (inside USA and Canada) or 724-776-4970 (outside USA), www.sae.org

Santoni, G. W., et al. 2011. "Aircraft Emissions of Methane and Nitrous Oxide During the Alternative Aviation Fuel Experiment." *Environ. Sci. Technol.* 45 (16):7075–7082. DOI: 10.1021/es200897h

Copyright National Academy of Sciences. All rights reserved.

Schauer, J. J., et al. 2002. "Measurement of Emissions from Air Pollution Sources. 5. C1–C32 Organic Compounds from Gasoline-Powered Motor Vehicles." *Environ. Sci. Technol.* 36 (6):1169–1180. DOI: 10.1021/es0108077.

Timko, M. T., et al. 2010. "Gas Turbine Engine Emissions—Part I: Volatile Organic Compounds and Nitrogen Oxides." *J. Eng. Gas Turb. Power*. 132 (6):061504. DOI: 10.1115/1.4000131.

Timko, M. T., et al. 2010. "Gas Turbine Engine Emissions—Part II: Chemical Properties of Particulate Matter." *J. Eng. Gas Turb. Power*. 132 (6):061505-061505. DOI: 10.1115/1.4000132.

Yook, S.-J., and Pui, D. Y. H. 2005. *Estimation of Penetration Efficiencies through NASA Sampling Lines*, submitted to NASA Glenn Research Center. National Aeronautics and Space Administration. Cleveland, OH.

Zeldovitch, Y. B. 1946. "The Oxidation of Nitrogen in Combustion Explosions." *Acta Physicochimica.* 21: 577–628.

Copyright National Academy of Sciences. All rights reserved.

APPENDIX O

List of Data Products

Two supplementary data products that accompany this report are available for download from the ACRP website http://www.trb.org/Publications/PubsACRPProjectReportsAll.aspx.

1. Spreadsheet containing emissions data "ACRP_02_54_emissions.xlsx" (Microsoft Excel.xlsx format).*
   i. The "Emissions" sheet containing average emission indices and fuel flows for each measured aircraft. Recommended substitutions to current data, engine family averages, and upper limits are also included. These tables are reproduced in their entirety in Appendix P.
   ii. The "PlumesPublish" sheet contains emission indices for each measured test point. The included data are Engine ID, Engine Type, Plume Index, Engine State, Start Time, Stop Time, Fuel Flow, % of Max Fuel Flow, Percent of Max Propeller RPM or % of Max Rated Thrust for Turbos, EI CO, EI HC (as CH_4), EI NO_x (as NO_2), EI PM # non-volatile (via APC), EI PM # Total (via EEPS), EI PM mass non-volatile (via MAAP), EI PM mass Total (via EEPS), EI CH_4, EI C_2H_6, EI C_2H_4, EI C_2H_2, EI benzene, EI Toluene, EI C2benzenes, EI naphthalene, EI acetone, EI acetaldehyde, EI formaldehyde, EI BC via SP-AMS, EI Org via SP-AMS, EI PbTot via SP-AMS, ambient temperature, and ambient pressure.
   iii. The "FuelFlows" sheet contains constants for the exponential fit to fuel flow, as described in Appendix J.
2. Presentation summarizing key findings (Microsoft PowerPoint.pptx format)

*Note that AEDT does not allow the saving of user-entered aircraft. Emissions indices and fuel flows reported in the Excel spreadsheet "Emissions" tab are appropriate for direct input into AEDT. A sample AEDT user-entered aircraft window is shown in Chapter 4, Sensitivity Analysis on Airport Emissions

Copyright National Academy of Sciences. All rights reserved.

APPENDIX P

Emission Index Data Tables

Several considerations apply to the data that follow:

1. Emission indices were calculated based on **a fuel composition of 3067 grams of CO_2 per kilogram of fuel** for AVGAS 100 LL and 3160 grams of CO_2 per kilogram of fuel for Jet A. The value for AVGAS was determined based on a fuel analysis of three AVGAS samples.
2. For safety reasons, including aircraft stability and engine temperature, **not all aircraft could achieve maximum power on the ground**. These states and other states not accessed are marked with the symbol "—".
3. Piston engine **power states have been defined based on how the pilot would usually operate the aircraft**. Two alternate measures of engine state are included: the fraction of maximum achieved propeller speed on the ground (% max RPM) and the fraction of maximum fuel flow (% max fuel flow). The fuel flow measure is expected to be most linear with thrust for propeller aircraft.
4. **Fuel flow gauges and readouts are not present in the cockpits of many aircraft**. When fuel flow data was not available, it was derived from engine manuals as described in Appendix J.
5. The research team included **four separate measures of PM emission indices**. These categories were based on recent recommendations and discussions of the SAE E-31 Committee on aircraft exhaust emission measurements and the ICAO CAEP Working Group 3 on emissions, but are extended to include total particle quantities as well as non-volatile particle quantities. The four measures are (1) non-volatile PM number **nvPMn**; (2) total PM number **tPMn**; (3) non-volatile PM mass **nvPMm**; and (4) total PM mass **tPMm**.
6. Comparison of PM emissions between different sampling systems requires the consideration of line losses (See Appendix I).

Copyright National Academy of Sciences. All rights reserved.

Unique ID	Engine Make	Engine Model	HP[a]	# Engines	Class	Engine State[b.] T/O	C/O	Cruise	App	Final App	Taxi	Idle	Engine State T/O	C/O	Cruise	App	Final App	Taxi	Idle
						% of max propellor speed							% of max fuel flow						
Recommended for Substitution in EDMS/AEDT																			
	Lycoming	O-320	150-160	1		100%	100%	91%	70%	69%	46%	34%	98%	98%	80%	41%	39%	18%	12%
Individual Engine Tests																			
1	Rotax	912	100	1		100%	100%	90%	66%	66%	58%	57%	72%	72%	50%	30%	30%	22%	13%
2	Continental	O-200-A	100	1		--	--	--	--	--	46%	--	--	--	--	--	--	19%	--
3	Continental	O-200-A	100	1		100%	100%	90%	71%	71%	41%	24%	90%	90%	70%	44%	44%	21%	14%
4	Continental	O-200-A	100	1		100%	100%	96%	64%	48%	40%	40%	90%	90%	82%	37%	25%	20%	20%
5	Continental	O-200-A	100	1		100%	85%	100%	65%	65%	46%	29%	90%	62%	90%	38%	38%	23%	15%
6	Continental	O-200-A	100	1		100%	100%	100%	83%	63%	46%	30%	90%	90%	90%	60%	35%	23%	16%
7	Lycoming	O-235-L2C	115	1		100%	100%	94%	77%	47%	43%	33%	98%	98%	81%	49%	20%	18%	14%
8	Lycoming	O-235-L2C	115	1		100%	100%	93%	77%	48%	43%	37%	98%	98%	81%	50%	21%	19%	15%
9	Lycoming	O-235-L2C	115	1		100%	100%	100%	67%	67%	67%	33%	98%	98%	98%	37%	37%	40%	14%
10	Lycoming	O-320-E2D	150	1		100%	100%	94%	68%	68%	51%	31%	100%	100%	86%	37%	37%	21%	11%
11	Lycoming	O-320-E2D	150	1		99%	99%	93%	57%	57%	43%	30%	100%	100%	86%	25%	25%	16%	11%
12.1	Lycoming	O-320-E2D	150	1		100%	100%	100%	91%	68%	45%	36%	100%	100%	100%	79%	37%	18%	13%
12.2	Lycoming	O-320-E2D	150	1		100%	100%	95%	68%	68%	55%	39%	100%	100%	92%	37%	37%	24%	14%
13	Lycoming	O-320-E2D	150	1		--	--	--	52%	65%	43%	30%	--	--	--	22%	34%	16%	11%
14	Lycoming	O-320-E2D	150	1		98%	98%	96%	74%	56%	35%	31%	99%	99%	92%	45%	25%	12%	11%
15	Lycoming	O-320-E2D	150	1		100%	100%	72%	70%	70%	43%	28%	100%	100%	58%	39%	39%	16%	10%
16	Lycoming	O-320-E2D	150	1		100%	100%	92%	67%	63%	50%	41%	100%	100%	81%	35%	31%	20%	15%
17	Lycoming	O-320-E2G	150	1		100%	100%	90%	69%	73%	48%	27%	100%	100%	77%	39%	43%	19%	10%
18	Lycoming	O-320-E2G	150	1		100%	100%	96%	87%	70%	46%	33%	100%	100%	92%	69%	39%	18%	12%
19	Lycoming	O-320-E3D	150	1		100%	100%	96%	67%	67%	42%	26%	100%	100%	93%	35%	35%	16%	9%
20	Lycoming	O-320-B2C	160	1	Helicopter	102%	102%	75%	--	--	--	58%	100%	100%	43%	--	--	--	24%
21	Lycoming	O-320-B2C	160	1	Helicopter	--	--	75%	--	--	--	--	--	--	43%	--	--	--	--
22	Lycoming	O-320-D2J	160	1		--	--	--	--	--	48%	32%	--	--	--	--	--	18%	10%
23	Lycoming	O-320-D3G	160	1		100%	100%	100%	57%	100%	43%	33%	100%	100%	100%	23%	100%	15%	11%
24	Lycoming	O-320-D3G	160	1		102%	102%	91%	65%	65%	43%	31%	100%	100%	75%	31%	31%	15%	10%
25	Lycoming	O-320-D3G	160	1		100%	100%	91%	81%	72%	64%	34%	100%	100%	75%	53%	40%	30%	11%
26	Lycoming	O-320-D3G	160	1		100%	100%	96%	58%	54%	42%	35%	100%	100%	87%	25%	22%	14%	11%
27	Lycoming	O-320-H2AD	160	1		92%	92%	88%	68%	68%	40%	32%	75%	75%	66%	35%	35%	14%	11%
28	Lycoming	O-320-H2AD	160	1		99%	99%	95%	91%	82%	45%	37%	94%	94%	84%	73%	54%	17%	13%
29	Franklin	6A4-165	165	1		100%	100%	91%	77%	45%	45%	32%	100%	100%	79%	50%	18%	18%	11%
30	Lycoming	O-360-A4M	180	1		100%	100%	95%	64%	64%	45%	40%	96%	96%	62%	35%	35%	15%	14%
31	Lycoming	O-360-C2E	180	1		100%	100%	91%	66%	68%	45%	40%	62%	62%	45%	28%	31%	18%	16%
32.1	Lycoming	O-360-F1A6	180	1		100%	97%	88%	85%	77%	42%	31%	100%	92%	70%	62%	48%	15%	10%
32.2	Lycoming	O-360-F1A6	180	1		100%	94%	90%	61%	61%	45%	24%	100%	84%	73%	28%	28%	17%	8%
33	Lycoming	O-360-A1A	180	2		97%	94%	88%	57%	57%	34%	37%	95%	88%	71%	26%	26%	12%	20%
34	Lycoming	O-360-A1G6D	180	2		100%	93%	85%	81%	74%	37%	41%	106%	83%	66%	58%	46%	14%	22%
35	Lycoming	IO-360-L2A	160	1	Fuel Injected	100%	100%	99%	69%	69%	48%	36%	100%	100%	64%	14%	14%	18%	12%
36	Lycoming	IO-360-A3B6D	200	1	Fuel Injected	99%	99%	70%	74%	78%	48%	30%	98%	98%	37%	25%	31%	11%	10%
37	Lycoming	IO-360-C1C6	200	1	Fuel Injected	100%	100%	91%	58%	50%	38%	26%	76%	76%	61%	25%	19%	19%	13%
38	Lycoming	IO-360-C1C6	200	1	Fuel Injected	102%	102%	81%	64%	64%	51%	37%	100%	100%	56%	32%	32%	20%	13%

Copyright National Academy of Sciences. All rights reserved.

Unique ID	Engine Make	Engine Model	HP[a]	# Engines	Class	Engine State[b] T/O	C/O	Cruise	App	Final App	Taxi	Idle	Engine State T/O	C/O	Cruise	App	Final App	Taxi	Idle
						% of max propellor speed							% of max fuel flow						
39	Lycoming	IO-520-1AB5	230	1	Fuel Injected	100%	100%	100%	77%	77%	45%	35%	100%	100%	56%	44%	44%	16%	15%
40	Continental	O-470-11	230	1		--	--	87%	65%	65%	39%	26%	--	--	71%	36%	36%	16%	10%
41	TCM	O-470-U	230	1		100%	100%	100%	68%	45%	45%	36%	100%	100%	61%	30%	16%	14%	3%
42	Lycoming	O-540-B4B5	235	1		100%	96%	84%	80%	56%	52%	40%	95%	84%	59%	52%	25%	22%	15%
43	Lycoming	O-540-A1D5	250	1		100%	96%	92%	65%	65%	42%	26%	96%	85%	75%	32%	32%	15%	9%
44	Lycoming	O-540-J3C5D	250	1		100%	100%	78%	63%	63%	37%	31%	100%	100%	52%	33%	33%	15%	13%
45	Lycoming	IO-540-C4B5	250	2	Fuel Injected	--	--	--	--	--	--	25%	--	--	--	--	--	--	11%
46	Lycoming	IO-540-C4B5	250	2	Fuel Injected	100%	94%	86%	51%	51%	47%	28%	100%	92%	73%	25%	25%	22%	13%
47.1	Lycoming	IO-540-C4B5	250	2	Fuel Injected	100%	100%	92%	80%	88%	42%	33%	98%	62%	54%	61%	50%	18%	15%
47.2	Lycoming	IO-540-C4B5	250	2	Fuel Injected	100%	100%	92%	68%	68%	56%	31%	100%	100%	87%	42%	42%	29%	14%
48	TCM	IO-540-BB	285	1	Fuel Injected	--	98%	94%	82%	82%	45%	25%	--	90%	80%	56%	56%	18%	10%
49	Lycoming	IO-540-K1G5D	300	1	Fuel Injected	93%	93%	90%	82%	82%	49%	37%	72%	72%	64%	51%	51%	19%	13%
50	Continental	IO-550-N	300	1	Fuel Injected	--	--	--	--	--	--	30%	--	--	--	--	--	--	15%
51	TCM	TSIO-520-C	300	1	Fuel Injected	96%	85%	96%	67%	67%	43%	27%	76%	61%	76%	34%	34%	16%	10%
52	TCM	IO-550-C	300	2	Fuel Injected	--	--	96%	75%	75%	43%	33%	--	--	89%	50%	50%	22%	17%
53	Unknown (Skybolt Experimental)			1		--	--	--	--	--	30%	--	--	--	--	--	--	11%	--
54	Garrett AiResearch	TPE331-6-252B	750	2	Turboprop	100%	100%	98%	98%	98%	91%	76%	100%	89%	56%	51%	51%	42%	26%
55	Pratt & Whitney Canada	PT6A-60A	1050lbs	2	Turboprop	--	--	80%	--	--	60%	52%	--	--	80%	--	--	60%	52%
56	Williams	FJ44-1AP	1965lbs	2	Turbofan	--	--	--	--	--	43%	--	--	--	--	--	--		--
57	General Electric	CF34-3A1	9140lbs	2	Turbofan	86%	86%	67%	56%	56%	30%	26%	100%	100%	50%	38%	38%	18%	16%
Engine Family Averages					Replicates														
	Continental	O-200	100		5	100%	96%	96%	71%	62%	44%	31%	90%	83%	83%	45%	35%	21%	16%
	Lycoming	O-235	115		3	100%	100%	96%	73%	54%	51%	34%	98%	98%	87%	45%	26%	26%	14%
	Lycoming	O-320	150-160		20	100%	100%	91%	70%	69%	46%	34%	98%	98%	80%	41%	39%	18%	12%
	Lycoming	O-360	180		6	99%	96%	90%	69%	67%	41%	36%	93%	84%	65%	40%	36%	15%	15%
	Lycoming	IO-360	200		4	100%	100%	85%	66%	65%	46%	32%	94%	94%	54%	24%	24%	17%	12%
	Lycoming	O-540	235-250		3	100%	97%	85%	69%	61%	44%	32%	97%	90%	62%	39%	30%	18%	13%
	Lycoming	IO-540	250-285		6	98%	97%	91%	73%	74%	48%	30%	92%	83%	72%	47%	45%	21%	13%
Upper Limit on Engine Family Averages at 95% Confidence																			
	Continental	O-200	100			100%	120%	112%	99%	93%	52%	52%	90%	128%	114%	78%	61%	26%	25%
	Lycoming	O-235	115			100%	100%	112%	99%	102%	110%	42%	98%	98%	129%	78%	66%	81%	18%
	Lycoming	O-320	150-160			104%	104%	109%	95%	91%	59%	49%	111%	111%	116%	78%	76%	26%	19%
	Lycoming	O-360	180			103%	104%	98%	98%	87%	54%	52%	133%	114%	91%	81%	59%	21%	29%
	Lycoming	IO-360	200			103%	103%	125%	89%	102%	63%	49%	130%	130%	93%	47%	52%	30%	16%
	Lycoming	O-540	235-250			100%	107%	116%	109%	82%	76%	63%	109%	128%	113%	87%	49%	35%	26%
	Lycoming	IO-540	250-285			109%	106%	99%	110%	116%	62%	43%	136%	127%	107%	86%	79%	34%	17%

Copyright National Academy of Sciences. All rights reserved.

Unique ID	Engine Make	Engine Model	HP[a]	# Engines	Class	Engine State[b.] T/O	C/O	Cruise	App	Final App	Taxi	Idle	Engine State T/O	C/O	Cruise	App	Final App	Taxi	Idle
						% of max propellor speed							% of max fuel flow						
Preexisting Data																			
FOCA[c.,e.]													**100%**	**85%**	**65%**	**45%**		**manual**	
ICAO[d.]													**100%**	**85%**		**30%**		**7%**	**manual**
FAEED162	diverse	Prop-200hp	150										100%	75%		53%	53%	11%	11%
FAEED160	diverse	Prop-300hp	225										100%	74%		46%	46%	8%	8%
FAEED165	diverse	Prop-500hp	350										100%	79%		38%	38%	10%	10%
FOCA	diverse	Prop>500hp	1200										100%	20%		10%	10%	0%	0%
FAEED159	TCM	O-200	100										100%	100%		56%	56%	18%	18%
FOCA	Lycoming	O-320-E2A	160										100%	80%		48%	48%	13%	13%
FAEED163	Lycoming	IO-320-DIAD	160		Fuel Injected								100%	66%		41%	41%	9%	9%
FOCA	Lycoming	O-360-A3A	180										100%	85%		45%	45%	13%	13%
FOCA	Lycoming	IO-360-A1B6	200		Fuel Injected								100%	78%		46%	46%	10%	10%
FAEED160	TCM	TSIO-360-C	225		Fuel Injected								100%	74%		46%	46%	8%	8%
FOCA	Lycoming	O-540-J3C5D	235										100%	84%		40%	40%	10%	10%
FOCA	Lycoming	IO-540-T4A5D	260		Fuel Injected								100%	89%		44%	44%	15%	15%
FOCA	TCM	IO-550-B	300		Fuel Injected								100%	99%		54%	54%	21%	21%
FOCA	Lycoming	TSIO-520-WB	325		Fuel Injected								100%	85%		52%	52%	23%	23%
FAEED165	Lycoming	TIO-540-J2B2	350		Fuel Injected								100%	79%		38%	38%	10%	10%
ICAO	General Electric	CF34-3A1											100%	82%		29%	29%	12%	12%
ICAO	Honeywell	AS907-1-1A											100%	83%		30%	30%	14%	14%
EDMS	Continental	6-285-B											92%	100%		50%	50%	43%	43%
EDMS	Curtiss-Wright	R-1820											100%	74%		28%	28%	8%	8%
EDMS	Lycoming	IO-320-D1AD			Fuel Injected								100%	67%		41%	41%	8%	8%
EDMS	Lycoming	IO-360-B			Fuel Injected								100%	70%		36%	36%	8%	8%
EDMS	Lycoming	O-200											100%	100%		56%	56%	18%	18%
EDMS	Lycoming	O-320											100%	75%		52%	52%	11%	11%
EDMS	Lycoming	TIO-540-J2B2			Fuel Injected								100%	79%		38%	38%	10%	10%
EDMS	Lycoming	TSIO-360-C			Fuel Injected								100%	74%		46%	46%	9%	9%
EDMS	Pratt & Whitney Canada	PT6A-60A	1050lbs		Turbofan								100%	91%		52%	52%	18%	18%
EDMS	Pratt & Whitney Canada	PT6A-114	600lbs		Turbofan								100%	89%		50%	50%	18%	18%
EDMS	Pratt & Whitney Canada	PT6A-67	1200lbs		Turbofan								100%	91%		52%	52%	19%	19%
EDMS	Pratt & Whitney Canada	PT6a-66	850lbs		Turbofan								100%	92%		54%	54%	21%	21%

Blank entries indicate that the data was not available or not of high enough quality to produce a value. The symbol "--" indicates that this engine state was not measured.

a. in lieu of horse power, turbofan engine power is stated in pounds of thrust b. The % of max propellor RPM achievable on the ground is used to convert a propellor RPM into a % power.

c. The FOCA (Swiss Federal Aviation Organization) power states are listed. d. The ICAO (International Civic Aviation Organization) power states are listed (% pounds of thrust).

e. FOCA data has power states that are measured based on a % of the maximum fuel flow.

Copyright National Academy of Sciences. All rights reserved.

Unique ID	Engine Make	Engine Model	EI HC (g/kg)							EI CO (g/kg)						
			T/O	C/O	Cruise	App	Final App	Taxi	Idle	T/O	C/O	Cruise	App	Final App	Taxi	Idle
Recommended for Substitution in EDMS/AEDT																
	Lycoming	O-320	35.5	35.5	39.1	39.6	50.0	42.5	96.6	905	905	525	770	857	700	767
Individual Engine Tests																
1	Rotax	912	79.0	79.0	70.7	78.9	78.9	87.8	100.9	808	808	795	1062	1062	819	816
2	Continental	O-200-A	--	--	--	--	--	53.3	--	--	--	--	--	--	247	--
3	Continental	O-200-A	88.5	88.5	84.2	80.0	80.0	126.9	239.9	1057	1057	623	745	745	634	789
4	Continental	O-200-A	46.5	46.5	38.5	57.2	74.2	110.6	143.9	901	901	491	845	909	923	963
5	Continental	O-200-A	26.0	28.4	26.0	30.9	30.9	27.4	170.7	1028	1082	1028	1009	1009	907	1096
6	Continental	O-200-A	31.4	31.4	23.9	23.9	32.0	35.0	136.9	1148	1148	1017	1107	442	993	1030
7	Lycoming	O-235-L2C	23.9	23.9	24.8	28.9	33.7	26.2	35.4	724	724	423	767	470	554	603
8	Lycoming	O-235-L2C	37.8	37.8	25.8	39.7	41.9	40.4	59.2	1113	1113	69	1047	538	636	748
9	Lycoming	O-235-L2C	48.8	48.8	31.1	58.1	58.1	70.0	131.0	1198	1198	199	34	34	643	107
10	Lycoming	O-320-E2D	18.5	18.5	10.9	25.2	25.2	12.3	134.2	792	792	576	1023	1023	95	979
11	Lycoming	O-320-E2D	61.1	61.1	35.8	81.7	81.7	29.6	116.8	985	985	422	1092	1092	889	657
12.1	Lycoming	O-320-E2D	28.9	28.9	43.5	36.5	44.3	0.0	78.7	897	897	660	755	1093	521	701
12.2	Lycoming	O-320-E2D	18.8	18.8	16.7	29.8	29.8	23.0	100.1	975	975	363	780	780	909	876
13	Lycoming	O-320-E2D	--	--	--	43.3	76.2	54.4	80.5	--	--	--	496	810	523	849
14	Lycoming	O-320-E2D	26.4	26.4	22.0	24.6	34.0	40.4	74.3	1207	1207	1136	744	488	1006	988
15	Lycoming	O-320-E2D	21.3	21.3	31.1	39.0	39.0	66.6	104.6	1006	1006	781	1058	1058	924	658
16	Lycoming	O-320-E2D	40.7	40.7	35.0	37.9	81.1	24.6	132.3	1280	1280	367	745	694	412	344
17	Lycoming	O-320-E2G	39.8	39.8	20.6	29.1	28.9	38.8	145.2	1028	1028	811	997	968	1228	1087
18	Lycoming	O-320-E2G	24.0	24.0	36.8	41.8	85.2	54.0	78.0	954	954	313	798	1058	484	720
19	Lycoming	O-320-E3D	40.6	40.6	40.7	43.5	43.5	73.8	172.0	941	941	690	763	763	733	706
20	Lycoming	O-320-B2C	33.8	33.8	45.9	--	--	--	48.8	835	835	979	--	--	--	785
21	Lycoming	O-320-B2C	--	--	99.3	--	--	--	--	--	--	348	--	--	--	--
22	Lycoming	O-320-D2J	--	--	--	--	--	45.5	111.2	--	--	--	--	--	580	707
23	Lycoming	O-320-D3G	37.9	37.9	39.0	42.5	47.3	44.5	53.1	810	810	610	932	742	879	720
24	Lycoming	O-320-D3G	66.7	66.7	81.9	57.7	57.7	70.8	91.4	852	852	139	1112	1112	1067	898
25	Lycoming	O-320-D3G	43.0	43.0	33.6	43.9	46.6	45.1	63.7	656	656	189	166	377	444	664
26	Lycoming	O-320-D3G	30.8	30.8	56.4	27.8	50.0	59.7	69.7	281	281	219	188	815	660	802
27	Lycoming	O-320-H2AD	30.7	30.7	23.3	34.0	34.0	29.6	129.7	947	947	404	887	887	293	617
28	Lycoming	O-320-H2AD	41.3	41.3	31.5	35.0	45.8	52.6	50.1	937	937	446	549	813	944	811
29	Franklin	6A4-165	59.4	59.4	40.7	230.5	120.6	191.0	359.5	709	709	91	607	815	697	864
30	Lycoming	O-360-A4M	44.3	44.3	51.5	48.4	48.4	53.9	121.5	925	925	146	1003	1003	657	649
31	Lycoming	O-360-C2E	32.7	32.7	23.2	40.4	37.3	161.2	95.2	1071	1071	245	1097	994	1101	1043
32.1	Lycoming	O-360-F1A6	37.7	29.8	31.6	36.4	43.8	81.5	93.0	1015	885	613	1117	1150	131	25
32.2	Lycoming	O-360-F1A6	25.4	20.5	19.7	26.9	26.9	80.0	200.4	1285	1097	165	1247	1247	1112	1120
33	Lycoming	O-360-A1A	25.4	27.0	27.1	49.6	21.3	69.8	89.3	1101	977	857	755	320	638	715
34	Lycoming	O-360-A1G6D	41.9	41.8	0.0	91.9	74.3	163.4	146.8	847	1120	205	1062	1062	802	983
35	Lycoming	IO-360-L2A	50.2	50.2	40.4	39.6	39.6	86.8	292.2	1229	1229	405	660	660	954	993
36	Lycoming	IO-360-A3B6D	48.9	48.9	24.5	41.6	30.3	161.0	217.0	627	627	25	375	53	1003	1066

Copyright National Academy of Sciences. All rights reserved.

Unique ID	Engine Make	Engine Model	EI HC g/kg							EI CO g/kg						
			T/O	C/O	Cruise	App	Final App	Taxi	Idle	T/O	C/O	Cruise	App	Final App	Taxi	Idle
37	Lycoming	IO-360-C1C6	57.7	57.7	55.8	167.6	185.9	206.3	289.1	707	707	270	969	721	915	743
38	Lycoming	IO-360-C1C6	24.4	34.9	32.2	47.8	47.8	53.4	169.0	807	799	481	907	907	806	1023
39	Lycoming	IO-520-1AB5	35.0	35.0	30.1	41.9	41.9	142.1	331.1	970	970	137	1009	1009	1011	873
40	Continental	O-470-11	--	--	59.6	33.1	33.1	47.9	185.6	--	--	451	525	525	807	354
41	TCM	O-470-U	68.7	68.7	39.2	116.0	159.3	101.5	203.1	997	997	33	460	802	929	729
42	Lycoming	O-540-B4B5	29.6	30.0	25.8	42.9	158.0	150.9	184.0	1173	881	107	1119	1177	723	722
43	Lycoming	O-540-A1D5	18.3	18.7	27.7	43.4	43.4	31.2	121.6	1106	995	602	1087	1087	883	973
44	Lycoming	O-540-J3C5D	34.9	34.9	63.6	282.3	282.3	313.7	141.9	1100	1100	637	688	688	412	614
45	Lycoming	IO-540-C4B5	--	--	--	--	--	--	305.4	--	--	--	--	--	--	638
46	Lycoming	IO-540-C4B5	32.5	27.9	81.7	79.3	50.3	76.3	239.1	1187	1006	641	817	911	385	771
47.1	Lycoming	IO-540-C4B5	37.3	27.8	11.6	28.0	35.8	101.1	300.2	1017	918	43	986	1078	471	902
47.2	Lycoming	IO-540-C4B5	18.1	18.1	19.8	30.2	30.2	78.9	256.3	1095	1095	553	1226	1226	1318	1118
48	TCM	IO-540-BB	--	15.1	13.5	27.2	27.2	45.2	255.0	--	784	802	750	750	779	649
49	Lycoming	IO-540-K1G5D	23.8	23.8	21.9	27.7	27.7	49.3	83.9	1004	1004	532	718	718	869	1090
50	Continental	IO-550-N	--	--	--	--	--	--	33.2	--	--	--	--	--	--	685
51	TCM	TSIO-520-C	149.3	251.1	149.3	297.7	297.7	779.8	852.0	1264	1357	1264	1050	1050	429	309
52	TCM	IO-550-C	--	--	41.1	29.9	29.9	280.5	221.1	--	--	648	848	848	755	664
53	Unknown (Skybolt Experimental)		--	--	--	--	--	415.2	--	--	--	--	--	--	635	--
54	Garrett AiResearch	TPE331-6-252B	8.2	6.2	5.6	9.3	9.3	17.4	45.3	2	2	9	19	19	31	56
55	Pratt & Whitney Canada	PT6A-60A	--	--	223.3	--	--	122.2	144.7	--	--	16	--	--	38	42
56	Williams	FJ44-1AP	--	--	--	--	--	0.0	--	--	--	--	--	--	57	--
57	General Electric	CF34-3A1	0.1	0.1	0.1	2.1	2.1	2.3	2.8	3	3	7	54	54	60	67
Engine Family Averages																
	Continental	O-200	48.1	48.7	43.1	48.0	54.3	70.7	172.8	1033	1047	790	927	776	741	969
	Lycoming	O-235	36.8	36.8	27.3	42.2	44.5	45.6	75.2	1012	1012	230	616	347	611	486
	Lycoming	O-320	35.5	35.5	39.1	39.6	50.0	42.5	96.6	905	905	525	770	857	700	767
	Lycoming	O-360	34.6	32.7	25.5	48.9	42.0	101.6	124.4	1041	1012	372	1047	963	740	756
	Lycoming	IO-360	45.3	47.9	38.2	74.2	75.9	126.9	241.8	843	841	295	728	585	920	956
	Lycoming	O-540	27.6	27.8	39.0	122.9	161.2	165.3	149.2	1127	992	448	965	984	672	770
	Lycoming	IO-540	27.9	22.5	29.7	38.5	34.2	70.2	240.0	1076	961	514	900	937	764	862
Upper Limit on Engine Family Averages at 95% Confidence																
	Continental	O-200	138.1	136.8	132.6	129.9	138.6	196.4	322.5	1359	1381	1662	1444	1566	1597	1388
	Lycoming	O-235	90.6	90.6	41.8	105.6	97.9	141.7	289.4	2100	2100	1001	2868	1524	826	1931
	Lycoming	O-320	63.9	63.9	85.4	68.6	91.6	84.8	170.2	1366	1366	1108	1371	1308	1334	1112
	Lycoming	O-360	55.4	55.9	68.6	107.1	90.3	225.0	235.6	1432	1262	1127	1469	1808	1674	1793
	Lycoming	IO-360	91.3	78.2	80.9	272.7	310.3	347.9	431.9	1694	1694	932	1589	1763	1186	1419
	Lycoming	O-540	64.1	63.5	130.8	716.8	675.2	775.4	286.0	1301	1463	1725	1996	2104	1702	1562
	Lycoming	IO-540	55.4	38.6	111.3	101.9	60.9	134.3	448.1	1344	1287	1303	1482	1537	1791	1405

Copyright National Academy of Sciences. All rights reserved.

Unique ID	Engine Make	Engine Model	EI HC g/kg						EI CO g/kg					
			T/O	C/O	Cruise	App	Final App	Taxi	Idle	T/O	C/O	Cruise	App	Final App	Taxi	Idle
Preexisting Data																
FOCA[c.,e.]																
ICAO[d.]																
FAEED162	diverse	Prop-200hp	11.8	12.4		19.3	19.3	36.9	36.9	1077	990		1222	1222	1077	1077
FAEED160	diverse	Prop-300hp	9.2	9.6		11.3	11.3	138.3	138.3	1082	961		995	995	592	592
FAEED165	diverse	Prop-500hp	12.4	16.6		13.4	13.4	68.1	68.1	1442	1471		1262	1262	1294	1294
FOCA	diverse	Prop>500hp	3.2	16.3		12.9	12.9	36.9	36.9	36	500		1262	1262	1294	1294
FAEED159	TCM	O-200	20.8	20.8		33.2	33.2	29.0	29.0	974	974		1188	1188	644	644
FOCA	Lycoming	O-320-E2A	12.6	15.1		13.7	13.7	16.0	16.0	816	837		696	696	690	690
FAEED163	Lycoming	IO-320-DIAD	11.4	9.6		12.2	12.2	36.1	36.1	1192	888		944	944	620	620
FOCA	Lycoming	O-360-A3A	15.3	12.9		16.4	16.4	27.4	27.4	1146	943		1083	1083	1081	1081
FOCA	Lycoming	IO-360-A1B6	15.5	16.7		20.6	20.6	48.3	48.3	1294	1306		1365	1365	1095	1095
FAEED160	TCM	TSIO-360-C	9.2	9.6		11.3	11.3	138.3	138.3	1082	961		995	995	592	592
FOCA	Lycoming	O-540-J3C5D	20.0	22.0		51.0	51.0	32.0	32.0	1327	1227		1425	1425	1210	1210
FOCA	Lycoming	IO-540-T4A5D	13.9	14.0		16.3	16.3	45.6	45.6	1010	978		819	819	1000	1000
FOCA	TCM	IO-550-B	12.7	12.3		11.5	11.5	42.6	42.6	827	795		1065	1065	1163	1163
FOCA	Lycoming	TSIO-520-WB	15.8	13.9		12.1	12.1	8.2	8.2	1018	1153		1299	1299	462	462
FAEED165	Lycoming	TIO-540-J2B2	12.4	16.6		13.4	13.4	68.1	68.1	1442	1471		1262	1262	1294	1294
ICAO	General Electric	CF34-3A1	0.1	0.1		0.1	0.1	4.0	4.0	0	0		2	2	43	43
ICAO	Honeywell	AS907-1-1A	0.0	0.0		0.1	0.1	4.3	4.3	1	1		3	3	30	30
EDMS	Continental	6-285-B	11.6	8.4		16.1	16.1	10.7	10.7	998	668		1020	1020	364	364
EDMS	Curtiss-Wright	R-1820	94.7	48.5		5.6	5.6	150.6	150.6	532	435		385	385	474	474
EDMS	Lycoming	IO-320-D1AD	11.4	9.6		12.2	12.2	36.1	36.1	1192	888		944	944	618	618
EDMS	Lycoming	IO-360-B	10.0	8.2		9.7	9.7	49.2	49.2	1199	983		691	691	897	897
EDMS	Lycoming	O-200	20.8	20.8		33.2	33.2	29.0	29.0	974	974		1188	1188	644	644
EDMS	Lycoming	O-320	11.8	12.4		19.4	19.4	36.9	36.9	1080	990		1220	1220	1080	1080
EDMS	Lycoming	TIO-540-J2B2	12.4	16.6		13.4	13.4	68.1	68.1	1442	1471		1260	1260	1294	1294
EDMS	Lycoming	TSIO-360-C	9.2	9.5		11.0	11.0	138.0	138.0	1080	961		995	995	592	592
EDMS	Pratt & Whitney Canada	PT6A-60A	0.0	0.0		0.5	0.5	25.7	25.7	4	5		19	19	154	154
EDMS	Pratt & Whitney Canada	PT6A-114	0.0	0.0		0.3	0.3	3.9	3.9	1	1		5	5	51	51
EDMS	Pratt & Whitney Canada	PT6A-67	0.0	0.0		0.1	0.1	13.8	13.8	2	3		13	13	131	131
EDMS	Pratt & Whitney Canada	PT6a-66	0.4	0.7		5.7	5.7	82.8	82.8	8	9		28	28	216	216

Copyright National Academy of Sciences. All rights reserved.

Unique ID	Engine Make	Engine Model	EI NOx (g/kg)							PM # Non-Volatile(via APC) (#/kg)						
			T/O	C/O	Cruise	App	Final App	Taxi	Idle	T/O	C/O	Cruise	App	Final App	Taxi	Idle
Recommended for Substitution in EDMS/AEDT																
	Lycoming	O-320	8.0	8.0	23.1	7.2	3.1	4.5	1.6	4.0E+15	4.0E+15	2.1E+15	2.2E+15	2.1E+15	1.6E+15	3.9E+15
Individual Engine Tests																
1	Rotax	912	4.8	4.8	6.6	1.1	1.3	1.0	1.3	1.2E+15	1.2E+15	1.1E+15	7.7E+14	7.7E+14	1.5E+15	6.6E+14
2	Continental	O-200-A	--	--	--	--	--	1.5	--	--	--	--	--	--	1.4E+13	--
3	Continental	O-200-A	4.2	4.2	17.4	8.8	2.5	3.5	2.5	8.4E+15	8.4E+15	2.9E+15	2.3E+15	2.3E+15	9.2E+15	7.7E+15
4	Continental	O-200-A	3.4	3.4	16.0	2.0	0.7	0.5	0.7	1.5E+15	1.5E+15	6.9E+15	2.0E+15	2.6E+15	3.3E+15	4.0E+15
5	Continental	O-200-A	4.7	8.0	4.7	2.8	2.8	2.2	0.4	5.0E+15	1.1E+15	5.0E+15	1.1E+14	1.1E+14	1.6E+15	4.6E+15
6	Continental	O-200-A	3.3	3.3	9.2	1.6	9.5	0.8	0.2	4.5E+15	4.5E+15	1.3E+15	2.9E+15	2.8E+15	2.0E+15	4.9E+15
7	Lycoming	O-235-L2C	11.9	11.9	25.8	6.4	7.3	2.4	1.8	3.6E+15	3.6E+15	1.7E+15	6.7E+15	1.2E+16	7.6E+15	6.7E+15
8	Lycoming	O-235-L2C	2.0	2.0	63.2	2.0	6.6	2.4	1.8	1.8E+15	1.8E+15	1.0E+15	2.9E+15	7.0E+15	5.3E+15	6.7E+15
9	Lycoming	O-235-L2C	2.7	2.7	40.6	20.5	11.0	4.1	11.0	5.1E+15	5.1E+15	5.8E+15	7.1E+13	7.1E+13	7.3E+14	1.9E+15
10	Lycoming	O-320-E2D	13.9	13.9	18.6	2.5	2.5	15.4	0.6	1.0E+15	1.0E+15	1.7E+15	7.2E+14	7.2E+14	6.0E+14	3.8E+15
11	Lycoming	O-320-E2D	3.0	3.0	20.5	0.7	1.2	1.0	1.2	1.0E+15	1.0E+15	2.4E+14	6.7E+13	6.7E+13	0.0E+00	2.9E+14
12.1	Lycoming	O-320-E2D	3.4	3.4	9.4	5.7	2.4	1.8	2.4	2.0E+15	2.0E+15	8.1E+14	7.6E+14	8.6E+14	2.0E+15	3.9E+15
12.2	Lycoming	O-320-E2D	5.2	5.2	29.7	5.4	5.4	1.8	0.9							
13	Lycoming	O-320-E2D	--	--	--	5.1	4.2	2.9	1.1	--	--	--	5.2E+15	7.2E+15	7.9E+15	6.0E+15
14	Lycoming	O-320-E2D	1.8	1.8	2.2	10.6	15.0	0.9	0.6	4.3E+15	4.3E+15	2.9E+15	4.1E+15	7.9E+15	4.7E+15	5.3E+15
15	Lycoming	O-320-E2D	3.0	3.0	2.7	2.3	2.3	1.5	1.4	3.0E+15	3.0E+15	3.6E+15	1.5E+15	1.5E+15	1.3E+15	6.8E+15
16	Lycoming	O-320-E2D	0.7	0.7	15.5	4.8	3.7	7.7	3.7	5.0E+15	5.0E+15	2.4E+15	9.3E+15	1.1E+15	7.4E+14	1.4E+15
17	Lycoming	O-320-E2G	5.9	5.9	14.2	2.7	2.6	0.4	0.6	6.0E+15	6.0E+15	6.8E+15	3.8E+15	3.7E+15	1.1E+15	6.5E+15
18	Lycoming	O-320-E2G	3.2	3.2	32.8	8.9	2.6	2.1	2.6	5.4E+14	5.4E+14	1.2E+15	6.9E+14	1.8E+15	3.2E+14	6.8E+14
19	Lycoming	O-320-E3D	5.6	5.6	7.9	2.6	0.6	1.0	0.6	6.9E+15	6.9E+15	1.9E+15	9.4E+13	9.4E+13	3.0E+14	1.0E+15
20	Lycoming	O-320-B2C	3.9	3.9	4.5	--	--	--	1.7	1.8E+16	1.8E+16	7.8E+15	--	--	--	2.2E+16
21	Lycoming	O-320-B2C	--	--	13.9	--	--	--	--	--	--	2.3E+15	--	--	--	--
22	Lycoming	O-320-D2J	--	--	--	--	1.9	4.1	1.9	--	--	--	--	--	6.4E+14	1.1E+15
23	Lycoming	O-320-D3G	5.7	5.7	15.2	1.3	1.2	1.1	1.2	3.9E+14	3.9E+14	1.2E+15	2.8E+14	1.9E+15	1.6E+14	3.4E+15
24	Lycoming	O-320-D3G	5.1	5.1	62.9	0.8	0.6	0.8	0.6	2.2E+15	2.2E+15	3.6E+14	3.7E+14	3.7E+14	1.0E+15	1.1E+15
25	Lycoming	O-320-D3G	22.7	22.7	60.0	42.8	2.4	28.5	2.4	6.4E+15	6.4E+15	1.0E+15	7.9E+14	8.0E+14	2.5E+15	3.9E+15
26	Lycoming	O-320-D3G	44.3	44.3	45.3	11.2	0.6	1.1	0.6	5.6E+14	5.6E+14	6.9E+13	1.4E+13	6.6E+13	2.2E+13	1.1E+14
27	Lycoming	O-320-H2AD	3.2	3.2	35.7	5.0	5.1	8.6	5.1	5.1E+15	5.1E+15	1.7E+15	5.3E+15	5.3E+15	4.3E+15	2.3E+15
28	Lycoming	O-320-H2AD	4.7	4.7	24.8	10.9	1.8	0.8	1.8	1.1E+15	1.1E+15	1.6E+14	2.4E+15	4.2E+14	8.8E+13	6.9E+14
29	Franklin	6A4-165	8.3	8.3	40.5	3.2	0.7	1.9	0.7	3.4E+15	3.4E+15	9.2E+15	1.2E+16	4.7E+15	7.2E+15	1.4E+16
30	Lycoming	O-360-A4M	3.2	3.2	52.2	0.7	0.2	2.5	0.2	4.8E+14	4.8E+14	8.0E+14	1.1E+15	1.1E+15	8.9E+14	8.8E+14
31	Lycoming	O-360-C2E	2.3	2.3	35.1	1.0	3.1	0.5	3.1	3.4E+15	3.4E+15	3.4E+15	4.8E+14	1.6E+14	3.5E+15	2.5E+15
32.1	Lycoming	O-360-F1A6	4.2	5.4	16.7	1.8	9.6	18.5	9.6	3.2E+15	3.8E+15	9.5E+14	3.5E+14	4.8E+14	1.7E+15	1.2E+15
32.2	Lycoming	O-360-F1A6	1.3	3.0	60.6	0.8	0.8	2.7	1.0	3.4E+14	2.0E+14	2.2E+15	3.3E+14	3.3E+14	4.0E+15	3.3E+15
33	Lycoming	O-360-A1A	2.0	4.5	3.9	2.9	1.0	1.3	1.0	1.2E+16	8.1E+15	6.3E+15	5.4E+15	5.1E+15	2.8E+15	3.7E+15
34	Lycoming	O-360-A1G6D	8.0	1.7	42.8	2.1	0.4	0.7	0.4	7.6E+15	4.0E+15	6.8E+15	3.3E+15	9.7E+14	2.5E+15	3.0E+15
35	Lycoming	IO-360-L2A	1.1	1.1	28.9	7.5	0.5	0.8	0.5	3.7E+15	3.7E+15	1.6E+15	2.9E+15	2.9E+15	1.4E+15	6.9E+15
36	Lycoming	IO-360-A3B6D	56.2	56.2	54.3	28.3	0.5	1.0	0.5	1.7E+16	1.7E+16	5.9E+14	5.4E+14	1.5E+14	4.4E+15	5.4E+15

Copyright National Academy of Sciences. All rights reserved.

Unique ID	Engine Make	Engine Model	EI NOx g/kg							PM # Non-Volatile(via APC) #/kg						
			T/O	C/O	Cruise	App	Final App	Taxi	Idle	T/O	C/O	Cruise	App	Final App	Taxi	Idle
37	Lycoming	IO-360-C1C6	8.0	8.0	40.5	1.6	0.0	1.2	0.0	2.0E+15	2.0E+15	3.6E+14	6.2E+14	5.4E+14	3.3E+15	4.2E+15
38	Lycoming	IO-360-C1C6	7.0	5.3	20.7	5.2	0.6	3.2	0.6	4.0E+15	2.3E+15	3.7E+14	7.2E+14	7.2E+14	9.5E+14	6.7E+15
39	Lycoming	IO-520-1AB5	3.2	3.2	58.0	2.4	0.7	0.5	0.7	1.2E+15	1.2E+15	4.2E+15	1.0E+16	1.0E+16	4.7E+15	6.8E+15
40	Continental	O-470-11	--	--	28.4	14.6	14.6	1.5	2.3	--	--	4.6E+14	1.2E+14	1.2E+14	1.4E+15	2.5E+15
41	TCM	O-470-U	3.3	3.3	96.8	5.4	0.2	0.6	0.2	1.2E+15	1.2E+15	1.3E+15	9.0E+14	4.8E+15	2.8E+15	4.4E+15
42	Lycoming	O-540-B4B5	1.3	7.9	47.3	1.7	1.6	2.2	1.6	1.5E+15	1.1E+15	1.5E+16	3.0E+15	1.2E+16	7.1E+15	6.9E+15
43	Lycoming	O-540-A1D5	3.3	4.8	22.7	2.2	2.2	1.1	0.7	4.9E+15	4.4E+15	4.0E+15	8.9E+15	8.9E+15	1.2E+16	9.3E+15
44	Lycoming	O-540-J3C5D	2.8	2.8	20.9	5.4	5.4	2.6	1.7	8.1E+15	8.1E+15	8.6E+15	1.2E+16	1.2E+16	7.5E+15	6.6E+15
45	Lycoming	IO-540-C4B5	--	--	--	--	--	--	0.6	--	--	--	--	--	--	
46	Lycoming	IO-540-C4B5	4.5	8.1	22.1	25.2	10.6	2.6	10.6	6.8E+15	4.5E+15	9.6E+15	1.6E+16	1.5E+16	1.6E+16	1.3E+16
47.1	Lycoming	IO-540-C4B5	3.6	9.9	72.1	2.9	0.1	8.6	0.1	1.6E+16	8.1E+15	2.3E+16	6.9E+15	3.8E+15	1.7E+15	7.5E+15
47.2	Lycoming	IO-540-C4B5	2.9	2.9	22.5	1.9	1.9	0.2	0.1	5.0E+15	5.0E+15	2.5E+15	2.3E+15	2.3E+15	4.4E+15	8.4E+15
48	TCM	IO-540-BB	--	9.9	8.7	9.0	9.0	1.0	0.5	--	1.5E+15	1.7E+15	2.0E+15	2.0E+15	1.5E+15	3.7E+15
49	Lycoming	IO-540-K1G5D	4.1	4.1	24.6	6.5	6.5	2.3	0.6	3.3E+15	3.3E+15	3.9E+15	6.8E+15	6.8E+15	4.7E+15	6.8E+15
50	Continental	IO-550-N	--	--	--	--	--	--	5.1	--	--	--	--	--	--	1.1E+15
51	TCM	TSIO-520-C	0.7	0.4	0.7	0.5	0.5	0.5	0.5	6.9E+15	7.1E+15	6.9E+15	6.5E+15	6.5E+15	3.2E+15	1.7E+15
52	TCM	IO-550-C	--	--	16.0	8.2	8.2	0.9	1.3	--	--	7.4E+15	6.6E+15	6.6E+15	1.0E+16	9.5E+15
53	Unknown (Skybolt Experimental)		--	--	--	--	--	0.0	--	--	--	--	--	--	5.5E+15	--
54	Garrett AiResearch	TPE331-6-252B	10.3	8.8	8.1	7.3	7.3	7.0	4.9	7.3E+14	8.3E+14	1.4E+15	2.6E+15	2.6E+15	3.5E+15	5.6E+15
55	Pratt & Whitney Canada	PT6A-60A	--	--	4.4	--	--	3.4	3.0	--	--	2.9E+15	--	--	1.5E+15	3.4E+15
56	Williams	FJ44-1AP	--	--	--	--	--	2.1	--	--	--	--	--	--	2.4E+15	--
57	General Electric	CF34-3A1	14.9	14.9	7.3	3.9	3.9	3.7	3.5	2.8E+14	2.8E+14	2.0E+14	8.6E+14	8.6E+14	7.0E+14	9.3E+14
Engine Family Averages																
	Continental	O-200	3.9	4.7	11.8	3.8	3.9	1.7	0.9	4.8E+15	3.9E+15	4.0E+15	1.8E+15	1.9E+15	3.2E+15	5.3E+15
	Lycoming	O-235	5.5	5.5	43.2	9.6	8.3	2.9	4.9	3.5E+15	3.5E+15	2.9E+15	3.2E+15	6.3E+15	4.5E+15	5.1E+15
	Lycoming	O-320	8.0	8.0	23.1	7.2	3.1	4.5	1.6	4.0E+15	4.0E+15	2.1E+15	2.2E+15	2.1E+15	1.6E+15	3.9E+15
	Lycoming	O-360	3.5	3.4	35.2	1.5	2.5	4.4	2.6	4.5E+15	3.3E+15	3.4E+15	1.8E+15	1.4E+15	2.6E+15	2.4E+15
	Lycoming	IO-360	18.1	17.7	36.1	10.6	0.4	1.5	0.4	6.7E+15	6.3E+15	7.3E+14	1.2E+15	1.1E+15	2.5E+15	5.8E+15
	Lycoming	O-540	2.5	5.2	30.3	3.1	3.1	1.9	1.3	4.8E+15	4.5E+15	9.1E+15	8.1E+15	1.1E+16	8.8E+15	7.6E+15
	Lycoming	IO-540	3.8	7.0	30.0	9.1	5.6	2.9	2.1	7.7E+15	4.5E+15	8.1E+15	6.7E+15	6.0E+15	5.6E+15	8.0E+15
Upper Limit on Engine Family Averages at 95% Confidence																
	Continental	O-200	6.1	11.7	30.7	14.6	16.2	5.0	4.3	1.4E+16	1.5E+16	1.2E+16	5.6E+15	5.9E+15	1.3E+16	1.1E+16
	Lycoming	O-235	29.3	29.3	124.2	51.3	18.5	7.3	27.7	1.1E+16	1.1E+16	1.4E+16	1.7E+16	3.2E+16	2.0E+16	1.7E+16
	Lycoming	O-320	30.7	30.7	61.6	28.0	10.1	19.5	4.2	1.3E+16	1.3E+16	6.7E+15	7.8E+15	7.6E+15	6.2E+15	1.5E+16
	Lycoming	O-360	9.7	6.9	90.5	3.8	11.9	22.4	11.8	1.6E+16	1.1E+16	1.0E+16	7.2E+15	6.2E+15	5.5E+15	5.4E+15
	Lycoming	IO-360	99.6	100.0	82.7	48.9	1.3	5.2	1.3	2.9E+16	2.9E+16	2.6E+15	4.8E+15	5.0E+15	7.6E+15	9.9E+15
	Lycoming	O-540	7.1	16.1	93.6	11.8	11.9	5.3	3.8	1.9E+16	2.0E+16	3.2E+16	2.9E+16	1.9E+16	2.0E+16	1.4E+16
	Lycoming	IO-540	6.0	16.1	97.6	35.4	18.2	12.1	12.8	2.5E+16	1.1E+16	3.2E+16	2.2E+16	2.1E+16	2.2E+16	1.8E+16

Copyright National Academy of Sciences. All rights reserved.

Unique ID	Engine Make	Engine Model	EI NOx g/kg						PM # Non-Volatile(via APC) #/kg						
			T/O	C/O	Cruise	App	Final App	Taxi	Idle	T/O	C/O	Cruise	App	Final App	Taxi	Idle
Preexisting Data																
FOCA[c.,e.]																
ICAO[d.]																
FAEED162	diverse	Prop-200hp	2.19	3.97		0.95	0.95	0.52	0.52	--	--	--	--	--	--	--
FAEED160	diverse	Prop-300hp	2.71	4.32		3.77	3.77	1.91	1.91	--	--	--	--	--	--	--
FAEED165	diverse	Prop-500hp	0.36	0.24		1.39	1.39	0.04	0.04	--	--	--	--	--	--	--
FOCA	diverse	Prop>500hp	0.99	2.38		13.64	13.64	22.00	22.00	--	--	--	--	--	--	--
FAEED159	TCM	O-200	4.87	4.87		1.14	1.14	1.58	1.58	--	--	--	--	--	--	--
FOCA	Lycoming	O-320-E2A	6.68	6.92		19.44	19.44	1.64	1.64	--	--	--	--	--	--	--
FAEED163	Lycoming	IO-320-DIAD	1.82	5.60		3.40	3.40	1.15	1.15	--	--	--	--	--	--	--
FOCA	Lycoming	O-360-A3A	3.51	5.81		2.99	2.99	1.43	1.43	--	--	--	--	--	--	--
FOCA	Lycoming	IO-360-A1B6	1.48	1.49		1.09	1.09	2.19	2.19	--	--	--	--	--	--	--
FAEED160	TCM	TSIO-360-C	2.71	4.32		3.77	3.77	1.91	1.91	--	--	--	--	--	--	--
FOCA	Lycoming	O-540-J3C5D	1.00	1.00		0.00	0.00	0.00	0.00	--	--	--	--	--	--	--
FOCA	Lycoming	IO-540-T4A5D	3.00	3.00		6.00	6.00	1.00	1.00	--	--	--	--	--	--	--
FOCA	TCM	IO-550-B	6.64	7.31		2.70	2.70	0.52	0.52	--	--	--	--	--	--	--
FOCA	Lycoming	TSIO-520-WB	2.96	2.09		1.17	1.17	3.54	3.54	--	--	--	--	--	--	--
FAEED165	Lycoming	TIO-540-J2B2	0.36	0.24		1.39	1.39	0.39	0.39	--	--	--	--	--	--	--
ICAO	General Electric	CF34-3A1	11.61	10.14		6.86	6.86	3.82	3.82	--	--	--	--	--	--	--
ICAO	Honeywell	AS907-1-1A	26.29	21.51		9.39	9.39	4.20	4.20	--	--	--	--	--	--	--
EDMS	Continental	6-285-B	5.88	5.50		4.72	4.72	0.46	0.46	--	--	--	--	--	--	--
EDMS	Curtiss-Wright	R-1820	1.72	2.09		6.50	6.50	0.00	0.00	--	--	--	--	--	--	--
EDMS	Lycoming	IO-320-D1AD	1.82	5.60		3.40	3.40	1.00	1.00	--	--	--	--	--	--	--
EDMS	Lycoming	IO-360-B	1.99	4.59		10.20	10.20	1.20	1.20	--	--	--	--	--	--	--
EDMS	Lycoming	O-200	4.87	4.87		1.10	1.10	1.60	1.60	--	--	--	--	--	--	--
EDMS	Lycoming	O-320	2.19	3.97		0.95	0.95	0.52	0.52	--	--	--	--	--	--	--
EDMS	Lycoming	TIO-540-J2B2	0.36	0.24		1.39	1.39	0.39	0.39	--	--	--	--	--	--	--
EDMS	Lycoming	TSIO-360-C	2.70	4.30		3.70	3.70	1.90	1.90	--	--	--	--	--	--	--
EDMS	Pratt & Whitney Canada	PT6A-60A	6.50	6.00		4.40	4.40	2.03	2.03	--	--	--	--	--	--	--
EDMS	Pratt & Whitney Canada	PT6A-114	7.30	7.00		5.30	5.30	2.75	2.75	--	--	--	--	--	--	--
EDMS	Pratt & Whitney Canada	PT6A-67	7.10	6.70		4.70	4.70	2.16	2.16	--	--	--	--	--	--	--
EDMS	Pratt & Whitney Canada	PT6a-66	6.20	5.90		4.10	4.10	1.70	1.70	--	--	--	--	--	--	--

Copyright National Academy of Sciences. All rights reserved.

Unique ID	Engine Make	Engine Model	PM # Total (via EEPS) #/kg							PM mass Non-Volatile (via MAAP) g/kg						
			T/O	C/O	Cruise	App	Final App	Taxi	Idle	T/O	C/O	Cruise	App	Final App	Taxi	Idle
Recommended for Substitution in EDMS/AEDT																
	Lycoming	O-320	1.1E+17	1.1E+17	1.2E+17	1.2E+17	9.4E+16	4.7E+16	5.8E+16	0.134	0.134	0.109	0.133	0.109	0.097	0.138
Individual Engine Tests																
1	Rotax	912	2.5E+17	2.5E+17	1.8E+17	1.8E+17	1.8E+17	1.0E+17	8.4E+16	0.045	0.045	0.026	0.005	0.005	0.001	0.000
2	Continental	O-200-A	--	--	--	--	--	8.1E+15	--	--	--	--	--	--	2.042	--
3	Continental	O-200-A	2.4E+17	2.4E+17	1.1E+17	1.1E+17	1.1E+17	1.2E+17	8.4E+16	0.043	0.043	0.029	0.008	0.008	0.025	0.071
4	Continental	O-200-A	9.8E+16	9.8E+16	2.4E+17	2.4E+17	5.0E+16	1.5E+17	2.1E+17	0.005	0.005	0.014	0.005	0.000	0.000	0.034
5	Continental	O-200-A	1.2E+17	5.8E+16	1.2E+17	--	--	1.6E+16	2.2E+16	0.733	0.337	0.733	0.061	0.061	0.036	1.722
6	Continental	O-200-A	8.2E+16	8.2E+16	1.1E+17	1.1E+17	2.4E+16	4.1E+16	2.9E+16	0.606	0.606	0.198	0.372	0.450	0.050	0.237
7	Lycoming	O-235-L2C	1.2E+17	1.2E+17	1.0E+17	1.0E+17	1.3E+17	1.0E+17	4.9E+16	0.273	0.273	0.516	0.970	2.837	0.840	0.937
8	Lycoming	O-235-L2C	8.0E+16	8.0E+16	1.6E+17	1.6E+17	4.0E+16	3.3E+16	2.6E+16	0.074	0.074	0.150	0.112	0.143	0.310	0.383
9	Lycoming	O-235-L2C	1.6E+17	1.6E+17	1.1E+17	1.1E+17	1.1E+17	4.9E+16	2.9E+16	0.140	0.140	0.063	0.000	0.000	0.000	0.095
10	Lycoming	O-320-E2D	9.1E+16	9.1E+16	1.4E+17	1.4E+17	1.4E+17	7.1E+16	3.3E+16	0.086	0.086	0.177	0.040	0.040	0.000	0.713
11	Lycoming	O-320-E2D	1.5E+17	1.5E+17	1.0E+17	1.0E+17	1.0E+17	1.7E+16	3.5E+16	0.008	0.008	0.003	0.000	0.000	0.002	0.015
12.1	Lycoming	O-320-E2D	9.6E+16	9.6E+16	8.1E+16	8.1E+16	3.1E+16	8.1E+16	4.4E+16	0.010	0.010	0.031	0.029	0.053	0.051	0.079
12.2	Lycoming	O-320-E2D								0.002	0.002	0.004	0.033	0.033	0.000	0.010
13	Lycoming	O-320-E2D	--	--	--	--	1.3E+17	1.3E+17	6.2E+16	--	--	--	0.328	0.732	0.268	0.059
14	Lycoming	O-320-E2D	8.8E+16	8.8E+16	8.6E+16	8.6E+16	4.8E+16	1.9E+16	1.9E+16	0.133	0.133	0.062	0.102	0.275	0.166	0.134
15	Lycoming	O-320-E2D	9.9E+16	9.9E+16	1.1E+17	1.1E+17	1.1E+17	6.2E+16	1.6E+17	0.077	0.077	0.115	0.061	0.061	0.271	0.294
16	Lycoming	O-320-E2D	1.4E+17	1.4E+17	0.0E+00	0.0E+00	0.0E+00	0.0E+00	2.9E+16	0.032	0.032	0.828	1.257	0.052	0.281	0.034
17	Lycoming	O-320-E2G	1.1E+17	1.1E+17	1.2E+17	1.2E+17	6.4E+16	4.5E+16	4.3E+16	0.217	0.217	0.318	0.084	0.271	0.000	0.800
18	Lycoming	O-320-E2G	8.4E+16	8.4E+16	0.0E+00	0.0E+00	0.0E+00	4.8E+16	4.6E+16	0.015	0.015	0.011	0.029	0.033	0.013	0.068
19	Lycoming	O-320-E3D	1.3E+17	1.3E+17	2.2E+17	2.2E+17	2.2E+17	5.1E+15	3.7E+16	0.140	0.140	0.025	0.014	0.014	0.006	0.012
20	Lycoming	O-320-B2C	4.7E+16	4.7E+16	6.9E+16	6.9E+16	6.9E+16	--	1.7E+17	1.430	1.430	0.091	--	--	--	0.000
21	Lycoming	O-320-B2C	--	--	5.3E+16	5.3E+16	5.3E+16	--	--	--	--	0.204	--	--	--	--
22	Lycoming	O-320-D2J	--	--	--	--	--	7.7E+15	1.2E+16	--	--	--	--	--	0.218	0.076
23	Lycoming	O-320-D3G	8.9E+16	8.9E+16	1.8E+17	1.8E+17	3.9E+16	2.3E+16	3.0E+16	0.001	0.001	0.049	0.000	0.015	0.008	0.005
24	Lycoming	O-320-D3G	1.0E+17	1.0E+17	1.5E+17	1.5E+17	1.5E+17	9.5E+16	8.1E+16	0.010	0.010	0.003	0.005	0.005	0.000	0.008
25	Lycoming	O-320-D3G	1.4E+17	1.4E+17	7.8E+16	7.8E+16	4.0E+16	4.8E+16	3.7E+16	0.044	0.044	0.019	0.048	0.007	0.004	0.011
26	Lycoming	O-320-D3G	1.1E+17	1.1E+17	1.6E+17	1.6E+17	1.8E+16	1.3E+16	7.2E+16	0.004	0.004	0.000	0.000	0.000	0.000	0.006
27	Lycoming	O-320-H2AD	1.1E+17	1.1E+17	4.2E+17	4.2E+17	4.2E+17	7.4E+16	4.3E+16	0.004	0.004	0.000	0.188	0.188	0.455	0.238
28	Lycoming	O-320-H2AD	9.9E+16	9.9E+16	1.2E+17	1.2E+17	5.7E+16	5.7E+16	9.1E+16	0.073	0.073	0.021	0.036	0.078	0.008	0.053
29	Franklin	6A4-165	7.4E+16	7.4E+16	1.9E+17	1.9E+17	2.2E+16	1.0E+17	1.0E+17	0.075	0.075	0.045	0.106	0.011	0.016	0.062
30	Lycoming	O-360-A4M	1.0E+17	1.0E+17	1.8E+17	1.8E+17	1.8E+17	4.3E+16	2.8E+16	0.007	0.007	0.000	0.074	0.074	0.001	0.102
31	Lycoming	O-360-C2E	1.2E+17	1.2E+17	1.4E+17	1.4E+17	5.8E+16	4.5E+16	3.0E+16	0.027	0.027	0.036	0.000	0.027	0.082	0.065
32.1	Lycoming	O-360-F1A6	1.2E+17	1.7E+17	1.8E+17	1.8E+17	8.3E+16	1.1E+16	3.6E+15	0.041	0.011	0.009	0.005	0.022	0.888	0.879
32.2	Lycoming	O-360-F1A6	2.7E+16	3.2E+16	5.1E+16	5.1E+16	5.1E+16	2.9E+16	2.2E+16	0.012	0.024	0.005	0.027	0.027	0.090	0.378
33	Lycoming	O-360-A1A	1.7E+17	1.6E+17	1.2E+17	1.2E+17	5.4E+16	6.2E+16	1.1E+17	0.068	0.027	0.038	0.031	0.195	0.019	0.004
34	Lycoming	O-360-A1G6D	1.7E+17	1.2E+17	1.9E+17	1.9E+17	7.1E+16	1.2E+17	1.2E+17	0.022	0.019	0.001	0.018	0.010	0.023	0.014
35	Lycoming	IO-360-L2A	9.8E+16	9.8E+16	1.6E+17	1.6E+17	1.6E+17	5.2E+16	6.6E+16	0.020	0.020	0.014	0.032	0.032	0.039	0.101
36	Lycoming	IO-360-A3B6D	2.2E+17	2.2E+17	1.4E+17	1.4E+17	3.4E+16	9.4E+16	1.2E+17	0.214	0.214	0.010	0.036	0.029	0.596	1.068

Copyright National Academy of Sciences. All rights reserved.

Unique ID	Engine Make	Engine Model	PM # Total (via EEPS) #/kg							PM mass Non-Volatile (via MAAP) g/kg						
			T/O	C/O	Cruise	App	Final App	Taxi	Idle	T/O	C/O	Cruise	App	Final App	Taxi	Idle
37	Lycoming	IO-360-C1C6	8.2E+16	8.2E+16	8.6E+16	8.6E+16	9.5E+15	6.3E+16	4.3E+16	0.022	0.022	0.002	0.000	0.000	0.050	0.022
38	Lycoming	IO-360-C1C6	1.0E+17	9.4E+16	7.8E+16	7.8E+16	7.8E+16	7.4E+16	7.0E+16	0.015	0.014	0.005	0.020	0.020	0.031	0.211
39	Lycoming	IO-520-1AB5	9.4E+16	9.4E+16	2.7E+17	2.7E+17	2.7E+17	6.4E+16	8.5E+16	0.019	0.019	0.075	0.093	0.093	0.107	0.224
40	Continental	O-470-11	--	--	2.1E+16	2.1E+16	2.1E+16	2.9E+16	2.5E+16	--	--	0.013	0.002	0.002	0.000	0.041
41	TCM	O-470-U	6.9E+16	6.9E+16	1.6E+17	1.6E+17	1.4E+17	1.5E+17	1.2E+17	0.011	0.011	0.011	0.068	0.027	0.160	0.059
42	Lycoming	O-540-B4B5	7.0E+16	8.5E+16	1.3E+17	1.3E+17	6.4E+16	4.7E+16	5.5E+16	0.017	0.011	0.016	0.046	0.106	0.103	0.043
43	Lycoming	O-540-A1D5	8.4E+16	6.6E+16	1.2E+17	1.2E+17	1.2E+17	1.3E+17	1.2E+17	0.298	0.287	0.181	0.412	0.412	0.152	0.789
44	Lycoming	O-540-J3C5D	8.6E+16	8.6E+16	1.5E+17	1.5E+17	1.5E+17	8.4E+16	4.4E+16	0.268	0.268	0.103	0.811	0.811	1.082	0.138
45	Lycoming	IO-540-C4B5	--	--	--	--	--	--	2.6E+14	--	--	--	--	--	--	0.000
46	Lycoming	IO-540-C4B5	1.4E+17	9.7E+16	1.8E+17	1.8E+17	1.7E+17	1.8E+17	1.3E+17	0.049	0.070	0.100	0.085	0.109	0.039	0.062
47.1	Lycoming	IO-540-C4B5	1.3E+17	1.3E+17	1.9E+17	1.9E+17	1.0E+17	2.8E+16	6.3E+16	0.052	0.026	0.012	0.015	0.014	0.705	0.057
47.2	Lycoming	IO-540-C4B5	4.5E+16	4.5E+16	2.8E+16	2.8E+16	2.8E+16	3.8E+15	5.0E+16	0.021	0.021	0.005	0.022	0.022	0.046	0.388
48	TCM	IO-540-BB	--	8.0E+16	9.7E+16	9.7E+16	9.7E+16	1.2E+17	9.3E+16	--	0.010	0.040	0.166	0.166	0.084	0.376
49	Lycoming	IO-540-K1G5D	7.1E+16	7.1E+16	1.2E+17	1.2E+17	1.2E+17	6.3E+16	8.5E+16	0.194	0.194	0.244	0.691	0.691	0.256	0.449
50	Continental	IO-550-N	--	--	--	--	--	--	2.2E+17	--	--	--	--	--	--	0.095
51	TCM	TSIO-520-C	8.6E+16	1.2E+17	8.6E+16	--	--	5.8E+16	3.9E+16	0.317	3.512	0.317	3.969	3.969	1.893	1.641
52	TCM	IO-550-C	--	--	9.6E+16	9.6E+16	9.6E+16	2.2E+17	1.8E+17	--	--	0.721	0.767	0.767	2.387	1.158
53	Unknown (Skybolt Experimental)		--	--	--	--	--	3.1E+16	--	--	--	--	--	--	1.162	--
54	Garrett AiResearch	TPE331-6-252B	3.4E+15	3.7E+15	4.1E+15	4.1E+15	4.1E+15	1.5E+16	2.8E+16	0.082	0.073	0.087	0.108	0.108	0.116	0.158
55	Pratt & Whitney Canada	PT6A-60A	--	--	2.0E+16	2.0E+16	2.0E+16	2.6E+16	3.4E+16	--	--	1.261	--	--	0.783	0.466
56	Williams	FJ44-1AP	--	--	--	--	--	4.3E+16	--	--	--	--	--	--	2.059	--
57	General Electric	CF34-3A1	5.7E+15	5.7E+15	5.5E+15	5.5E+15	5.5E+15	7.6E+15	7.0E+15	0.106	0.106	0.002	0.004	0.004	0.005	0.006
Engine Family Averages																
	Continental	O-200	1.3E+17	1.2E+17	1.5E+17	1.5E+17	6.1E+16	6.6E+16	8.7E+16	0.347	0.248	0.244	0.112	0.130	0.431	0.516
	Lycoming	O-235	1.2E+17	1.2E+17	1.2E+17	1.2E+17	9.4E+16	6.1E+16	3.5E+16	0.163	0.163	0.243	0.361	0.993	0.383	0.472
	Lycoming	O-320	1.1E+17	1.1E+17	1.2E+17	1.2E+17	9.4E+16	4.7E+16	5.8E+16	0.134	0.134	0.109	0.133	0.109	0.097	0.138
	Lycoming	O-360	1.2E+17	1.2E+17	1.4E+17	1.4E+17	8.2E+16	5.2E+16	5.3E+16	0.029	0.019	0.015	0.026	0.059	0.184	0.240
	Lycoming	IO-360	1.2E+17	1.2E+17	1.2E+17	1.2E+17	6.9E+16	7.1E+16	7.4E+16	0.068	0.068	0.008	0.022	0.020	0.179	0.350
	Lycoming	O-540	8.0E+16	7.9E+16	1.3E+17	1.3E+17	1.1E+17	8.7E+16	7.4E+16	0.195	0.189	0.100	0.423	0.443	0.446	0.323
	Lycoming	IO-540	9.6E+16	8.5E+16	1.2E+17	1.2E+17	1.0E+17	7.8E+16	6.9E+16	0.079	0.064	0.080	0.196	0.200	0.226	0.222
Upper Limit on Engine Family Averages at 95% Confidence																
	Continental	O-200	3.6E+17	3.8E+17	3.5E+17	4.9E+17	2.5E+17	2.4E+17	3.7E+17	1.546	1.143	1.315	0.670	0.814	2.932	3.090
	Lycoming	O-235	2.9E+17	2.9E+17	2.5E+17	2.5E+17	3.0E+17	2.2E+17	8.8E+16	0.599	0.599	1.276	2.644	7.870	2.211	2.314
	Lycoming	O-320	1.6E+17	1.6E+17	3.3E+17	3.3E+17	3.0E+17	1.2E+17	1.5E+17	0.854	0.854	0.530	0.772	0.497	0.395	0.627
	Lycoming	O-360	2.5E+17	2.5E+17	2.8E+17	2.8E+17	2.1E+17	1.5E+17	1.8E+17	0.087	0.041	0.059	0.094	0.240	1.075	1.119
	Lycoming	IO-360	3.2E+17	3.2E+17	2.4E+17	2.4E+17	2.8E+17	1.3E+17	1.7E+17	0.379	0.379	0.026	0.074	0.066	1.064	1.892
	Lycoming	O-540	1.2E+17	1.3E+17	2.1E+17	2.1E+17	3.0E+17	2.7E+17	2.6E+17	0.859	0.854	0.454	2.069	1.965	2.820	2.070
	Lycoming	IO-540	2.4E+17	1.8E+17	3.1E+17	3.1E+17	2.5E+17	2.7E+17	1.8E+17	0.327	0.275	0.355	0.983	0.982	1.008	0.742

Copyright National Academy of Sciences. All rights reserved.

Unique ID	Engine Make	Engine Model	PM # Total (via EEPS) #/kg							PM mass Non-Volatile (via MAAP) g/kg						
			T/O	C/O	Cruise	App	Final App	Taxi	Idle	T/O	C/O	Cruise	App	Final App	Taxi	Idle
Preexisting Data																
FOCA[c.,e.]																
ICAO[d.]																
FAEED162	diverse	Prop-200hp	--	--	--	--	--	--	--	--	--	--	--	--	--	--
FAEED160	diverse	Prop-300hp	--	--	--	--	--	--	--	--	--	--	--	--	--	--
FAEED165	diverse	Prop-500hp	--	--	--	--	--	--	--	--	--	--	--	--	--	--
FOCA	diverse	Prop>500hp	--	--	--	--	--	--	--	--	--	--	--	--	--	--
FAEED159	TCM	O-200	--	--	--	--	--	--	--	--	--	--	--	--	--	--
FOCA	Lycoming	O-320-E2A	--	--	--	--	--	--	--	--	--	--	--	--	--	--
FAEED163	Lycoming	IO-320-DIAD	--	--	--	--	--	--	--	--	--	--	--	--	--	--
FOCA	Lycoming	O-360-A3A	--	--	--	--	--	--	--	--	--	--	--	--	--	--
FOCA	Lycoming	IO-360-A1B6	--	--	--	--	--	--	--	--	--	--	--	--	--	--
FAEED160	TCM	TSIO-360-C	--	--	--	--	--	--	--	--	--	--	--	--	--	--
FOCA	Lycoming	O-540-J3C5D	--	--	--	--	--	--	--	--	--	--	--	--	--	--
FOCA	Lycoming	IO-540-T4A5D	--	--	--	--	--	--	--	--	--	--	--	--	--	--
FOCA	TCM	IO-550-B	--	--	--	--	--	--	--	--	--	--	--	--	--	--
FOCA	Lycoming	TSIO-520-WB	--	--	--	--	--	--	--	--	--	--	--	--	--	--
FAEED165	Lycoming	TIO-540-J2B2	--	--	--	--	--	--	--	--	--	--	--	--	--	--
ICAO	General Electric	CF34-3A1	--	--	--	--	--	--	--	--	--	--	--	--	--	--
ICAO	Honeywell	AS907-1-1A	--	--	--	--	--	--	--	--	--	--	--	--	--	--
EDMS	Continental	6-285-B	--	--	--	--	--	--	--	--	--	--	--	--	--	--
EDMS	Curtiss-Wright	R-1820	--	--	--	--	--	--	--	--	--	--	--	--	--	--
EDMS	Lycoming	IO-320-D1AD	--	--	--	--	--	--	--	--	--	--	--	--	--	--
EDMS	Lycoming	IO-360-B	--	--	--	--	--	--	--	--	--	--	--	--	--	--
EDMS	Lycoming	O-200	--	--	--	--	--	--	--	--	--	--	--	--	--	--
EDMS	Lycoming	O-320	--	--	--	--	--	--	--	--	--	--	--	--	--	--
EDMS	Lycoming	TIO-540-J2B2	--	--	--	--	--	--	--	--	--	--	--	--	--	--
EDMS	Lycoming	TSIO-360-C	--	--	--	--	--	--	--	--	--	--	--	--	--	--
EDMS	Pratt & Whitney Canada	PT6A-60A	--	--	--	--	--	--	--	--	--	--	--	--	--	--
EDMS	Pratt & Whitney Canada	PT6A-114	--	--	--	--	--	--	--	--	--	--	--	--	--	--
EDMS	Pratt & Whitney Canada	PT6A-67	--	--	--	--	--	--	--	--	--	--	--	--	--	--
EDMS	Pratt & Whitney Canada	PT6a-66	--	--	--	--	--	--	--	--	--	--	--	--	--	--

Copyright National Academy of Sciences. All rights reserved.

Unique ID	Engine Make	Engine Model	PM mass Total (via EEPS) g/kg T/O	C/O	Cruise	App	Final App	Taxi	Idle	Fuel Spec	H/C Ratio	Arom %
Recommended for Substitution in EDMS/AEDT												
	Lycoming	O-320	0.197	0.197	0.177	0.269	0.132	0.148	0.466	AVGAS 100LL	2.32	<10%
Individual Engine Tests												
1	Rotax	912	0.292	0.292	0.393	0.205	0.205	0.307	0.104	AVGAS 100LL	2.32	<10%
2	Continental	O-200-A	--	--	--	--	--	0.000	--	AVGAS 100LL	2.32	<10%
3	Continental	O-200-A	0.314	0.314	0.142	0.089	0.089	1.215	0.971	AVGAS 100LL	2.32	<10%
4	Continental	O-200-A	0.169	0.169	0.292	0.202	0.097	0.607	0.802	AVGAS 100LL	2.32	<10%
5	Continental	O-200-A	0.199	0.057	0.199	0.080	0.080	0.040	0.282	AVGAS 100LL	2.32	<10%
6	Continental	O-200-A	0.151	0.151	0.136	0.155	0.083	0.065	0.142	AVGAS 100LL	2.32	<10%
7	Lycoming	O-235-L2C	0.163	0.163	0.212	0.597	0.932	0.398	0.516	AVGAS 100LL	2.32	<10%
8	Lycoming	O-235-L2C	0.158	0.158	0.298	0.174	0.189	0.152	0.283	AVGAS 100LL	2.32	<10%
9	Lycoming	O-235-L2C	0.545	0.545	0.249	0.136	0.136	0.187	0.289	AVGAS 100LL	2.32	<10%
10	Lycoming	O-320-E2D	0.107	0.107	0.220	0.060	0.060	0.074	0.238	AVGAS 100LL	2.32	<10%
11	Lycoming	O-320-E2D	0.165	0.165	0.166	0.073	0.073	0.060	0.170	AVGAS 100LL	2.32	<10%
12.1	Lycoming	O-320-E2D	0.106	0.106	0.091	0.114	0.053	0.452	0.136	AVGAS 100LL	2.32	<10%
12.2	Lycoming	O-320-E2D								AVGAS 100LL	2.32	<10%
13	Lycoming	O-320-E2D	--	--	--	0.244	0.508	0.494	0.907	AVGAS 100LL	2.32	<10%
14	Lycoming	O-320-E2D	0.184	0.184	0.147	0.133	0.114	0.056	0.132	AVGAS 100LL	2.32	<10%
15	Lycoming	O-320-E2D	0.167	0.167	0.250	0.181	0.181	0.106	1.074	AVGAS 100LL	2.32	<10%
16	Lycoming	O-320-E2D	0.237	0.237	0.000	2.133	0.000	0.000	0.092	AVGAS 100LL	2.32	<10%
17	Lycoming	O-320-E2G	0.172	0.172	0.267	0.152	0.122	0.037	0.203	AVGAS 100LL	2.32	<10%
18	Lycoming	O-320-E2G	0.052	0.052	0.000	0.071	0.000	0.000	0.131	AVGAS 100LL	2.32	<10%
19	Lycoming	O-320-E3D	0.291	0.291	0.394	0.200	0.200	0.150	0.188	AVGAS 100LL	2.32	<10%
20	Lycoming	O-320-B2C	0.849	0.849	0.274	--	--	--	3.894	AVGAS 100LL	2.32	<10%
21	Lycoming	O-320-B2C	--	--	0.049	--	--	--	--	AVGAS 100LL	2.32	<10%
22	Lycoming	O-320-D2J	--	--	--	--	--	0.000	0.019	AVGAS 100LL	2.32	<10%
23	Lycoming	O-320-D3G	0.062	0.062	0.136	0.047	0.037	0.014	0.106	AVGAS 100LL	2.32	<10%
24	Lycoming	O-320-D3G	0.092	0.092	0.121	0.056	0.056	0.399	0.402	AVGAS 100LL	2.32	<10%
25	Lycoming	O-320-D3G	0.235	0.235	0.136	0.193	0.130	0.088	0.112	AVGAS 100LL	2.32	<10%
26	Lycoming	O-320-D3G	0.101	0.101	0.122	0.055	0.079	0.076	0.237	AVGAS 100LL	2.32	<10%
27	Lycoming	O-320-H2AD	0.236	0.236	0.551	0.434	0.434	0.433	0.244	AVGAS 100LL	2.32	<10%
28	Lycoming	O-320-H2AD	0.093	0.093	0.093	0.158	0.058	0.072	0.110	AVGAS 100LL	2.32	<10%
29	Franklin	6A4-165	0.144	0.144	0.235	0.379	0.196	0.270	0.854	AVGAS 100LL	2.32	<10%
30	Lycoming	O-360-A4M	0.093	0.093	0.144	0.493	0.493	0.051	0.046	AVGAS 100LL	2.32	<10%
31	Lycoming	O-360-C2E	0.107	0.107	0.135	0.054	0.068	0.201	0.091	AVGAS 100LL	2.32	<10%
32.1	Lycoming	O-360-F1A6	0.163	0.226	0.216	0.117	0.084	0.822	0.708	AVGAS 100LL	2.32	<10%
32.2	Lycoming	O-360-F1A6	0.014	0.011	0.020	0.000	0.000	0.160	0.370	AVGAS 100LL	2.32	<10%
33	Lycoming	O-360-A1A	0.294	0.162	0.145	0.248	0.265	1.170	0.975	AVGAS 100LL	2.32	<10%
34	Lycoming	O-360-A1G6D	0.212	0.168	0.170	0.155	0.082	0.404	0.721	AVGAS 100LL	2.32	<10%
35	Lycoming	IO-360-L2A	0.142	0.142	0.210	0.201	0.201	0.083	0.403	AVGAS 100LL	2.32	<10%
36	Lycoming	IO-360-A3B6D	0.872	0.872	0.084	0.164	0.035	1.581	2.011	AVGAS 100LL	2.32	<10%

Copyright National Academy of Sciences. All rights reserved.

Unique ID	Engine Make	Engine Model	PM mass Total (via EEPS) g/kg T/O	C/O	Cruise	App	Final App	Taxi	Idle	Fuel Spec	H/C Ratio	Arom %
37	Lycoming	IO-360-C1C6	0.099	0.099	0.091	0.049	0.147	0.203	0.176	AVGAS 100LL	2.32	<10%
38	Lycoming	IO-360-C1C6	0.109	0.088	0.062	0.075	0.075	0.138	0.431	AVGAS 100LL	2.32	<10%
39	Lycoming	IO-520-1AB5	0.063	0.063	0.240	0.512	0.512	0.255	0.359	AVGAS 100LL	2.32	<10%
40	Continental	O-470-11	--	--	0.089	0.091	0.091	0.180	0.260	AVGAS 100LL	2.32	<10%
41	TCM	O-470-U	0.115	0.115	0.186	0.100	0.474	0.564	0.428	AVGAS 100LL	2.32	<10%
42	Lycoming	O-540-B4B5	0.079	0.081	0.139	0.103	0.203	0.194	0.189	AVGAS 100LL	2.32	<10%
43	Lycoming	O-540-A1D5	0.212	0.191	0.233	0.779	0.779	1.106	1.847	AVGAS 100LL	2.32	<10%
44	Lycoming	O-540-J3C5D	0.131	0.131	0.210	0.240	0.240	0.409	0.167	AVGAS 100LL	2.32	<10%
45	Lycoming	IO-540-C4B5	--	--	--	--	--	--	0.923	AVGAS 100LL	2.32	<10%
46	Lycoming	IO-540-C4B5	0.182	0.193	0.557	0.877	1.771	1.140	1.155	AVGAS 100LL	2.32	<10%
47.1	Lycoming	IO-540-C4B5	0.312	0.237	0.273	0.317	0.139	0.451	0.166	AVGAS 100LL	2.32	<10%
47.2	Lycoming	IO-540-C4B5	0.182	0.182	0.070	0.096	0.096	0.037	0.543	AVGAS 100LL	2.32	<10%
48	TCM	IO-540-BB	--	0.094	0.122	0.159	0.159	0.352	1.016	AVGAS 100LL	2.32	<10%
49	Lycoming	IO-540-K1G5D	0.117	0.117	0.220	0.325	0.325	0.138	0.290	AVGAS 100LL	2.32	<10%
50	Continental	IO-550-N	--	--	--	--	--	--	0.659	AVGAS 100LL	2.32	<10%
51	TCM	TSIO-520-C	0.403	0.497	0.403	0.609	0.609	0.578	0.537	AVGAS 100LL	2.32	<10%
52	TCM	IO-550-C	--	--	0.272	0.269	0.269	4.126	2.607	AVGAS 100LL	2.32	<10%
53	Unknown (Skybolt Experimental)		--	--	--	--	--	0.405	--	AVGAS 100LL	2.32	<10%
54	Garrett AiResearch	TPE331-6-252B	0.003	0.003	0.004	0.009	0.009	0.011	0.020	JET A	1.90	
55	Pratt & Whitney Canada	PT6A-60A	--	--	0.040	--	--	0.033	0.091	JET A	1.90	
56	Williams	FJ44-1AP	--	--	--	--	--	0.515	--	JET A	1.90	
57	General Electric	CF34-3A1	0.105	0.105	0.004	0.008	0.008	0.010	0.010	JET A	1.90	
Engine Family Averages												
	Continental	O-200	0.208	0.173	0.192	0.132	0.087	0.386	0.549	AVGAS 100LL	2.32	<10%
	Lycoming	O-235	0.289	0.289	0.253	0.302	0.419	0.246	0.363	AVGAS 100LL	2.32	<10%
	Lycoming	O-320	0.197	0.197	0.177	0.269	0.132	0.148	0.466	AVGAS 100LL	2.32	<10%
	Lycoming	O-360	0.147	0.128	0.138	0.178	0.165	0.468	0.485	AVGAS 100LL	2.32	<10%
	Lycoming	IO-360	0.306	0.300	0.112	0.122	0.115	0.501	0.755	AVGAS 100LL	2.32	<10%
	Lycoming	O-540	0.141	0.134	0.194	0.374	0.407	0.570	0.734	AVGAS 100LL	2.32	<10%
	Lycoming	IO-540	0.198	0.165	0.248	0.355	0.498	0.424	0.682	AVGAS 100LL	2.32	<10%
Upper Limit on Engine Family Averages at 95% Confidence												
	Continental	O-200	0.441	0.511	0.423	0.315	0.111	1.847	1.821			
	Lycoming	O-235	1.245	1.245	0.440	1.404	2.336	0.817	0.934			
	Lycoming	O-320	0.597	0.597	0.475	1.349	0.439	0.519	2.365			
	Lycoming	O-360	0.400	0.319	0.306	0.631	0.636	1.596	1.452			
	Lycoming	IO-360	1.508	1.515	0.323	0.351	0.350	2.797	3.444			
	Lycoming	O-540	0.430	0.372	0.404	1.911	1.794	2.620	4.881			
	Lycoming	IO-540	0.460	0.326	0.776	1.211	2.489	1.627	1.732			

Copyright National Academy of Sciences. All rights reserved.

Unique ID	Engine Make	Engine Model	PM mass Total (via EEPS) g/kg T/O	C/O	Cruise	App	Final App	Taxi	Idle	Fuel Spec	H/C Ratio	Arom %
Preexisting Data												
FOCA[c.,e.]												
ICAO[d.]												
FAEED162	diverse	Prop-200hp	0.10	0.07		0.04	0.04	0.05	0.05			
FAEED160	diverse	Prop-300hp	0.10	0.07		0.40	0.40	0.50	0.50			
FAEED165	diverse	Prop-500hp	0.10	0.70		0.40	0.40	0.50	0.50			
FOCA	diverse	Prop>500hp	0.10	0.10		0.10	0.10	0.10	0.10	AVGAS 100LL	1.857	
FAEED159	TCM	O-200	0.10	0.07		0.04	0.04	0.05	0.05			
FOCA	Lycoming	O-320-E2A	0.10	0.07		0.04	0.04	0.05	0.05	AVGAS 100LL	1.857	
FAEED163	Lycoming	IO-320-DIAD	0.10	0.07		0.04	0.04	0.05	0.05			
FOCA	Lycoming	O-360-A3A	0.10	0.07		0.04	0.04	0.05	0.05	AVGAS 100LL	1.857	
FOCA	Lycoming	IO-360-A1B6	0.10	0.20		0.50	0.50	0.10	0.10	AVGAS 100LL	1.857	
FAEED160	TCM	TSIO-360-C	0.10	0.07		0.04	0.04	0.05	0.05			
FOCA	Lycoming	O-540-J3C5D	--	--		--	--	--	--	AVGAS 100LL	1.857	
FOCA	Lycoming	IO-540-T4A5D	0.10	0.07		0.40	0.40	0.05	0.05	AVGAS 100LL	1.857	
FOCA	TCM	IO-550-B	0.10	0.07		0.04	0.04	0.05	0.05	AVGAS 100LL	1.857	
FOCA	Lycoming	TSIO-520-WB	0.10	0.07		0.04	0.04	0.05	0.05	AVGAS 100LL	1.857	
FAEED165	Lycoming	TIO-540-J2B2	0.10	0.07		0.04	0.04	0.05	0.05			
ICAO	General Electric	CF34-3A1	--	--	--	--	--	--	--	JP-5	1.92	20.3
ICAO	Honeywell	AS907-1-1A	--	--	--	--	--	--	--	Jet A	1.866	16.5
EDMS	Continental	6-285-B	--	--	--	--	--	--	--			
EDMS	Curtiss-Wright	R-1820	--	--	--	--	--	--	--			
EDMS	Lycoming	IO-320-D1AD	--	--	--	--	--	--	--			
EDMS	Lycoming	IO-360-B	--	--	--	--	--	--	--			
EDMS	Lycoming	O-200	--	--	--	--	--	--	--			
EDMS	Lycoming	O-320	--	--	--	--	--	--	--			
EDMS	Lycoming	TIO-540-J2B2	--	--	--	--	--	--	--			
EDMS	Lycoming	TSIO-360-C	--	--	--	--	--	--	--			
EDMS	Pratt & Whitney Canada	PT6A-60A	--	--	--	--	--	--	--			
EDMS	Pratt & Whitney Canada	PT6A-114	--	--	--	--	--	--	--			
EDMS	Pratt & Whitney Canada	PT6A-67	--	--	--	--	--	--	--			
EDMS	Pratt & Whitney Canada	PT6a-66	--	--	--	--	--	--	--			

Copyright National Academy of Sciences. All rights reserved.

Unique ID	Engine Make	Engine Model	Fuel Flow T/O (kg/sec)	Fuel Flow C/O (kg/sec)	Fuel Flow Cruise (kg/sec)	Fuel Flow App (kg/sec)	Fuel Flow Final App (kg/sec)	Fuel Flow Taxi (kg/sec)	Fuel Flow Idle (kg/sec)	Ambient Baro bar	Ambient Baro kPa	Ambient Temp K	Ambient Temp C	Ambient Humidity kg/kg	Ambient Humidity vol/vol
Recommended for Substitution in EDMS/AEDT															
	Lycoming	O-320	0.010	0.010	0.007	0.004	0.004	0.002	0.001	0.97	96.5	291.9	18.8	7.2E-03	1.2%
Individual Engine Tests															
1	Rotax	912	0.0033	0.0033	0.0023	0.0014	0.0014	0.0010	0.0006	1.01	100.5	295.5	22.3	1.3E-02	2.0%
2	Continental	O-200-A	--	--	--	--	--	0.0014	--	1.01	100.6	292.7	19.5	6.8E-03	1.1%
3	Continental	O-200-A	0.0067	0.0067	0.0045	0.0033	0.0033	0.0015	0.0010	1.02	102.5	291.7	18.6	6.3E-03	1.0%
4	Continental	O-200-A	0.0067	0.0067	0.0060	0.0027	0.0018	0.0015	0.0015	1.02	102.4	291.8	18.6	5.8E-03	0.9%
5	Continental	O-200-A	0.0067	0.0046	0.0067	0.0028	0.0028	0.0017	0.0011	1.01	101.3	288.7	15.5	4.3E-03	0.7%
6	Continental	O-200-A	0.0067	0.0067	0.0067	0.0044	0.0026	0.0017	0.0012	1.02	101.7	295.3	22.2	8.7E-03	1.4%
7	Lycoming	O-235-L2C	0.0070	0.0070	0.0058	0.0035	0.0015	0.0013	0.0010	1.02	101.9	292.7	19.5	8.7E-03	1.4%
8	Lycoming	O-235-L2C	0.0070	0.0070	0.0058	0.0036	0.0015	0.0013	0.0011	1.02	101.8	293.3	20.2	8.7E-03	1.4%
9	Lycoming	O-235-L2C	0.0070	0.0070	0.0070	0.0026	0.0026	0.0029	0.0010	1.03	102.7	288.6	15.5	6.0E-03	1.0%
10	Lycoming	O-320-E2D	0.0103	0.0103	0.0089	0.0038	0.0038	0.0022	0.0011	1.02	101.5	285.4	12.2	4.3E-03	0.7%
11	Lycoming	O-320-E2D	0.0102	0.0102	0.0088	0.0026	0.0026	0.0017	0.0011	1.01	100.6	294.5	21.3	1.2E-02	2.0%
12.1	Lycoming	O-320-E2D	0.0103	0.0103	0.0068	0.0081	0.0038	0.0018	0.0013	1.02	102.0	294.0	20.8	7.3E-03	1.2%
12.2	Lycoming	O-320-E2D	0.0103	0.0103	0.0060	0.0038	0.0038	0.0024	0.0014	1.02	101.6	283.7	10.5	4.6E-03	0.7%
13	Lycoming	O-320-E2D	--	--	--	0.0023	0.0035	0.0017	0.0011	1.02	102.0	292.4	19.3	5.0E-03	0.8%
14	Lycoming	O-320-E2D	0.0119	0.0119	0.0110	0.0054	0.0030	0.0015	0.0013	1.02	101.6	294.6	21.5	8.7E-03	1.4%
15	Lycoming	O-320-E2D	0.0103	0.0103	0.0061	0.0040	0.0040	0.0018	0.0010	1.01	100.7	293.0	19.9	6.8E-03	1.1%
16	Lycoming	O-320-E2D	0.0103	0.0103	0.0053	0.0036	0.0032	0.0021	0.0015	1.02	102.3	296.2	23.1	6.5E-03	1.0%
17	Lycoming	O-320-E2G	0.0103	0.0103	0.0079	0.0040	0.0045	0.0020	0.0010	1.01	101.5	286.0	12.8	4.3E-03	0.7%
18	Lycoming	O-320-E2G	0.0103	0.0103	0.0064	0.0071	0.0040	0.0018	0.0012	1.02	102.4	294.2	21.0	6.5E-03	1.1%
19	Lycoming	O-320-E3D	0.0103	0.0103	0.0096	0.0036	0.0036	0.0016	0.0009	1.01	101.2	295.8	22.6	1.0E-02	1.6%
20	Lycoming	O-320-B2C	0.0103	0.0103	0.0045	--	--	--	0.0025	1.01	101.5	287.1	14.0	4.3E-03	0.7%
21	Lycoming	O-320-B2C	--	--	0.0045	--	--	--	--	1.01	101.3	290.3	17.1	4.3E-03	0.7%
22	Lycoming	O-320-D2J	--	--	--	--	--	0.0018	0.0011	1.02	102.3	293.6	20.4	6.2E-03	1.0%
23	Lycoming	O-320-D3G	0.0103	0.0103	0.0068	0.0024	0.0103	0.0015	0.0011	1.01	101.3	292.9	19.8	9.2E-03	1.5%
24	Lycoming	O-320-D3G	0.0103	0.0103	0.0077	0.0032	0.0032	0.0015	0.0010	1.01	100.6	293.3	20.1	1.2E-02	1.9%
25	Lycoming	O-320-D3G	0.0103	0.0103	0.0078	0.0054	0.0041	0.0031	0.0011	1.03	102.7	289.3	16.2	6.1E-03	1.0%
26	Lycoming	O-320-D3G	0.0103	0.0103	0.0067	0.0025	0.0022	0.0015	0.0012	1.00	100.5	296.5	23.4	1.3E-02	2.0%
27	Lycoming	O-320-H2AD	0.0077	0.0077	0.0060	0.0036	0.0036	0.0014	0.0012	1.02	102.4	292.1	18.9	6.3E-03	1.0%
28	Lycoming	O-320-H2AD	0.0097	0.0097	0.0087	0.0075	0.0056	0.0017	0.0013	1.02	102.4	293.9	20.8	6.3E-03	1.0%
29	Franklin	6A4-165	0.0103	0.0103	0.0060	0.0052	0.0018	0.0018	0.0012	1.01	101.1	295.5	22.4	1.0E-02	1.6%
30	Lycoming	O-360-A4M	0.0105	0.0105	0.0068	0.0039	0.0039	0.0017	0.0015	1.00	100.5	297.0	23.8	1.3E-02	2.0%
31	Lycoming	O-360-C2E	0.0110	0.0110	0.0049	0.0039	0.0042	0.0020	0.0017	1.02	102.1	291.0	17.9	7.0E-03	1.1%
32.1	Lycoming	O-360-F1A6	0.0110	0.0100	0.0077	0.0068	0.0052	0.0017	0.0011	1.02	102.3	294.8	21.6	6.5E-03	1.0%
32.2	Lycoming	O-360-F1A6	0.0110	0.0092	0.0080	0.0031	0.0031	0.0018	0.0009	1.02	101.5	286.3	13.1	4.0E-03	0.6%
33	Lycoming	O-360-A1A	0.0104	0.0097	0.0068	0.0029	0.0029	0.0014	0.0022	1.00	100.4	294.7	21.5	1.3E-02	2.0%
34	Lycoming	O-360-A1G6D	0.0116	0.0091	0.0076	0.0064	0.0050	0.0015	0.0024	1.03	102.6	290.9	17.7	6.0E-03	1.0%
35	Lycoming	IO-360-L2A	0.0106	0.0106	0.0068	0.0015	0.0015	0.0019	0.0013	1.01	101.2	294.2	21.1	9.9E-03	1.6%
36	Lycoming	IO-360-A3B6D	0.0116	0.0116	0.0044	0.0029	0.0037	0.0014	0.0012	1.03	102.7	290.3	17.1	6.3E-03	1.0%
37	Lycoming	IO-360-C1C6	0.0091	0.0091	0.0072	0.0030	0.0023	0.0023	0.0015	1.00	100.4	296.9	23.7	1.3E-02	2.0%
38	Lycoming	IO-360-C1C6	0.0113	0.0113	0.0053	0.0036	0.0036	0.0023	0.0015	1.01	101.5	292.6	19.4	7.8E-03	1.3%

Copyright National Academy of Sciences. All rights reserved.

Unique ID	Engine Make	Engine Model	Fuel Flow kg/sec							Ambient					
			T/O	C/O	Cruise	App	Final App	Taxi	Idle	Baro bar	Baro kPa	Temp K	Temp C	Humidity kg/kg	Humidity vol/vol
39	Lycoming	IO-520-1AB5	0.0140	0.0140	0.0079	0.0061	0.0061	0.0023	0.0020	1.02	101.9	295.4	22.2	7.4E-03	1.2%
40	Continental	O-470-11	--	--	0.0109	0.0055	0.0055	0.0024	0.0016	1.02	101.9	287.1	13.9	4.3E-03	0.7%
41	TCM	O-470-U	0.0110	0.0110	0.0067	0.0033	0.0018	0.0015	0.0004	1.01	101.2	293.1	19.9	9.6E-03	1.5%
42	Lycoming	O-540-B4B5	0.0108	0.0095	0.0076	0.0059	0.0028	0.0025	0.0018	1.01	101.4	293.1	19.9	8.2E-03	1.3%
43	Lycoming	O-540-A1D5	0.0227	0.0191	0.0109	0.0072	0.0072	0.0021	0.0019	1.02	101.9	284.1	10.9	4.3E-03	0.7%
44	Lycoming	O-540-J3C5D	0.0155	0.0155	0.0080	0.0052	0.0052	0.0024	0.0020	1.01	100.7	294.2	21.0	6.8E-03	1.1%
45	Lycoming	IO-540-C4B5	--	--	--	--	--	--	0.0018	1.02	102.0	292.0	18.9	5.0E-03	0.8%
46	Lycoming	IO-540-C4B5	0.0178	0.0164	0.0091	0.0044	0.0044	0.0039	0.0022	1.01	101.1	296.2	23.0	1.0E-02	1.6%
47.1	Lycoming	IO-540-C4B5	0.0170	0.0108	0.0094	0.0106	0.0087	0.0031	0.0025	1.02	102.3	293.3	20.1	6.4E-03	1.0%
47.2	Lycoming	IO-540-C4B5	0.0174	0.0174	0.0110	0.0073	0.0073	0.0051	0.0024	1.02	101.5	287.2	14.0	4.1E-03	0.7%
48	TCM	IO-540-BB	--	0.0151	0.0129	0.0101	0.0101	0.0049	0.0027	1.01	100.7	292.7	19.6	6.8E-03	1.1%
49	Lycoming	IO-540-K1G5D	0.0122	0.0122	0.0109	0.0087	0.0087	0.0032	0.0023	1.02	102.0	283.7	10.6	4.3E-03	0.7%
50	Continental	IO-550-N	--	--	--	--	--	--	0.0031	1.01	101.3	289.2	16.0	4.3E-03	0.7%
51	TCM	TSIO-520-C	0.0166	0.0113	0.0166	0.0060	0.0060	0.0037	0.0022	1.01	100.8	291.9	18.8	6.8E-03	1.1%
52	TCM	IO-550-C	--	--	0.0113	0.0101	0.0101	0.0044	0.0034	1.01	101.3	288.1	14.9	4.3E-03	0.7%
53	Unknown (Skybolt Experimental)		--	--	--	--	--	0.0011	--	1.02	101.7	294.5	21.3	8.7E-03	1.4%
54	Garrett AiResearch	TPE331-6-252B	0.0567	0.0504	0.0315	0.0292	0.0292	0.0239	0.0148	1.01	101.3	283.8	10.6	5.9E-03	1.0%
55	Pratt & Whitney Canada	PT6A-60A	--	--	0.0600	--	--	0.0450	0.0605	1.02	101.7	292.9	19.7	8.7E-03	1.4%
56	Williams	FJ44-1AP	--	--	--	--	--		--	1.01	100.6	293.3	20.2	6.8E-03	1.1%
57	General Electric	CF34-3A1	0.3276	0.3276	0.1644	0.1260	0.1260	0.0592	0.0529	1.02	101.6	285.4	12.3	4.4E-03	0.7%
Engine Family Averages															
	Continental	O-200	0.007	0.006	0.006	0.003	0.003	0.002	0.001	1.02	101.7	292.0	18.9	6.4E-03	1.0%
	Lycoming	O-235	0.007	0.007	0.006	0.003	0.002	0.002	0.001	1.02	102.1	291.5	18.4	7.8E-03	1.3%
	Lycoming	O-320	0.010	0.010	0.007	0.004	0.004	0.002	0.001	0.97	96.5	291.9	18.8	7.2E-03	1.2%
	Lycoming	O-360	0.011	0.010	0.007	0.004	0.004	0.002	0.002	0.85	84.7	292.4	19.3	8.1E-03	1.3%
	Lycoming	IO-360	0.011	0.011	0.006	0.003	0.003	0.002	0.001	1.01	101.4	293.5	20.3	9.1E-03	1.5%
	Lycoming	O-540	0.016	0.015	0.009	0.006	0.005	0.002	0.002	1.01	101.3	290.5	17.3	6.5E-03	1.0%
	Lycoming	IO-540	0.016	0.014	0.011	0.008	0.008	0.004	0.002	0.85	84.7	290.8	17.7	6.1E-03	1.0%
Upper Limit on Engine Family Averages at 95% Confidence															
	Continental	O-200	0.0067	0.0095	0.0092	0.0058	0.0045	0.0019	0.0018						
	Lycoming	O-235	0.0070	0.0070	0.0093	0.0056	0.0047	0.0058	0.0013						
	Lycoming	O-320	0.0118	0.0118	0.0109	0.0081	0.0078	0.0027	0.0020						
	Lycoming	O-360	0.0120	0.0118	0.0098	0.0088	0.0065	0.0022	0.0031						
	Lycoming	IO-360	0.0143	0.0143	0.0101	0.0056	0.0062	0.0033	0.0018						
	Lycoming	O-540	0.0421	0.0356	0.0166	0.0106	0.0145	0.0032	0.0024						
	Lycoming	IO-540	0.0244	0.0222	0.0148	0.0151	0.0138	0.0066	0.0032						

Copyright National Academy of Sciences. All rights reserved.

Unique ID	Engine Make	Engine Model	Fuel Flow kg/sec						Ambient					
			T/O	C/O	Cruise	App	Final App	Taxi	Idle	Baro bar	Baro kPa	Temp K	Temp C	Humidity kg/kg	Humidity vol/vol
Preexisting Data															
FOCA[c.,e.]															
ICAO[d.]															
FAEED162	diverse	Prop-200hp	0.0112	0.0084		0.0059	0.0059	0.0012	0.0012						
FAEED160	diverse	Prop-300hp	0.0168	0.0125		0.0077	0.0077	0.0014	0.0014						
FAEED165	diverse	Prop-500hp	0.0327	0.0258		0.0125	0.0125	0.0032	0.0032						
FOCA	diverse	Prop>500hp	0.2243	0.0449		0.0220	0.0220	0.0010	0.0010						
FAEED159	TCM	O-200	0.0057	0.0057		0.0032	0.0032	0.0010	0.0010						
FOCA	Lycoming	O-320-E2A	0.0100	0.0080		0.0048	0.0048	0.0013	0.0013						
FAEED163	Lycoming	IO-320-DIAD	0.0116	0.0077		0.0047	0.0047	0.0010	0.0010						
FOCA	Lycoming	O-360-A3A	0.0120	0.0102		0.0054	0.0054	0.0016	0.0016						
FOCA	Lycoming	IO-360-A1B6	0.0136	0.0106		0.0062	0.0062	0.0014	0.0014						
FAEED160	TCM	TSIO-360-C	0.0168	0.0125		0.0077	0.0077	0.0014	0.0014						
FOCA	Lycoming	O-540-J3C5D	0.0166	0.0140		0.0066	0.0066	0.0016	0.0016						
FOCA	Lycoming	IO-540-T4A5D	0.0167	0.0148		0.0074	0.0074	0.0025	0.0025						
FOCA	TCM	IO-550-B	0.0182	0.0180		0.0098	0.0098	0.0038	0.0038						
FOCA	Lycoming	TSIO-520-WB	0.0270	0.0230		0.0140	0.0140	0.0061	0.0061						
FAEED165	Lycoming	TIO-540-J2B2	0.0327	0.0258		0.0125	0.0125	0.0032	0.0032						
ICAO	General Electric	CF34-3A1	0.4070	0.3343		0.1190	0.1190	0.0496	0.0496						
ICAO	Honeywell	AS907-1-1A	0.3470	0.2880		0.1040	0.1040	0.0480	0.0480						
EDMS	Continental	6-285-B	0.0193	0.0209		0.0105	0.0105	0.0091	0.0091						
EDMS	Curtiss-Wright	R-1820	0.1469	0.1086		0.0407	0.0407	0.0112	0.0112						
EDMS	Lycoming	IO-320-D1AD	0.0116	0.0077		0.0047	0.0047	0.0010	0.0010						
EDMS	Lycoming	IO-360-B	0.0130	0.0090		0.0046	0.0046	0.0010	0.0010						
EDMS	Lycoming	O-200	0.0057	0.0057		0.0032	0.0032	0.0010	0.0010						
EDMS	Lycoming	O-320	0.0112	0.0084		0.0059	0.0059	0.0012	0.0012						
EDMS	Lycoming	TIO-540-J2B2	0.0327	0.0258		0.0125	0.0125	0.0032	0.0032						
EDMS	Lycoming	TSIO-360-C	0.0168	0.0125		0.0077	0.0077	0.0015	0.0015						
EDMS	Pratt & Whitney Canada	PT6A-60A	0.0750	0.0680		0.0390	0.0390	0.0138	0.0138						
EDMS	Pratt & Whitney Canada	PT6A-114	0.0504	0.0449		0.0250	0.0250	0.0090	0.0090						
EDMS	Pratt & Whitney Canada	PT6A-67	0.0870	0.0790		0.0450	0.0450	0.0164	0.0164						
EDMS	Pratt & Whitney Canada	PT6a-66	0.0710	0.0650		0.0380	0.0380	0.0151	0.0151						

Copyright National Academy of Sciences. All rights reserved.

Unique ID	Engine Make	Engine Model	Manufacturer Test Organisation	Test Location	---Test Dates--- From	To
Recommended for Substitution in EDMS/AEDT						
	Lycoming	O-320	Aerodyne Research Inc	New England, USA	2014/10/06	2015/10/16
Individual Engine Tests						
1	Rotax	912	Aerodyne Research Inc	New England, USA	2015/06/09	2015/06/09
2	Continental	O-200-A	Aerodyne Research Inc	New England, USA	2014/10/08	2014/10/08
3	Continental	O-200-A	Aerodyne Research Inc	New England, USA	2015/06/04	2015/06/04
4	Continental	O-200-A	Aerodyne Research Inc	New England, USA	2015/06/03	2015/06/03
5	Continental	O-200-A	Aerodyne Research Inc	New England, USA	2014/10/09	2014/10/09
6	Continental	O-200-A	Aerodyne Research Inc	New England, USA	2014/10/07	2014/10/07
7	Lycoming	O-235-L2C	Aerodyne Research Inc	New England, USA	2014/10/07	2014/10/07
8	Lycoming	O-235-L2C	Aerodyne Research Inc	New England, USA	2014/10/07	2014/10/07
9	Lycoming	O-235-L2C	Aerodyne Research Inc	New England, USA	2015/06/04	2015/06/04
10	Lycoming	O-320-E2D	Aerodyne Research Inc	New England, USA	2014/10/09	2014/10/09
11	Lycoming	O-320-E2D	Aerodyne Research Inc	New England, USA	2015/06/09	2015/06/09
12.1	Lycoming	O-320-E2D	Aerodyne Research Inc	New England, USA	2015/06/05	2015/06/05
12.2	Lycoming	O-320-E2D	Aerodyne Research Inc	New England, USA	2015/10/15	2015/10/15
13	Lycoming	O-320-E2D	Aerodyne Research Inc	New England, USA	2014/10/06	2014/10/06
14	Lycoming	O-320-E2D	Aerodyne Research Inc	New England, USA	2014/10/07	2014/10/07
15	Lycoming	O-320-E2D	Aerodyne Research Inc	New England, USA	2014/10/08	2014/10/08
16	Lycoming	O-320-E2D	Aerodyne Research Inc	New England, USA	2015/06/03	2015/06/03
17	Lycoming	O-320-E2G	Aerodyne Research Inc	New England, USA	2014/10/09	2014/10/09
18	Lycoming	O-320-E2G	Aerodyne Research Inc	New England, USA	2015/06/04	2015/06/04
19	Lycoming	O-320-E3D	Aerodyne Research Inc	New England, USA	2015/06/08	2015/06/08
20	Lycoming	O-320-B2C	Aerodyne Research Inc	New England, USA	2014/10/09	2014/10/09
21	Lycoming	O-320-B2C	Aerodyne Research Inc	New England, USA	2014/10/10	2014/10/10
22	Lycoming	O-320-D2J	Aerodyne Research Inc	New England, USA	2015/06/03	2015/06/03
23	Lycoming	O-320-D3G	Aerodyne Research Inc	New England, USA	2015/06/08	2015/06/08
24	Lycoming	O-320-D3G	Aerodyne Research Inc	New England, USA	2015/06/09	2015/06/09
25	Lycoming	O-320-D3G	Aerodyne Research Inc	New England, USA	2015/06/04	2015/06/04
26	Lycoming	O-320-D3G	Aerodyne Research Inc	New England, USA	2015/06/09	2015/06/09
27	Lycoming	O-320-H2AD	Aerodyne Research Inc	New England, USA	2015/06/03	2015/06/03
28	Lycoming	O-320-H2AD	Aerodyne Research Inc	New England, USA	2015/06/04	2015/06/04
29	Franklin	6A4-165	Aerodyne Research Inc	New England, USA	2015/06/08	2015/06/08
30	Lycoming	O-360-A4M	Aerodyne Research Inc	New England, USA	2015/06/09	2015/06/09
31	Lycoming	O-360-C2E	Aerodyne Research Inc	New England, USA	2015/06/05	2015/06/05
32.1	Lycoming	O-360-F1A6	Aerodyne Research Inc	New England, USA	2015/06/03	2015/06/03
32.2	Lycoming	O-360-F1A6	Aerodyne Research Inc	New England, USA	2015/10/15	2015/10/15
33	Lycoming	O-360-A1A	Aerodyne Research Inc	New England, USA	2015/06/09	2015/06/09
34	Lycoming	O-360-A1G6D	Aerodyne Research Inc	New England, USA	2015/06/04	2015/06/04
35	Lycoming	IO-360-L2A	Aerodyne Research Inc	New England, USA	2015/06/08	2015/06/08
36	Lycoming	IO-360-A3B6D	Aerodyne Research Inc	New England, USA	2015/06/04	2015/06/04

Copyright National Academy of Sciences. All rights reserved.

Unique ID	Engine Make	Engine Model	Manufacturer Test Organisation	Test Location	---Test Dates--- From	To
37	Lycoming	IO-360-C1C6	Aerodyne Research Inc	New England, USA	2015/06/09	2015/06/09
38	Lycoming	IO-360-C1C6	Aerodyne Research Inc	New England, USA	2015/06/08	2015/06/08
39	Lycoming	IO-520-1AB5	Aerodyne Research Inc	New England, USA	2015/06/05	2015/06/05
40	Continental	O-470-11	Aerodyne Research Inc	New England, USA	2014/10/10	2014/10/10
41	TCM	O-470-U	Aerodyne Research Inc	New England, USA	2015/06/08	2015/06/08
42	Lycoming	O-540-B4B5	Aerodyne Research Inc	New England, USA	2015/06/08	2015/06/08
43	Lycoming	O-540-A1D5	Aerodyne Research Inc	New England, USA	2014/10/10	2014/10/10
44	Lycoming	O-540-J3C5D	Aerodyne Research Inc	New England, USA	2014/10/08	2014/10/08
45	Lycoming	IO-540-C4B5	Aerodyne Research Inc	New England, USA	2014/10/06	2014/10/06
46	Lycoming	IO-540-C4B5	Aerodyne Research Inc	New England, USA	2015/06/08	2015/06/08
47.1	Lycoming	IO-540-C4B5	Aerodyne Research Inc	New England, USA	2015/06/03	2015/06/03
47.2	Lycoming	IO-540-C4B5	Aerodyne Research Inc	New England, USA	2015/10/15	2015/10/15
48	TCM	IO-540-BB	Aerodyne Research Inc	New England, USA	2014/10/08	2014/10/08
49	Lycoming	IO-540-K1G5D	Aerodyne Research Inc	New England, USA	2014/10/10	2014/10/10
50	Continental	IO-550-N	Aerodyne Research Inc	New England, USA	2014/10/09	2014/10/09
51	TCM	TSIO-520-C	Aerodyne Research Inc	New England, USA	2014/10/08	2014/10/08
52	TCM	IO-550-C	Aerodyne Research Inc	New England, USA	2014/10/09	2014/10/09
53	Unknown (Skybolt Experimental)		Aerodyne Research Inc	New England, USA	2014/10/07	2014/10/07
54	Garrett AiResearch	TPE331-6-252B	Aerodyne Research Inc	New England, USA	2015/10/16	2015/10/16
55	Pratt & Whitney Canada	PT6A-60A	Aerodyne Research Inc	New England, USA	2014/10/07	2014/10/07
56	Williams	FJ44-1AP	Aerodyne Research Inc	New England, USA	2014/10/08	2014/10/08
57	General Electric	CF34-3A1	Aerodyne Research Inc	New England, USA	2015/10/15	2015/10/15
Engine Family Averages						
	Continental	O-200	Aerodyne Research Inc			
	Lycoming	O-235	Aerodyne Research Inc			
	Lycoming	O-320	Aerodyne Research Inc			
	Lycoming	O-360	Aerodyne Research Inc			
	Lycoming	IO-360	Aerodyne Research Inc			
	Lycoming	O-540	Aerodyne Research Inc			
	Lycoming	IO-540	Aerodyne Research Inc			
Upper Limit on Engine Family Averages at 95% Confidence						
	Continental	O-200				
	Lycoming	O-235				
	Lycoming	O-320				
	Lycoming	O-360				
	Lycoming	IO-360				
	Lycoming	O-540				
	Lycoming	IO-540				

Copyright National Academy of Sciences. All rights reserved.

Unique ID	Engine Make	Engine Model	Manufacturer Test Organisation	Test Location	---Test Dates--- From	To
Preexisting Data						
FOCA[c.,e.]						
ICAO[d.]						
FAEED162	diverse	Prop-200hp	FAA Aircraft Emissions Database		7/12/2002	
FAEED160	diverse	Prop-300hp	FAA Aircraft Emissions Database		7/12/2002	
FAEED165	diverse	Prop-500hp	FAA Aircraft Emissions Database		7/12/2002	
FOCA	diverse	Prop>500hp	FOCA		9/11/1997	
FAEED159	TCM	O-200	FAA Aircraft Emissions Database		7/12/2002	
FOCA	Lycoming	O-320-E2A	FOCA		4/21/2006	
FAEED163	Lycoming	IO-320-DIAD	FAA Aircraft Emissions Database		10/18/2002	
FOCA	Lycoming	O-360-A3A	FOCA		10/19/2005	
FOCA	Lycoming	IO-360-A1B6	FOCA		10/19/2005	
FAEED160	TCM	TSIO-360-C	FAA Aircraft Emissions Database		7/12/2002	
FOCA	Lycoming	O-540-J3C5D	FOCA		11/6/2006	
FOCA	Lycoming	IO-540-T4A5D	FOCA		12/15/2006	
FOCA	TCM	IO-550-B	FOCA		10/19/2005	
FOCA	Lycoming	TSIO-520-WB	FOCA		4/21/2006	
FAEED165	Lycoming	TIO-540-J2B2	FAA Aircraft Emissions Database		7/12/2002	
ICAO	General Electric	CF34-3A1	ICAO		23/3/1991	
ICAO	Honeywell	AS907-1-1A	ICAO			
EDMS	Continental	6-285-B	AP-42 Table II-1-7			
EDMS	Curtiss-Wright	R-1820	EPA 420-92-009 Table 5-7			
EDMS	Lycoming	IO-320-D1AD	AP-42 Table II-1-7			
EDMS	Lycoming	IO-360-B	AP-42 Table II-1-7			
EDMS	Lycoming	O-200	AP-42 Table II-1-7			
EDMS	Lycoming	O-320	AP-42 Table II-1-7			
EDMS	Lycoming	TIO-540-J2B2	AP-42 Table II-1-7			
EDMS	Lycoming	TSIO-360-C	AP-42 Table II-1-7			
EDMS	Pratt & Whitney Canada	PT6A-60A	P & W Canada			
EDMS	Pratt & Whitney Canada	PT6A-114	P & W Canada			
EDMS	Pratt & Whitney Canada	PT6A-67	P & W Canada			
EDMS	Pratt & Whitney Canada	PT6a-66	P & W Canada			

Copyright National Academy of Sciences. All rights reserved.

Abbreviations and acronyms used without definitions in TRB publications:

A4A	Airlines for America
AAAE	American Association of Airport Executives
AASHO	American Association of State Highway Officials
AASHTO	American Association of State Highway and Transportation Officials
ACI–NA	Airports Council International–North America
ACRP	Airport Cooperative Research Program
ADA	Americans with Disabilities Act
APTA	American Public Transportation Association
ASCE	American Society of Civil Engineers
ASME	American Society of Mechanical Engineers
ASTM	American Society for Testing and Materials
ATA	American Trucking Associations
CTAA	Community Transportation Association of America
CTBSSP	Commercial Truck and Bus Safety Synthesis Program
DHS	Department of Homeland Security
DOE	Department of Energy
EPA	Environmental Protection Agency
FAA	Federal Aviation Administration
FAST	Fixing America's Surface Transportation Act (2015)
FHWA	Federal Highway Administration
FMCSA	Federal Motor Carrier Safety Administration
FRA	Federal Railroad Administration
FTA	Federal Transit Administration
HMCRP	Hazardous Materials Cooperative Research Program
IEEE	Institute of Electrical and Electronics Engineers
ISTEA	Intermodal Surface Transportation Efficiency Act of 1991
ITE	Institute of Transportation Engineers
MAP-21	Moving Ahead for Progress in the 21st Century Act (2012)
NASA	National Aeronautics and Space Administration
NASAO	National Association of State Aviation Officials
NCFRP	National Cooperative Freight Research Program
NCHRP	National Cooperative Highway Research Program
NHTSA	National Highway Traffic Safety Administration
NTSB	National Transportation Safety Board
PHMSA	Pipeline and Hazardous Materials Safety Administration
RITA	Research and Innovative Technology Administration
SAE	Society of Automotive Engineers
SAFETEA-LU	Safe, Accountable, Flexible, Efficient Transportation Equity Act: A Legacy for Users (2005)
TCRP	Transit Cooperative Research Program
TDC	Transit Development Corporation
TEA-21	Transportation Equity Act for the 21st Century (1998)
TRB	Transportation Research Board
TSA	Transportation Security Administration
U.S.DOT	United States Department of Transportation

Copyright National Academy of Sciences. All rights reserved.

TRANSPORTATION RESEARCH BOARD
500 Fifth Street, NW
Washington, DC 20001

ADDRESS SERVICE REQUESTED

NON-PROFIT ORG.
U.S. POSTAGE
PAID
COLUMBIA, MD
PERMIT NO. 88

National Academy of Sciences. All rights reserved.

The National Academies of
SCIENCES • ENGINEERING • MEDICINE

The nation turns to the National Academies of Sciences, Engineering, and Medicine for independent, objective advice on issues that affect people's lives worldwide.
www.national-academies.org

ISBN 978-0-309-44601-3